Bachelor's Thesis

Biotechnology and Food Technology

Laboratory Technology

2013

Hanna Mark

PRE-TENSIONING METHOD FOR PRODUCTION OF FIBER-REINFORCED COMPOSITE POLES FOR ROOT CANAL POSTS

TURUN AMMATTIKORKEAKOULU
TURKU UNIVERSITY OF APPLIED SCIENCES

BACHELOR´S THESIS | ABSTRACT
TURKU UNIVERSITY OF APPLIED SCIENCES

Biotechnology and food Technology | Laboratory Technology

2013| Pages 68 (+8)

Instructors: Mika Jokinen, Principal Lecturer (TUAS); Lippo Lassila, Head of the Laboratory (UTU/TCBC)

Hanna Mark

PRE-TENSIONING METHOD FOR PRODUCTION OF FIBER-REINFORCED COMPOSITE POLES FOR ROOT CANAL POSTS

In this study some experimental glass fiber-reinforced composite poles with a dental resin matrix were prepared and their mechanical properties evaluated. A three-point bending test was carried out to determine the flexural strength, load and Young's modulus of bending of the poles and the work needed to break the pole structure. The poles were manufactured with a pre-tensioning method, using a special device designed and built for that purpose only. The poles will later on be milled into root canal posts used in dentistry to fix severe dental damage.

The materials used in this study are commonly used in dentistry. The matrix resin consists of Bis-GMA and TEGDMA monomers and Camphorquinone and DMAEMA light-curing initiators.

In the pre-tensioning method applied in this study the reinforcing fibers are pre-tensioned using different weights. The matrix resin is light-cured onto the tensioned fibers. Releasing the pre-tension creates a small, reinforcing compression in the material. The pole-shape was created by forcing the resin-impregnated fiber roving through a round-shaped nozzle. In addition, the effect of heat post-curing on the mechanical properties of the poles was evaluated.

The special pole-manufacturing device enables 3-17 kg pre-tensioning, several light-curing speeds, adjustable light intensity, nozzles of different sizes and heat post-curing at up to 150 °C.

The effect of the pre-tensioning on the mechanical properties of the poles was not evident. The highest mechanical values in the pre-tensioning range of 3-17 kg were achieved using 7 kg of weight. The slow speed that enables longer polymerization time was shown to enhance the mechanical properties while using the polymerization light at full intensity seemed to have just the opposite effect. Heat post-curing proved to be essential for the manufacturing process.

The highest flexural strength was achieved using low light intensity, slow speed, 10 kg of pre-tensioning weight, a nozzle size of 2.7 mm and post-curing at 120 °C for 1 h.

It is possible to use the device and the method to create poles for root canal posts. Some test milling was carried out but the final milling process is still under development and the gained results could not be directly compared to the mechanical properties of any product on the market. The results of this study can be used for further development of the method.

KEYWORDS:

FRC, fiber-reinforced composite, resin, light-curing, pre-tension, pre-stress, root canal post

OPINNÄYTETYÖ (AMK) | TIIVISTELMÄ
TURUN AMMATTIKORKEAKOULU

Bioalat | Laboratoriotekniikka

2013 | Sivumäärä 68 (+8)

Ohjaaja(t): Mika Jokinen (TuAMK), Lippo Lassila (UTU/TCBC)

Hanna Mark

LASIKUITUVAHVISTEISTEN KOMPOSIITTITANKOJEN ESIJÄNNITYSMENETELMÄ JUURIKANAVANASTOJEN VALMISTUKSEEN

Työssä valmistettiin kokeellisia lasikuituvahvisteisia komposiittitankoja, joita on tarkoitus käyttää myöhemmin juurikanavanastojen valmistukseen. Juurikanavanastoja käytetään hammashoidossa suurten hammaskudosvaurioiden korjaamiseen. Valmistettujen tankojen mekaanisia ominaisuuksia tutkittiin kolmipistetaivutustestin avulla. Tangoista määritettiin taivutuslujuus, maksimivoima, kimmokerroin ja työ, joka tarvitaan tangon murtamiseen.

Käytetyt materiaalit ovat yleisesti hammaslääketieteessä käytettäviä materiaaleja. Matriisihartsi koostuu Bis-GMA- ja TEGDMA –monomeereista, sekä kamforikinonista ja DMAEMA:sta, jotka mahdollistavat seoksen polymeroinnin valon avulla. Lisäksi työssä sovellettiin esijännitystekniikkaa, jossa lasikuituvahvisteet asetetaan painojen avulla esijännitykseen ja matriisihartsi polymeroidaan niiden ympärille. Esijännityksen purkaminen luo materiaaliin pienen, vahvistavan puristusjännityksen. Tangon muoto saatiin aikaan pakottamalla hartsilla impregnoitu, esijännitetty lasikuitunippu kulkemaan pyöreän suuttimen läpi. Työssä testattiin myös kuumentamalla tehtävän jälkipolymeroinnin vaikutusta valmistettujen tankojen mekaanisiin ominaisuuksiin.

Työtä varten oli suunniteltu ja valmistettu erikoislaite. Laite mahdollistaa 3-17 kg:n esijännityksen, useita eri veto- eli polymerointinopeuksia, säädettävän polymerointivalon intensiteetin, erikokoisten suuttimien käytön ja jälkipolymeroinnin uunissa aina 150 °C asti.

Työn perusteella ei voitu yksiselitteisesti osoittaa esijännityksen merkitystä tankojen vahvuuteen. Tuloksissa on kuitenkin havaittavissa huippukohta, joka saattaa viitata mahdolliseen optimijännitykseen. Hidas vetonopeus mahdollisti pidemmän polymerointiajan ja se paransi mekaanisia ominaisuuksia. Polymerointivalon käyttämisellä maksimi-intensiteetillä taas vaikutti olevan päinvastainen vaikutus. Jälkipolymerointi osoittautui tulosten perusteella tärkeäksi osaksi tankojen valmistusprosessia. Taivutuslujuudeltaan vahvin tanko saatiin käyttämällä alhaista valon intensiteettiä, hidasta veto/polymerointinopeutta, 10 kg esijännitystä, 2,7 mm suutinta ja jälkipolymerointia 120 °C:ssa 1 h ajan.

Menetelmän avulla voidaan valmistaa komposiittitankoja, joita voidaan käyttää juurikanavanastojen valmistukseen. Sorvausmenetelmä vaatii kuitenkin vielä kehitystä, eikä tangoista saatuja tuloksia voi suoraan verrata mihinkään markkinoilla olevaan tuotteeseen. Työssä selvitettiin kuitenkin menetelmän tärkeimmät parametrit, joita voidaan käyttää jatkokehityksessä.

ASIASANAT:

FRC, lasikuituvahvisteinen komposiitti, hartsi, valokovetus, esijännitys, juurikanavanasta

CONTENT

APPENDICES

FIGURES

TABLES

LIST OF ABBREVIATIONS (OR) SYMBOLS

Bis-GMA	Bisphenol A glycerolate dimethacrylate, CAS 1565-94-2
CQ	Camphorquinone, CAS 10373-78-1
DMAEMA	2-(Dimethylamino)ethyl methacrylate, CAS 2867-47-2
FRC	Fiber-reinforced composite
MMA	Methyl methacrylate
TEGDMA	Triethylene glycol dimethacrylate, CAS 109-16-0

1 INTRODUCTION

In this study some experimental glass fiber-reinforced poles with dental resin matrix were prepared and their mechanical properties were evaluated. The poles were manufactured by using a special device designed and built for that purpose only. The poles will later on be milled into root canal posts used in dentistry to fix severe dental damage.

Root canal posts are subjected to occlusion forces and therefore need to have enough strength and flexibility to resist breaking and damaging the tooth. They also need to be biocompatible, non-toxic and moisture resistant. The materials used in this study are biomaterials commonly used in dentistry. To enhance the strength of the fiber-reinforced pole structure a pre-tensioning method widely used when building concrete elements is applied. To evaluate the ability of this method to create a new root canal post that is able to compete with those already on the market, flexural strength, Young's modulus, load and the work needed to break the structure in three-point bending are studied.

The focus of this study is on learning the effects of the different parameters of the manufacturing process on the mechanical properties of the product. Other important properties required of the material are a high degree of conversion and suitable radio-opacity and translucency. The manufactured poles should also have proper dimensions for the subsequent milling process and in addition to that, no delamination of the material should occur and there should be no air bubbles in the structure of the poles.

This study is part of an ongoing research process started somewhere in 2004-2005 by Lippo Lassila, (D.D.S.) and Filip Keulemans, (D.D.S, PhD). They started to study the effect of pre-tensioning on fiber-reinforced dental composites in the biomaterials research group led by Professor Pekka Vallittu in the Turku Institute of Dentistry. Today the work continues at Turku Clinical Biomaterials Centre (TCBC).

I would like to thank Professor Pekka Vallittu for the opportunity to work in his interdisciplinary research group. I would also like to thank my supervisors DSc Mika Jokinen from Turku University of Applied Sciences and D.D.S Lippo Lassila from Turku Clinical Biomaterials Centre (TCBC). A special thank you is also owed to Stick Tech Ltd for material support. I am also very grateful for the pictures I received from lab.tech. Pasi Saarenmaa (Turku University Technical Laboratory) and lab.tech. Genevieve Alfont (TCBC). I also greatly appreciate all the support and help I have received from the TCBC lab girls.

2 BIOMATERIALS

The European Society for Biomaterials (ESB) has defined a biomaterial as follows: “Material intended to interface with biological systems to evaluate, treat, augment or replace any tissue, organ or function of the body” (Williams 1999). Materials used in direct contact with tissues, blood or body fluids are called biomaterials. Biomaterials are used to create implants; they are used in dental restorative materials (Figure 1), in prostheses and in bone cements. They are used whenever there is a need to repair or replace a part of a living system. Biomaterials can be synthetic or of biological origin. Synthetic materials are metals, ceramics, polymers or composites i.e. combinations of these. Biological materials are derived from biological molecules or living tissues such as bones or dentin for example. (Rich 2002)

Figure 1. Dental restorative materials are biomaterials. (Photograph G. Alfont)

Biomaterials have high standards. They have to be biocompatible, which means that they should not cause any tissue damage or other harmful reactions within the body. The mechanical strength of the material must be sufficient enough for the intended purpose. Usually the best result is achieved when the mechanical properties imitate the properties of the surrounding or replaced tissue. Biomaterials also need to be ductile; one should be able to modify them as

needed. They also need to be able remain intact during the sterilization process. Non-biodegradable materials should not undergo any decomposition or degradation inside the body and biodegradable materials should have a controlled degradation process. (Rich 2002)

3 DENTAL RESINS

Dental resins are monomer mixtures used in dentistry. They can be found in dental composites, pit and fissure sealants, dentine bonding agents, cements, adhesives, dentures and elastomeric impression materials (Sideridou *et al.* 2002). Dental resins are in direct contact with the living tissues so they are classified as biomaterials. The dental resin monomers used today are mostly based on methyl methacrylate (MMA) (Figure 2). MMA or its polymer, polymethyl methacrylate (PMMA) is still widely used in medical applications and also as a denture material, but it has some drawbacks as a restorative material. It is a linear, thermoplastic polymer with large polymerization shrinkage and a high thermal expansion coefficient. This means that the polymerization process and variations in temperature cause dimensional changes in the polymer. This may result in detaching of the cavity filling. PMMA also lacks in strength when compared to tooth enamel and its polarity causes water absorption and plasticization of material. (Darvell, 2009)

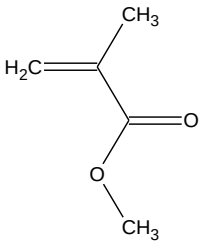

Figure 2. MMA molecule.

Bisphenol-A-glycidyl dimethacrylate (Bis-GMA)

Dimethacrylates, such as Bis-GMA are widely used in dentistry today. Bis-GMA is a dental resin monomer molecule that has many advantages compared to MMA/PMMA. It is not as volatile as MMA which makes it less harmful. It has a large molecule size which reduces polymerization shrinkage and the sterically hindered structure increases the elastic modulus of the resin. Its water absorption and plasticization are reduced due to reduced polarity and it has more than one functional group to enable cross-linking. Bis-GMA contains a bisphenol-A molecule in its structure (Figure 3). It can be seen as a bisphenol-A based molecule terminated at each end by the methacrylate group. (Darvell, 2009; Sideridou *et al.* 2002)

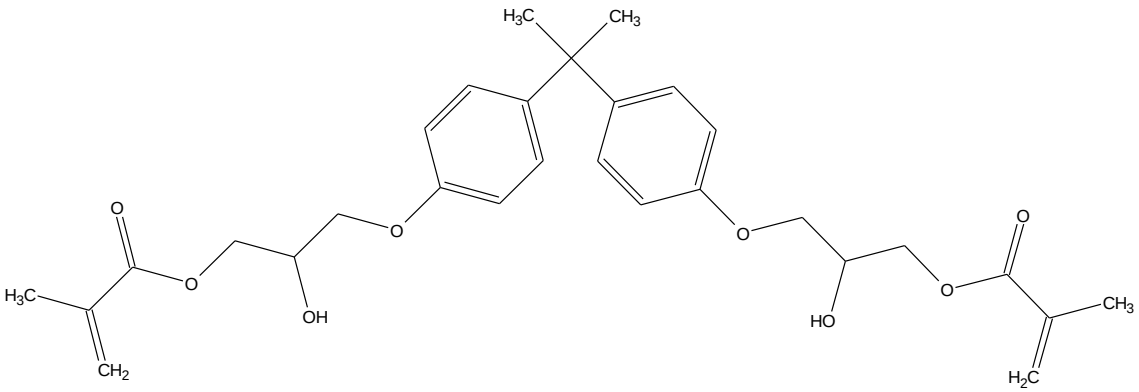

Figure 3. Bis-GMA molecule.

The Bis-GMA monomer is a highly viscous, honey-like substance and it needs to be diluted to be usable. Triethyleneglycol dimethacrylate (TEGDMA) is commonly used as a diluent for Bis-GMA. The TEGDMA molecule is also a monomer, so it can be polymerized to be part of the final polymer structure (Figure 4). This is important because leaching residual monomers are hazardous in a living, biological environment. The TEGDMA molecule has two functional vinyl groups to form cross-linking structures. (Darvell, 2009; Sideridou *et al.* 2002)

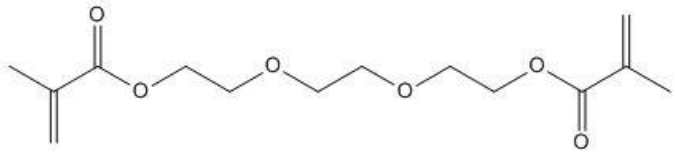

Figure 4. TEGDMA molecule.

4 POLYMERIZATION

4.1 Polymerization reaction

Both MMA and Bis-GMA polymerize via free radical reaction of carbon-carbon double bonds. There are many polymerization systems used in dentistry. A polymerization reaction can be activated chemically, thermally or by light, depending on the initiator-activator system used. Light curing is the most simple and common way. Using a diketone-tertiary amine system, such as camphorquinone (CQ) and dimethylaminoethylmetharylate (DMAEMA), it is possible to use visible, blue light to polymerize Bis-GMA-TEGDMA resin (Figures 5 and 6). The DMAEMA molecule can also be polymerized to be part of the final polymer structure to avoid residual monomer leaching. (Darvell 2009)

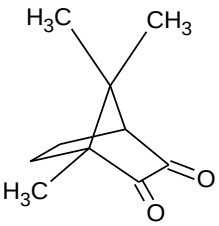

Figure 5. CQ molecule.

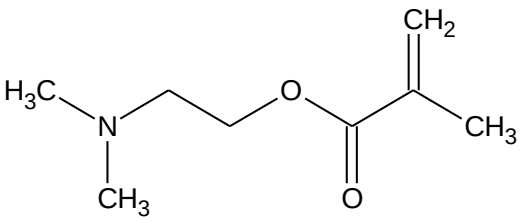

Figure 6. DMAEMA molecule.

When the blue light from the light source hits the resin containing light curing initiator-activator system, the diketone gets into excited state and reacts with tertiary amine to form an exited-state complex, which then results in free radical molecule formation and the initiation of the polymerization reaction. The light starts the reaction and the chain propagation continues until the polymer becomes too viscous and the fraction of reacting double bonds becomes too low, or until the free radicals are lost. The reaction does not result in full conversion of all of the double bonds into polymer chain links. Typical conversion for dental materials is more around 50-75 % of the double bonds. The polymerization reaction is dependent on the intensity and the wavelength of the light source and the exposure time used. (Darvell 2009)

Studies have shown that heat post-curing can enhance the properties of some resin composites. Heating the material after light-curing improves the polymerization and is expected to result in better mechanical properties of the polymer composite. It also reduces the amount of unreacted residual monomers making the material more biocompatible. The post-curing temperature has been shown to have more influence on the result than the post-curing time. (Ferracane et Condon 1992, Bagis et Rueggeberg 1997, Bagis et Rueggeberg 2000)

4.2 Curing lamps

Camphorquinone has the strongest absorption at visible light wavelengths from 430 to 480 nm, the maximum being at 470 nm. The light source used should meet this demand. The possible sources are quartz-halogen lamps, plasma arc lamps and light-emitting diodes, i.e. LED lamps (Figure 7). Quartz-halogen and plasma arc lamps are not as specific as LEDs and often need heat and wavelength filters. Also the emitted power varies according to the device. LEDs are relatively low-power output devices compared to quartz-halogens and plasma arcs. (Darvell 2009)

The light intensity for a basic dentist's LED curing light is about 1200 mW/cm^2. (3M 2009)

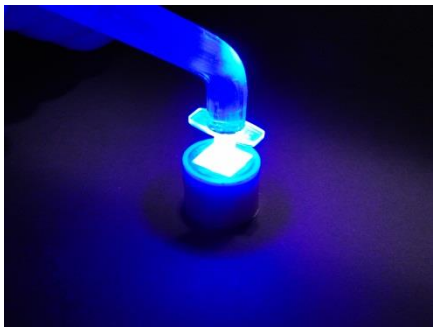

Figure 7. Dental LED light-curing device.

With a more specific emission spectrum and high intensity it is possible to use shorter exposure times. However, high intensities and short exposure times may result in early termination of the polymer chains causing lower molar mass for the final polymer. Fast polymerization leaves no time for relaxation of the polymer network and causes stress inside the material. (Rueggeberg 2011)

4.3 Depth of cure

The intensity of the irradiation falls with a growing distance to the light source and also as it passes through the material, and most rapidly at the wavelengths that are the most efficiently absorbed. The light is also scattered due to possible air bubbles and filling materials. As a result, there is a certain depth of cure that can be expected for a given light exposure time and intensity. This means that with a certain light source, exposure time and distance, there is a maximum thickness of material that can be expected to be properly cured. (Darvell 2009)

A recommended exposure time using a dental light-curing device for an about 2 mm thick Filtek™ Z250 dental restorative material layer is 20-40 s (3M 2005) and for fiber-reinforced post material EverStick® with a diameter of 0.9-1.5 mm 40 s (StickTech 2011).

4.4 Oxygen inhibition

The oxygen in air can react with free radicals. This phenomenon inhibits the free radical polymerization and yields polymers with uncured, sticky surfaces. This can be an advantage. That is the case when building up a dental restoration in layers. The sticky surface can be removed by polishing and in some cases the formation of an oxygen inhibition layer can be prevented by using a suitable material, such as Mylar foil, on the surface while curing. Vacuum systems can also be used to solve the problem. Polymerization at a temperature above ~110 C has been shown to eliminate oxygen inhibition and it can also be affected by the viscosity and the filler content of the material. (Darvell 2009; Gauthier *et al.* 2005)

5 COMPOSITES

5.1 Properties of composites

Resins are often used in combination with fillers or reinforcing fibers to achieve better properties. These combination materials are called composites (Figure 8). Composite properties are determined by the materials used, the manufacturing process and the environment of the final product, especially temperature and moisture. Composite structures can have different material mixing ratios and the distribution of the materials may vary. The structures easily capture air bubbles which cause porosity. (Saarela *et al.* 2007)

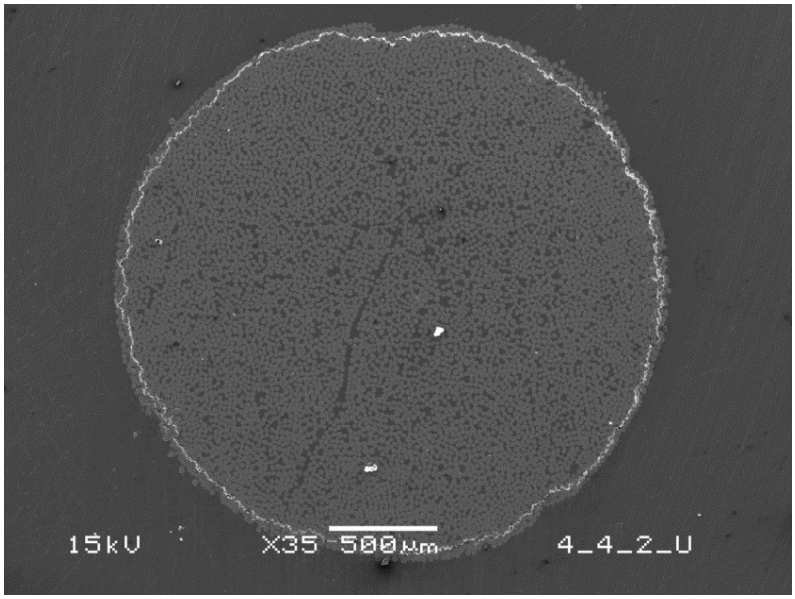

Figure 8. Microscopic image of a cross-sectional surface of a fiber-reinforced composite.

5.2 Fiber-reinforced composites

Fiber-reinforced composites (FRCs) are combinations of polymer matrix and reinforcing fibers. The load applied to the composite structure is transferred to the fibers and carried by them. The structure can have different fiber orientations; they can be continuous unidirectional rovings, bidirectional weaves

or random oriented mats (Figure 9). They can also be short random oriented fibers. Fiber orientation has an effect on the strength of the FRC. Reinforcing only occurs in the direction of the fibers. For example for continuous unidirectional fibers the highest strength and elastic modulus are achieved when the direction of the stress is the same as the direction of the fibers. With continuous bidirectional weaves the reinforcing effect is divided in two directions, which gives lower strength values, but on the other hand the toughness of the material increases. (Vallittu 2008)

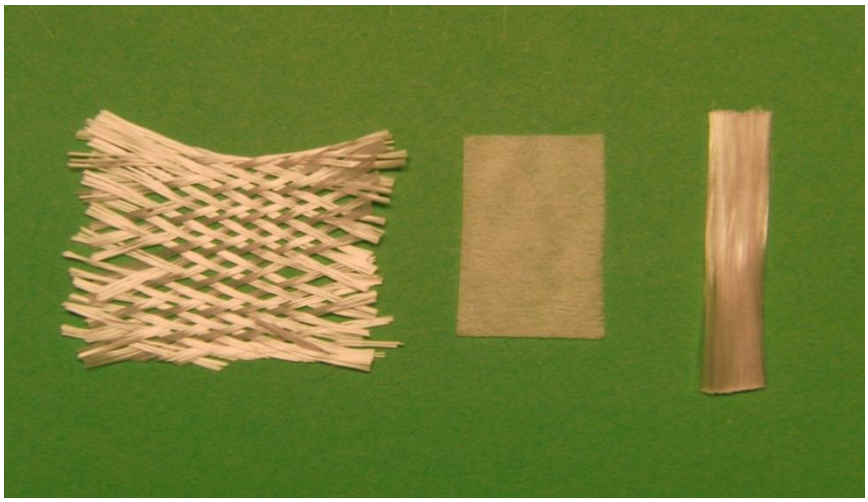

Figure 9. Glass fiber weave, mat and roving.

From the many types of fibers, glass fibers are commonly used in clinical applications. There are also different kinds of glass fibers but the most popular one is the E-glass. It has good electrical, mechanical and chemical properties and it is not expensive. The colorless appearance is one of the benefits of the glass fibers and it is also possible to have good adhesion between the resin matrix and the glass fibers due to silane coating. Silanes are molecules that have both inorganic and organic properties and they can be attached to a glass surface to create a coating that improves the bonding between the inorganic glass and the organic polymer matrix. (Vallittu 2008, Saarela *et al.* 2007)

5.3 Impregnation

When working with fiber-reinforcements, it is essential to make sure that all of the fibers are well impregnated. This means that the fibers should be fully covered with the matrix resin before curing. Inadequate wetting of fibers by the resin results in poor adhesion between the materials and the mechanical properties will not reach the optimal values. (Vallittu 2008)

5.4 Pultrusion

There are many ways to manufacture composites. A common way to prepare FRC poles is pultrusion. It is used to make sports equipment such as ski stick rods. In pultrusion the impregnated reinforcements are pulled through a nozzle or a mold to give them the desired shape and to cure the material. When using a pultrusion method it is important to make sure that the material is strong enough to be pulled and the tension should be as even as possible throughout the reinforcing fibers. Pultrusion products have high reinforcement content and good mechanical properties in the axial direction. (Saarela *et al.* 2007)

5.5 Pre-stress and pre-tension

Pre-stressing is a technique used to enhance the mechanical properties of concrete buildings. In pre-stressing a concrete matrix is applied on to pre-tensioned reinforcements. When the concrete has set, the pre-tensioning is released and the reinforcements strive to their original length causing a compressive pre-stress on the structure. This structure is stronger and more efficient to resist tensile forces because to be able to break the structure one must first overcome the pre-stress. The stress also causes the small cracks to close after removing the load that caused the crack. When using the pre-stress technique one should note that the compressive strength of the matrix material should be higher than the pre-tensioning stress and the adhesion between the reinforcements and the matrix should be adequate enough to endure the process and assure the load transfer between the phases. (Schlichting *et al.* 2010)

This same technique can be applied to a glass fiber reinforced resin matrix system. If the compressive strength of the resin matrix is not high enough, the stress caused by the tensioning will break the composite structure. The applicable amount of fibers and the pre-tensioning load that can be used are dependent on the compressive strength of the resin matrix. The fibers should also be placed symmetrically and the tension should be even across the whole fiber bundle. Asymmetrical placement and uneven tensioning leads to curving of the structure. (Schlichting *et al.* 2010)

Some studies have been made concerning pre-stressing and FRCs. Schlichting *et al.* have studied the influence of pre-stressing on the flexural properties of composite resin reinforced with pre-tensioned glass fibers. The study showed that pre-stressing can increase the flexural strength of a composite resin material but it has very limited effect on the flexural modulus. (Schlichting 2010)

Keulemans *et al.* have conducted some experiments using pre-stressed dental fiber-reinforced composites. In the study FRC rods with a diameter of 1.4 mm were prepared using different pre-tensioning weights and the mechanical properties of the rods were evaluated in a three-point bending test. The results showed that there is an optimal pre-tensioning level for the FRC rods. Pre-tensioning enhances the mechanical properties up to a certain point and when the point is exceeded the flexural properties decrease significantly. The observed optimal pre-tensioning level for the rods was 44-52 MPa. (Keulemans 2012)

6 ROOT CANAL POSTS

A tooth can be divided into two parts; the visible part is the crown and the part inside the gums is the root. The crown surface consists of enamel and the inner part of the tooth of dentin (Figure 10). In the middle of the structure there is the root canal and the pulp. The pulp houses the soft tissue, such as nerves. Sometimes the pulpal tissue may get infected and the tooth needs endodontic root canal treatment. The treatment requires that the dentist drills an entrance through the enamel and the dentin, and removes the tissue and disinfects the root. The procedure can cause massive dental tissue loss and the strength of the tooth is weakened. To restore the tooth a reconstruction of the crown with a core build-up is required. Root canal posts are rods that are placed into the root canal of a tooth to increase the retention of the core restoration. (Fokkinga 2007)

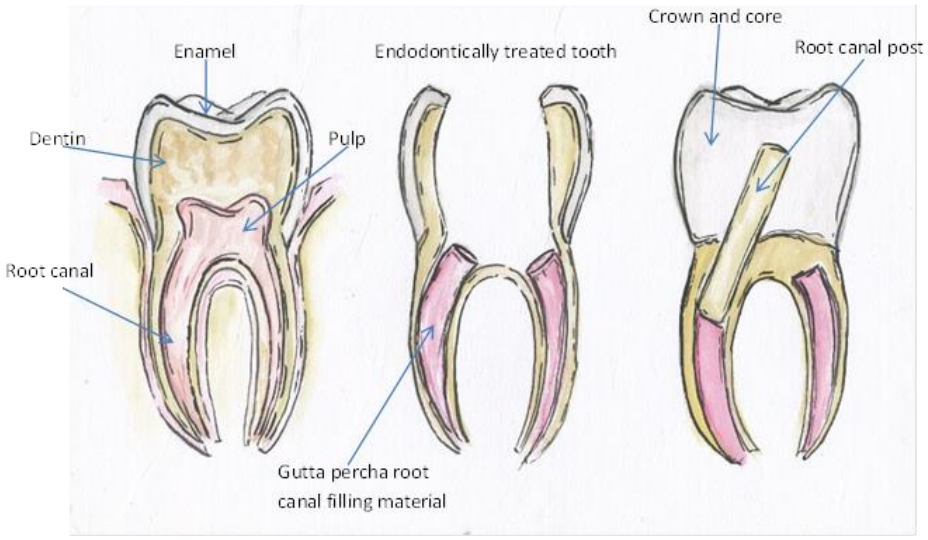

Figure 10. Root canal treated tooth and a root canal post. (Picture G. Alfont)

Root canal posts can be custom-made cast posts made in the dental laboratory, they can be prefabricated or *in situ* polymerized individually formed FRC posts. They can be made out of metal, ceramics or fiber-reinforced composites. The

posts can have different designs to enhance the retention to the structure (Figure 11). The post needs to have good bonding with the luting cement and the core material to have strong structure. The adhesion between the materials can be increased by mixing cross-linked and linear monomers to create semi-interpenetrating network polymer matrix. The retention is also affected by the length and the diameter of the post. (Le Bell-Rönnlöf 2007)

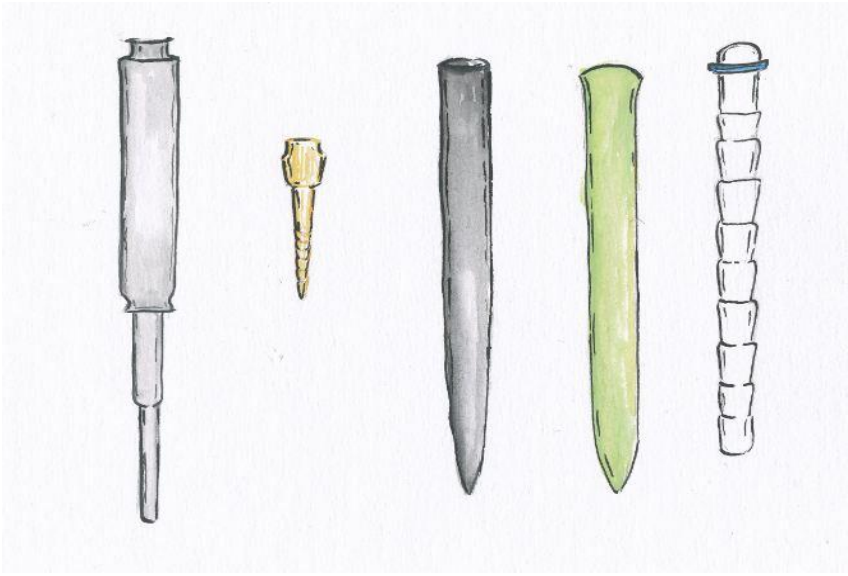

Figure 11. Different kinds of root canal post designs. (Picture G. Alfont)

FRC posts

Contemporary dentistry has high demands for good esthetics. This has also affected the focus of current post and core research. FRCs have good esthetic properties. Tooth-like color or translucency enhance the esthetic appearance of the build-up and help light-curing through the post. A major advantage for FRCs is that they can be adjusted to have a similar modulus of elasticity as dentin (Table 1). A post material with an excessively elevated elastic modulus causes stress to be transferred to the less rigid dentin and results in root fractures. It is more desirable for the post to failure before the tooth fractures. One more thing that is expected of a good root canal post material is radio-opacity. It is

necessary for a dentist to be able to see the post in an x-ray image. The Radio-opacity of the FRC posts can be enhanced by adding radio-opaque fillers into the resin matrix. (Le Bell-Rönnlöf 2007)

Table 1. Mechanical properties of some dental and post materials. (According to Le Bell-Rönnlöf 2007)

Material	Flexural Strength (Mpa) (Transverse strength)	Elastic modulus (Gpa) (E-modulus)	Notice
Dentin	30-105*	15	*ultimate tensile strength
Enamel	10*	50-84	*ultimate tensile strength
Titanium	550-930*	117	*ultimate tensile strength
Stainless steel	841-924*	177-202	*ultimate tensile strength
Gold alloy	469-759*	77-108	*ultimate tensile strength
Zirconia post	900-1200	200-210	Cosmopost, Ivoclar
Carbon fibre post	1154	82	Composipost, RTD
Glass fibre post	990	29	Parapost Fiberwhite, ColteneWhaledent
Glass fibre post	1145	16	Everstick, StickTech

7 MECHANICAL TESTS

A three-point bending test is used to determine the flexural properties of materials. With the test it is possible to determine the flexural strength and the flexural modulus of the material. The test also reveals the force and the work needed to break the specimen. In the three-point bending test a load is applied on a test specimen with known dimensions. The jig consisting of the specimen holder and the head used to apply the force also have a certain setup and dimensions (Figure 12).

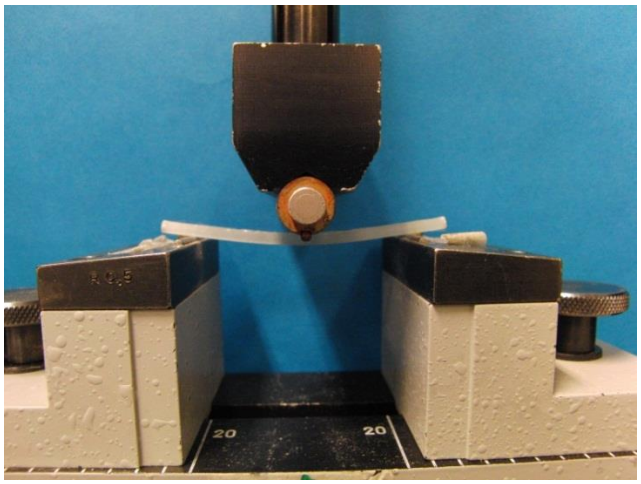

Figure 12. 3-point bending test.

The three-point bending test can be presented as a stress-strain curve (Figure 13). Stress (σ) is defined as being force (F) per area (A). Strain (ε) is the ratio between the change in length (ΔL) and the initial length (L_0) of the test specimen. It is a measure of the amount of deformation caused by the applied force. Modulus of elasticity (E) is the slope of the linear segment of the curve and it is a measure of the material's stiffness and resistance to deformation. A high modulus value indicates high stiffness. The highest point of the curve gives the force or the stress needed to break the specimen and the work done can be

determined from the area under the graph when plotting the load (F) readings against the bending extension readings (d). (Outinen *et al.* 1998)

Stress $\sigma = F/A$ (N/m^2=Pa)

Strain $\varepsilon = \Delta L/L_0$

Modulus of elasticity $E = \sigma/\varepsilon$ (Pa)

Work $W = Fd$ (Nm=J)

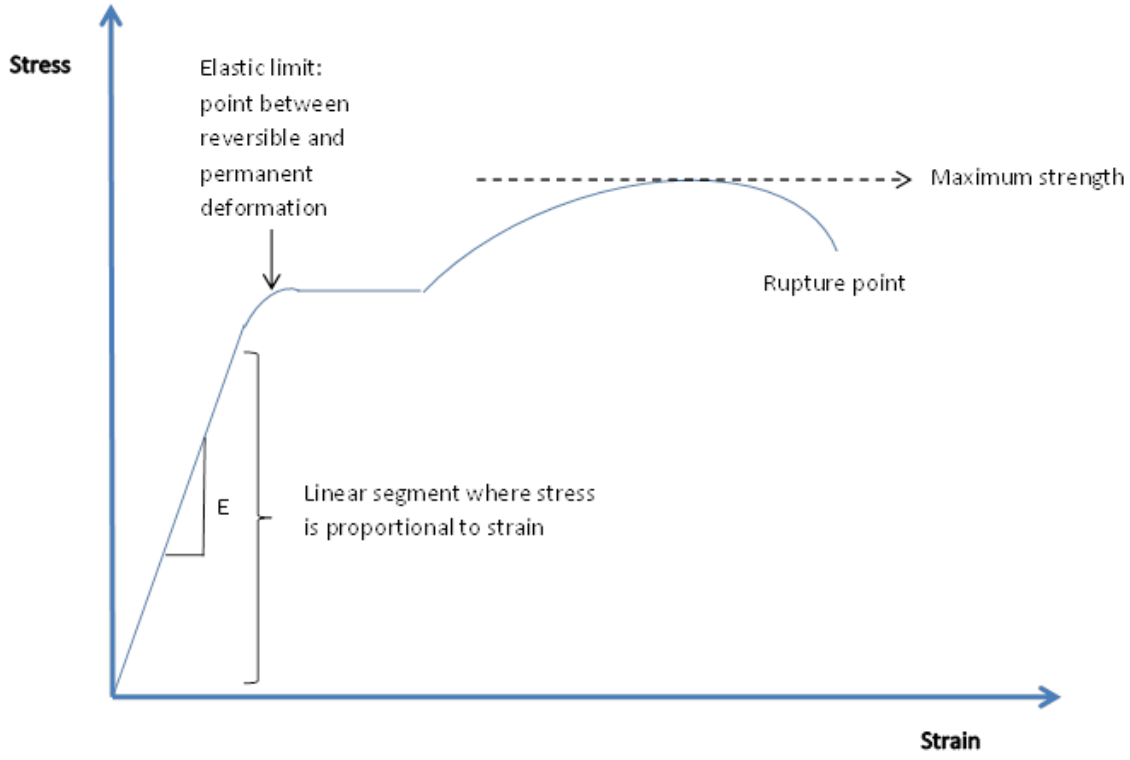

Figure 13. Stress-Strain curve.

The formulae used for calculating the Young's modulus and the flexural strength (Max bending stress) for circular cross sectional specimens in a three-point bending test by the Nexygen program (LLOYD instruments):

$$Young's\ modulus\ of\ bending\ E_b = \frac{P}{\delta} * \frac{4L^3}{3\pi D^4}$$

where

P=applied force (N)

δ=deflection (mm)

L=span length (mm)

D=diameter of the specimen (mm)

$$Maximum\ bending\ stress\ f_{max} = \frac{M_{max} * y_{max}}{I}$$

where

Half thickness of the specimen y_{max}=D/2

Maximum bending moment M_{max}=PL/4

$$Moment\ of\ inertia\ I = \frac{\pi D^4}{64}$$

Testing small sized specimens such as root canal posts may easily lead to incorrect results. Flexural strength and elastic modulus determined by the three point bending test depend on the diameter of the specimen and the span length of the test set-up. When using a constant span length, specimens with smaller diameter give higher results than the specimens with larger diameter. So, it is very important to use the same span length and the dimensions of the specimens should be as similar as possible when comparing the strength values. (Vallittu 2008)

The correlations between the manufacturing parameters and the mechanical test results are studied using Spearman rank-order correlation coefficient. It is a non-parametric test that does not require normal distribution. The coefficient varies between 1 and -1, coefficient value 1 meaning full positive correlation and -1 meaning full negative correlation. Value 0 means that there is no correlation between the variables. The P-value gives the probability associated with the risk of error. The comparisons are made using T-test. A T-test value that is lower than 0.05 indicates significant difference between the compared values. (Holopainen *et al.* 2004)

8 FRC POLE MANUFACTURING DEVICE

A special device was designed and built for manufacturing the pre-tensioned FRC-poles used in this study (Figure 14). The device consists of two gutters enabling two poles to be manufactured at the same time. The maximum length of the pole is 198 cm. An impregnated fiber roving is first attached to the upper hook above the gutter and then it is attached to the lower weight holder. Weights are added to create the pretension. Then the roving is guided through a nozzle and it is fitted into a nozzle holder. Next the machine is set to pull the nozzle through the fiber roving at a certain speed. Normally in pultrusion techniques the fibers are pulled through the nozzle but in this technique the nozzle is pulled through the fibers. The technique can be seen as a kind of reverse pultrusion. The curing lamps are situated in the nozzle holder about one centimeter below the nozzle. There are three LED lamps placed circularly around the roving. The distance from the lamps to the roving is about one centimeter. The intensity of the curing lamps can be adjusted. After the light-curing the nozzle and the nozzle holder are removed and the motor is run back to zero position. It is possible also to post-cure the material in pretension by pulling the gutter around the fiber roving and closing it. The gutter can be heated up to 150 °C.

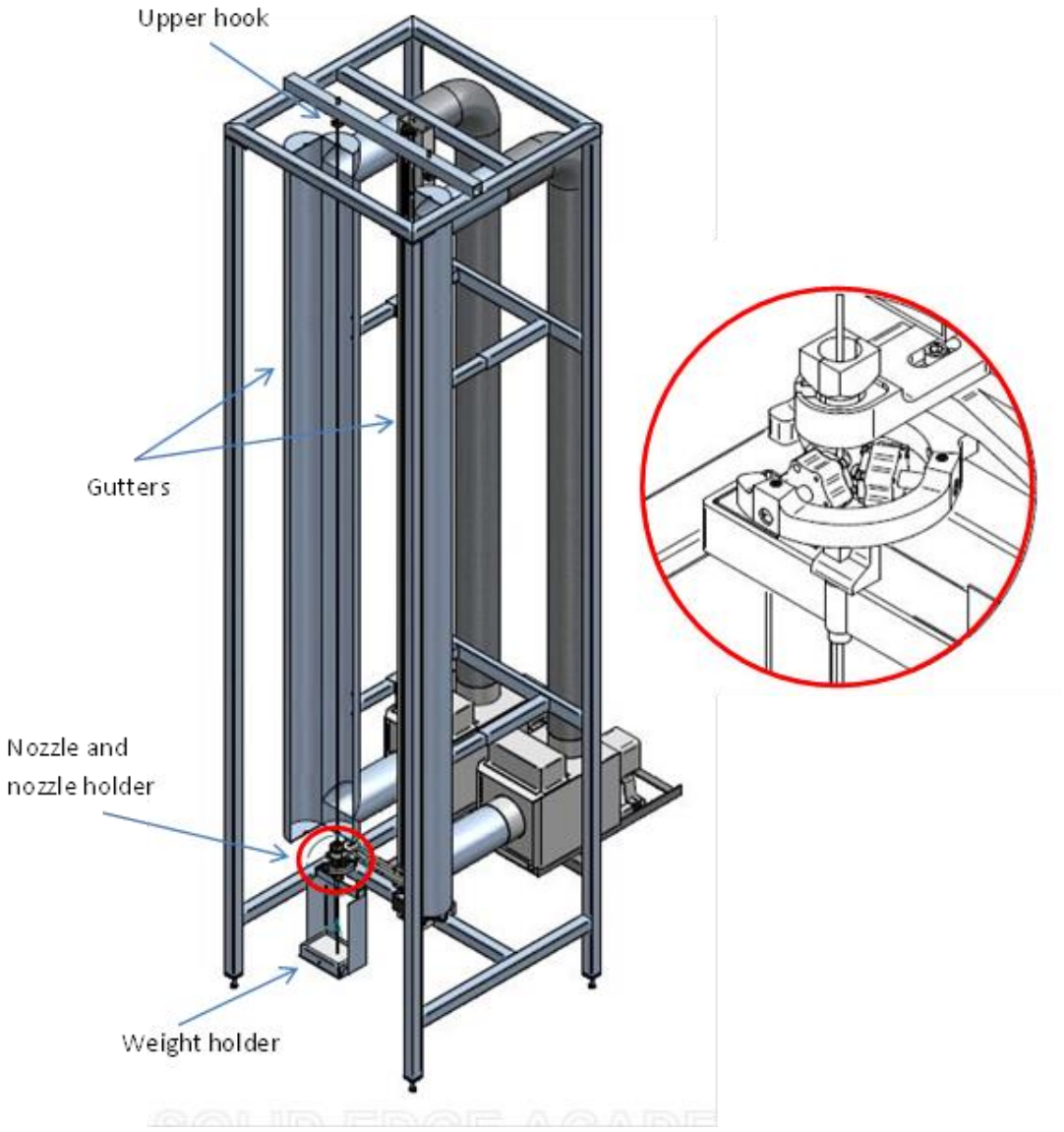

Figure 14. FRC pole manufacturing device. (Picture Pasi Saarenmaa)

9 FRC POLE MANUFACTURING PROCESS

The following materials and devices were used in this study (Tables 2 and 3):

Table 2. Materials used in this study.

Materials						
Reagent	**Usage**	**Manufacturer**	**Catalog no**	**Purity**	**Batch/lot. No**	**Notice**
Bis-GMA	Resin 60 w-%	Esschem	X 950 0000	min 85 %	688-07, 688-51	
TEGDMA	Resin 40 w-%	Aldrich	261 548	95 %	STBC4723V, STBC5193V	
DMAEMA	Resin 0,7 w-%	Aldrich	234 907	98 %	1437599V	
CQ	Resin 0,7 w-%	Aldrich	124 893	97 %	S12442V, STBC7007V	
Glass fiber		Ahlström	R338-4800		1103010507	Epoxy-silanized E-glass, Tex 4800g/1000m

Table 3. Devices used in this study.

Devices				
Machine	**Usage**	**Type/model**	**Manufacturer**	**Notice**
Handlightcuring unit	Attaching the fibers to the device	Elipar S10	3M ESPE	
Load Cell 2500N	Mechanical testing	LLOYD 2500N	LLOYD Instruments, Ametek Inc. USA	Sensitivity 2,0 mV/V +/- 0,05%, nonlinearity <0,05% FSR
Universal material testing device	Mechanical testing	LR30K+	LLOYD Instruments, Ametek Inc. USA	
RMS multimeter	Oven temperature testing	Fluke 179	Fluke corp. USA	
LED radiometer	Light intensity measurement		Kerr, USA	
Motor	FRC-pole manufacture device	43HGAC-2,33	HSI Inc. Waterbury CT, USA	B43HGO-2,33-060, 2,33VDC
LED Blue light	FRC-pole manufacture device	Luxeon III Star LXHL-LB3C	Philips Lumileds Lighting Co	Blue 470 nm

The test specimens were prepared using silane coated E-glass fibers and Bis-GMA-TEGDMA -resin with light-curing initiator and activator. The effects of the following parameters on the mechanical properties of the test specimens were tested in three-point bending:

1. Light intensity and speed with oven post-curing (120 °C, 60 min)

   Light intensities 1, 2, 3 and 4

   Speeds (2, 3, 4, 5, 6, 7 and 8) mm/s

2. Light intensity and speed without oven post-curing

   Light intensities 1, 2, 3 and 4

   Speeds (2, 3, 4, 5, 6, 7 and 8) mm/s

3. The effect of pre-tensioning

   Weights (3, 7, 10, 14 and 17) kg

4. The effect of post-curing

   Temperatures (100, 120 and 130) °C

   Times (15, 30 and 60) min

5. The effect of the nozzle size

   Diameters (2.6, 2.7 and 2.8) mm

The manufacturing process was started by cutting pieces of about 420 cm from the glass fiber roving. The cut pieces were folded to create double rovings and wetted thoroughly with 60/40 (w/w) Bis-GMA-TEGDMA resin, containing 0.7 w-% CQ and DMAEMA light-curing initiators. The rovings were allowed to impregnate overnight in room temperature, under a fume hood and wrapped in foil (Figure 15).

Figure 15. Fiber roving impregnation.

The next day the fibers were attached to the device. The fibers were first fastened to the upper hook and then to the weight holder down below (Figures 16 and 17). A dental hand light-curing device was used to cure the knots at both ends. Weights were added and the roving was guided through the nozzle (Figure 18). The motor was set to run the nozzle up the roving at a desired speed and the LED-curing lights were switched on with a desired intensity (Figure 19). The nozzle cup gathered the excess resin and was emptied with a plastic Pasteur pipette a few times during a run. Post-cured groups were heated with the machine oven. Only one pole was prepared per group because of the time-consuming manufacturing process. The pole was then cut to pieces for a three-point bending test. Eight 65 mm pieces were cut from the middle of the

pole for the mechanical testing. The diameters of the test specimens were measured by using a digital caliper and the values were entered to the testing program. The used crosshead speed was 5 mm/min and the specimen holder span was 50 mm.

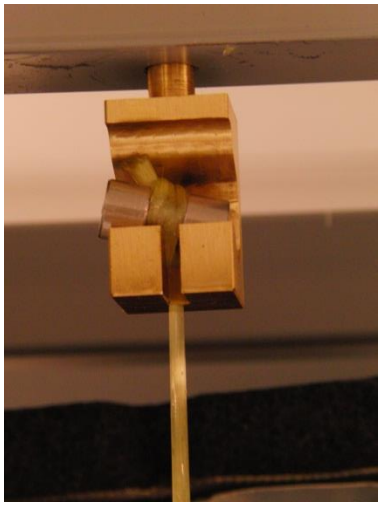

Figure 16. Upper attaching hook of the device.

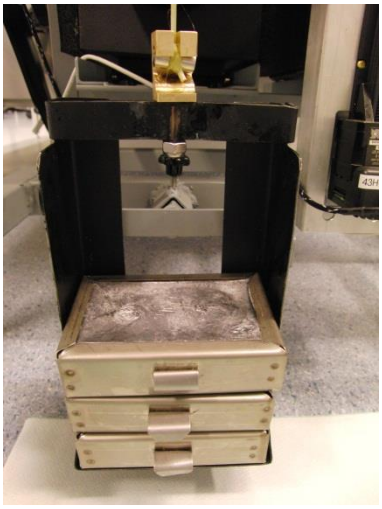

Figure 17. Weight holder.

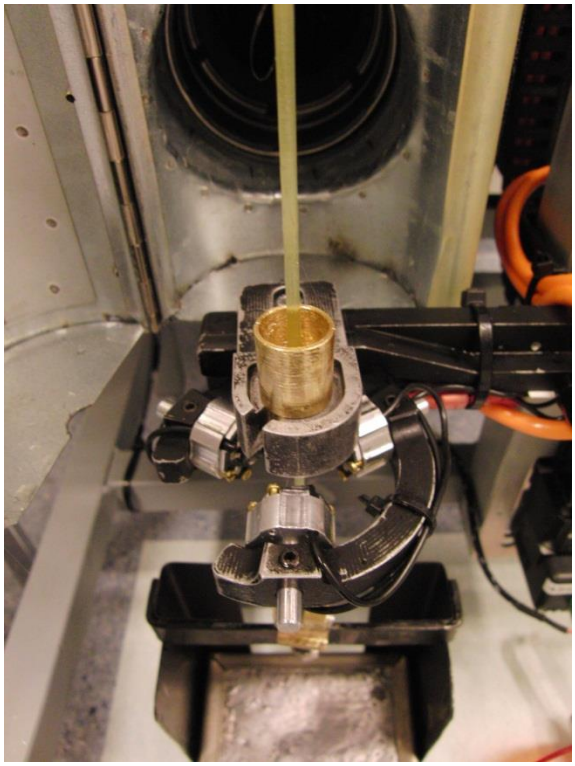

Figure 18. The nozzle and the nozzle holder.

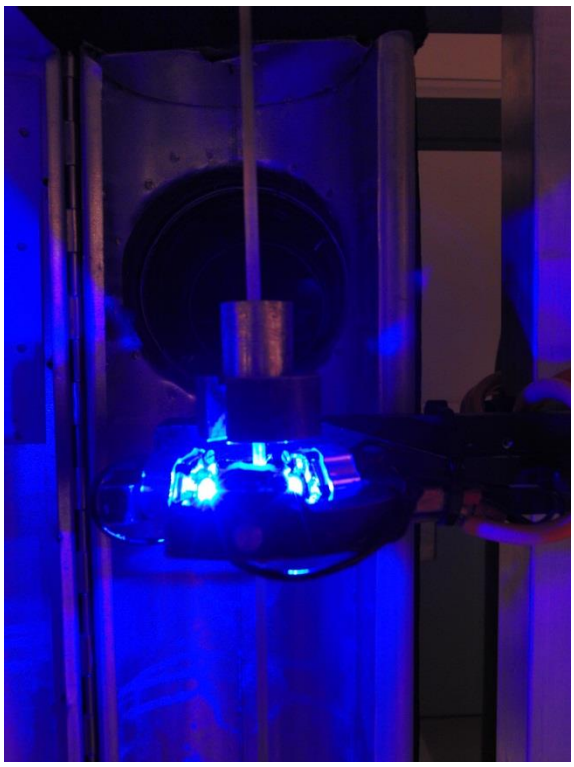

Figure 19. The device in action.

The light intensity was selected from the control panel by adjusting the Dim-button (Figure 20). The used intensities were 1/4, 2/4, 3/4, and 4/4 rounds.

Figure 20. Control panel and the light intensity switch.

Some challenges were met during the manufacturing process. First of all the glass fiber roving had some bad parts in it (Figure 21). The parts may possibly be due to a precipitation of silane coating. These parts caused uneven tension along the roving. Also the diameter of the poles was not perfectly symmetrical.

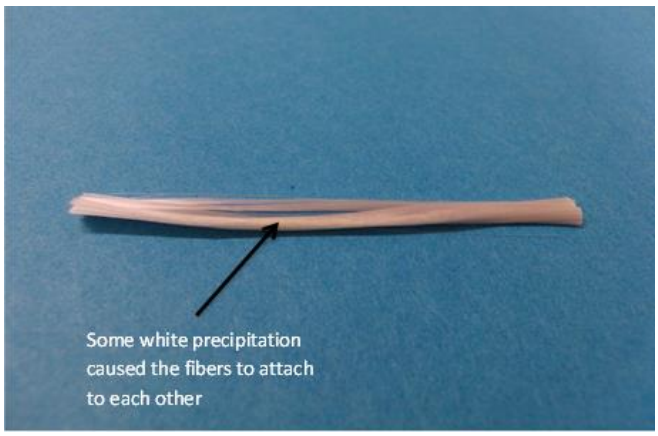

Figure 21. Problem-causing precipitation on a glass fiber roving.

The nozzle was replaced by a new one after studying the effect of the light intensity and speed with oven and without oven post-curing. The new nozzle did not fit perfectly into the nozzle holder and some tape was used to get better fitting. Also the light-curing lamps from the right-hand side gutter broke down at the same time and the rest of the studies were carried out using the left-hand side gutter. The temperatures of the two gutter-ovens were tested using an RMS multimeter and the light intensities were checked with a dental LED radiometer. The temperatures were measured from the middle of the gutter (120 °C, 60 min) and the light intensities by pressing the lamps one by one against the radiometer detector. The two gutters and the old and the new nozzle were also compared by manufacturing some poles and comparing the test results.

The poles that were manufactured at a speed of 2 mm/s and at light intensities 3 and 4 needed some extra procedures. The nozzle and the nozzle holder were lifted 3 mm further up than with other groups. This was because otherwise the pole would have been cured onto the nozzle and the system would have got stuck (Figure 22).

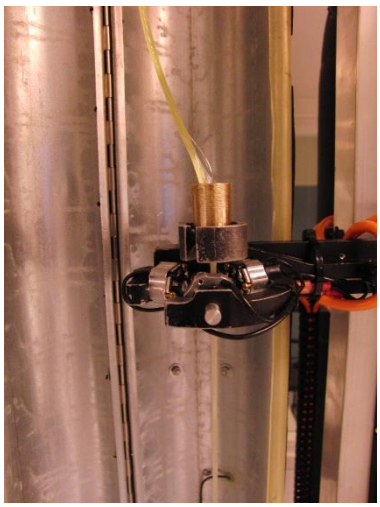

Figure 22. A problem with low speed and high light intensity.

Also high speeds (7 and 8 mm/s) and low light intensity (1/4) without post-curing caused some problems. The poles were really soft and wet when removed from the device. They were cured and hardened when stored on a table overnight. The group with light intensity 1/4 and speed 8 mm/s without oven was left undone because of this problem.

Some test-milling was done to the manufactured poles (Figures 23 and 24). The milling process was carried out by using a ZirkonZahn CAD/CAM milling system.

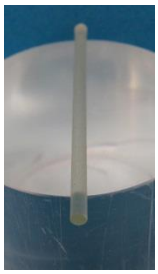

Figure 23. Manufactured FRC pole.

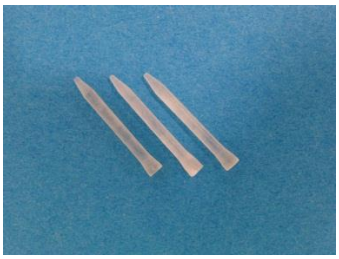

Figure 24. Test-milled root canal posts.

10 RESULTS

10.1 Light intensity and speed with oven post-curing

The test specimens were prepared using a nozzle with a diameter of 2.7 mm and 10.3 kg of pre-tensioning weight. Post-curing was performed at 120 °C for 60 min. The average length of the prepared poles was 152 cm (min 123 cm and max 177 cm) and the diameter varied from 2.65 mm to 2.70 mm, the average being 2.68 mm. The three-point bending test results are listed below (Tables 4-9 and Figures 25-30). The raw data for all the studies can be found in Appendix 1.

Table 4. Max bending stress and Young's modulus by light intensity after oven post-curing.

Group		Max bending stress at max load (MPa)	SD (MPa)	Young's modulus (GPa)	SD (GPa)
1/4	2 mm/s	1470,0	71,2	51,7	1,2
	3 mm/s	1253,1	56,5	49,6	1,8
	4 mm/s	1304,9	65,4	48,2	2,6
	5 mm/s	1262,7	127,2	46,5	1,4
	6 mm/s	1137,1	93,7	46,5	3,4
	7 mm/s	1211,9	73,4	45,1	1,8
	8 mm/s	1191,7	49,4	44,3	1,9
2/4	2 mm/s	1409,0	88,6	50,2	1,7
	3 mm/s	1430,0	76,2	49,2	2,3
	4 mm/s	1381,6	88,1	47,6	1,6
	5 mm/s	1327,1	60,4	50,0	1,8
	6 mm/s	1271,5	53,4	46,7	1,3
	7 mm/s	1227,9	98,8	49,9	1,3
	8 mm/s	1139,5	72,3	46,2	3,7
3/4	2 mm/s	1190,8	48,0	51,7	3,0
	3 mm/s	1363,9	96,0	52,3	1,5
	4 mm/s	1320,0	112,5	52,4	1,6
	5 mm/s	1214,8	115,0	48,6	1,3
	6 mm/s	1211,0	109,4	50,0	2,0
	7 mm/s	1216,8	71,2	49,4	3,1
	8 mm/s	1182,9	92,8	45,2	0,9
4/4	2 mm/s	1219,2	90,9	52,5	0,7
	3 mm/s	1187,0	55,1	50,9	1,8
	4 mm/s	1046,1	60,7	52,4	2,8
	5 mm/s	1010,1	98,7	41,2	3,2
	6 mm/s	952,7	93,0	40,5	3,6
	7 mm/s	910,0	151,2	30,9	8,5
	8 mm/s	913,0	82,4	33,4	2,5

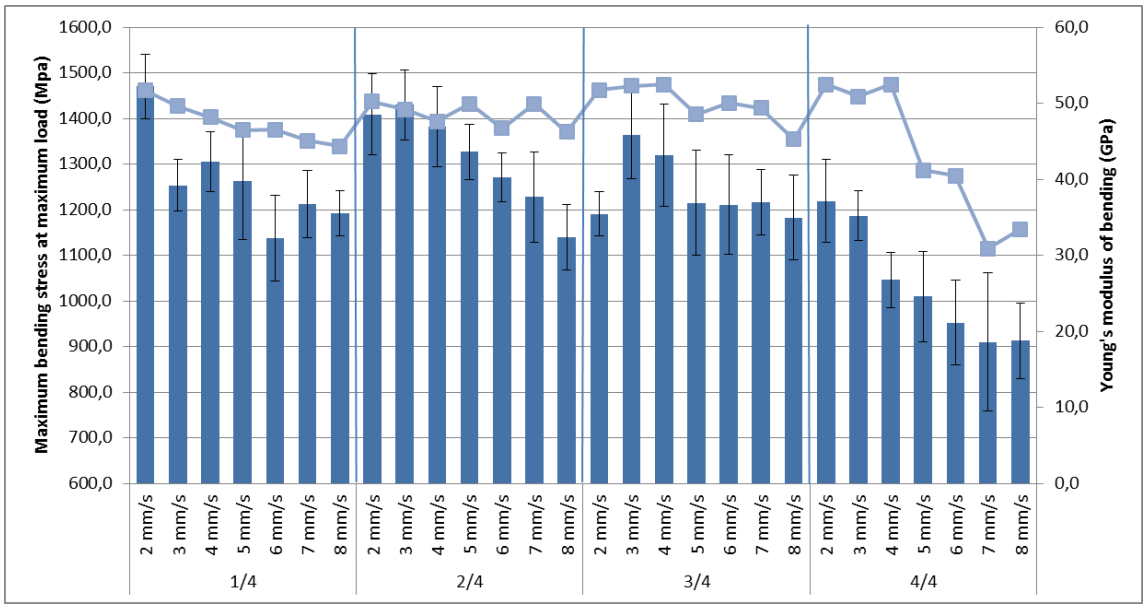

Figure 25. Max bending stress (bar) and Young's modulus (line) by light intensity after oven post-curing.

Table 5. Max bending stress and Young's modulus by speed after oven post-curing.

Group		Max bending stress at max load (MPa)	SD (MPa)	Young's modulus (GPa)	SD (GPa)
2 mm/	1/4	1470,0	71,2	51,7	1,2
	2/4	1409,0	88,6	50,2	1,7
	3/4	1190,8	48,0	51,7	3,0
	4/4	1219,2	90,9	52,5	0,7
3 mm/	1/4	1253,1	56,5	49,6	1,8
	2/4	1430,0	76,2	49,2	2,3
	3/4	1363,9	96,0	52,3	1,5
	4/4	1187,0	55,1	50,9	1,8
4 mm/	1/4	1304,9	65,4	48,2	2,6
	2/4	1381,6	88,1	47,6	1,6
	3/4	1320,0	112,5	52,4	1,6
	4/4	1046,1	60,7	52,4	2,8
5 mm/	1/4	1262,7	127,2	46,5	1,4
	2/4	1327,1	60,4	50,0	1,8
	3/4	1214,8	115,0	48,6	1,3
	4/4	1010,1	98,7	41,2	3,2
6 mm/	1/4	1137,1	93,7	46,5	3,4
	2/4	1271,5	53,4	46,7	1,3
	3/4	1211,0	109,4	50,0	2,0
	4/4	952,7	93,0	40,5	3,6
7 mm/	1/4	1211,9	73,4	45,1	1,8
	2/4	1227,9	98,8	49,9	1,3
	3/4	1216,8	71,2	49,4	3,1
	4/4	910,0	151,2	30,9	8,5
8 mm/	1/4	1191,7	49,4	44,3	1,9
	2/4	1139,5	72,3	46,2	3,7
	3/4	1182,9	92,8	45,2	0,9
	4/4	913,0	82,4	33,4	2,5

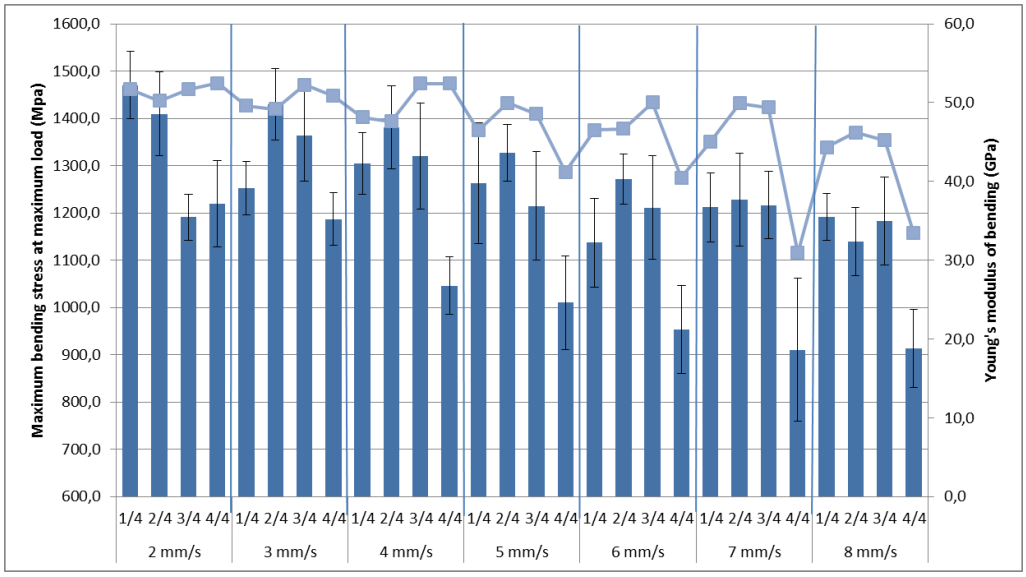

Figure 26. Max bending stress (bar) and Young's modulus (line) by speed after oven post-curing.

Table 6. Max load by light intensity after oven post-curing.

Group		Load at Maximum Load (N)	SD (N)
1/4	2 mm/s	225,5	11,0
	3 mm/s	193,7	8,3
	4 mm/s	199,7	8,1
	5 mm/s	192,0	18,7
	6 mm/s	169,0	14,0
	7 mm/s	182,3	8,8
	8 mm/s	177,2	8,1
2/4	2 mm/s	211,8	12,9
	3 mm/s	217,4	10,8
	4 mm/s	205,9	12,8
	5 mm/s	203,7	8,0
	6 mm/s	195,0	9,0
	7 mm/s	188,9	14,0
	8 mm/s	173,2	10,8
3/4	2 mm/s	181,7	6,8
	3 mm/s	208,5	14,8
	4 mm/s	201,6	18,0
	5 mm/s	182,3	16,8
	6 mm/s	186,0	16,8
	7 mm/s	184,0	11,3
	8 mm/s	179,1	13,7
4/4	2 mm/s	180,7	12,3
	3 mm/s	181,2	8,2
	4 mm/s	158,1	9,2
	5 mm/s	151,9	14,9
	6 mm/s	143,3	15,0
	7 mm/s	135,7	23,1
	8 mm/s	133,4	12,0

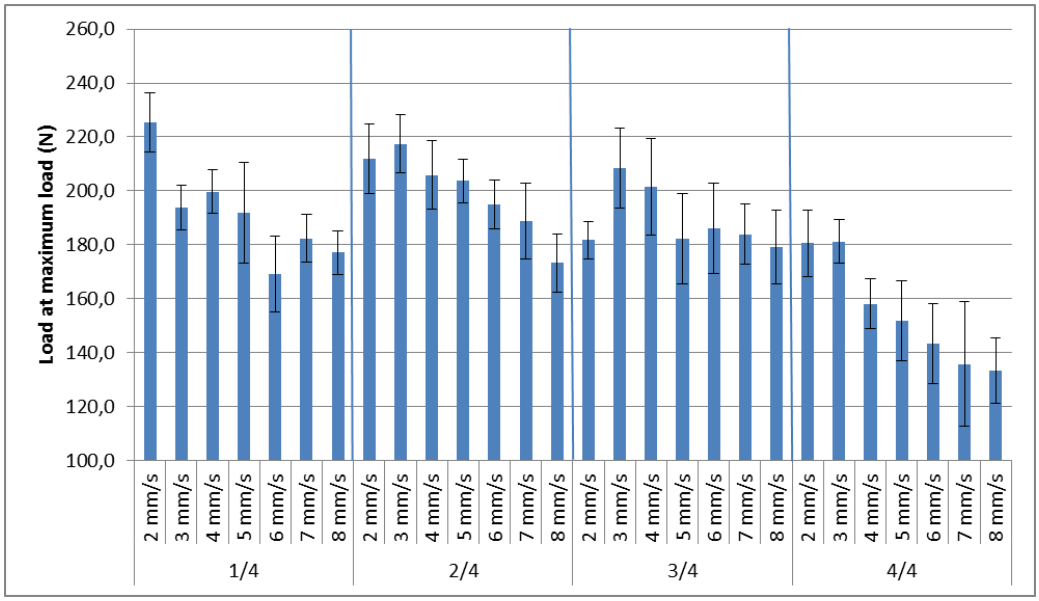

Figure 27. Max load by light intensity after oven post-curing.

Table 7. Max load by speed after oven post-curing.

Group		Load at Maximum Load (N)	SD (N)
2 mm/s	**1/4**	225,5	11,0
	2/4	211,8	12,9
	3/4	181,7	6,8
	4/4	180,7	12,3
3 mm/s	**1/4**	193,7	8,3
	2/4	217,4	10,8
	3/4	208,5	14,8
	4/4	181,2	8,2
4 mm/s	**1/4**	199,7	8,1
	2/4	205,9	12,8
	3/4	201,6	18,0
	4/4	158,1	9,2
5 mm/s	**1/4**	192,0	18,7
	2/4	203,7	8,0
	3/4	182,3	16,8
	4/4	151,9	14,9
6 mm/s	**1/4**	169,0	14,0
	2/4	195,0	9,0
	3/4	186,0	16,8
	4/4	143,3	15,0
7 mm/s	**1/4**	182,3	8,8
	2/4	188,9	14,0
	3/4	184,0	11,3
	4/4	135,7	23,1
8 mm/s	**1/4**	177,2	8,1
	2/4	173,2	10,8
	3/4	179,1	13,7
	4/4	133,4	12,0

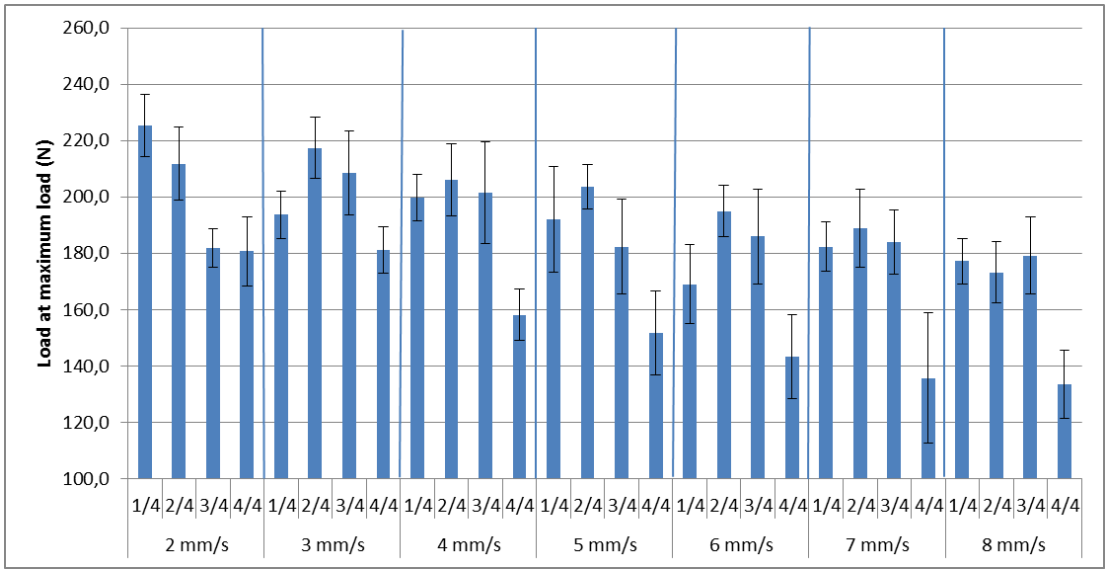

Figure 28. Max load by speed after oven post-curing.

Table 8. Work by intensity after oven post-curing.

Group		Work from preload to Break (Ncm)	SD (Ncm)
1/4	2 mm/s	85,7	18,1
	3 mm/s	86,1	29,0
	4 mm/s	119,0	34,4
	5 mm/s	104,6	21,9
	6 mm/s	96,2	27,2
	7 mm/s	80,9	16,7
	8 mm/s	93,3	28,8
2/4	2 mm/s	143,7	20,7
	3 mm/s	112,0	16,4
	4 mm/s	135,1	33,5
	5 mm/s	105,5	24,3
	6 mm/s	106,5	25,0
	7 mm/s	94,5	18,6
	8 mm/s	91,8	25,3
3/4	2 mm/s	74,3	5,4
	3 mm/s	123,0	16,2
	4 mm/s	97,4	22,1
	5 mm/s	98,6	30,5
	6 mm/s	102,2	14,4
	7 mm/s	94,9	18,6
	8 mm/s	102,1	24,8
4/4	2 mm/s	86,0	11,6
	3 mm/s	98,7	23,6
	4 mm/s	79,6	20,8
	5 mm/s	79,0	21,0
	6 mm/s	72,3	11,8
	7 mm/s	81,8	8,8
	8 mm/s	69,6	16,4

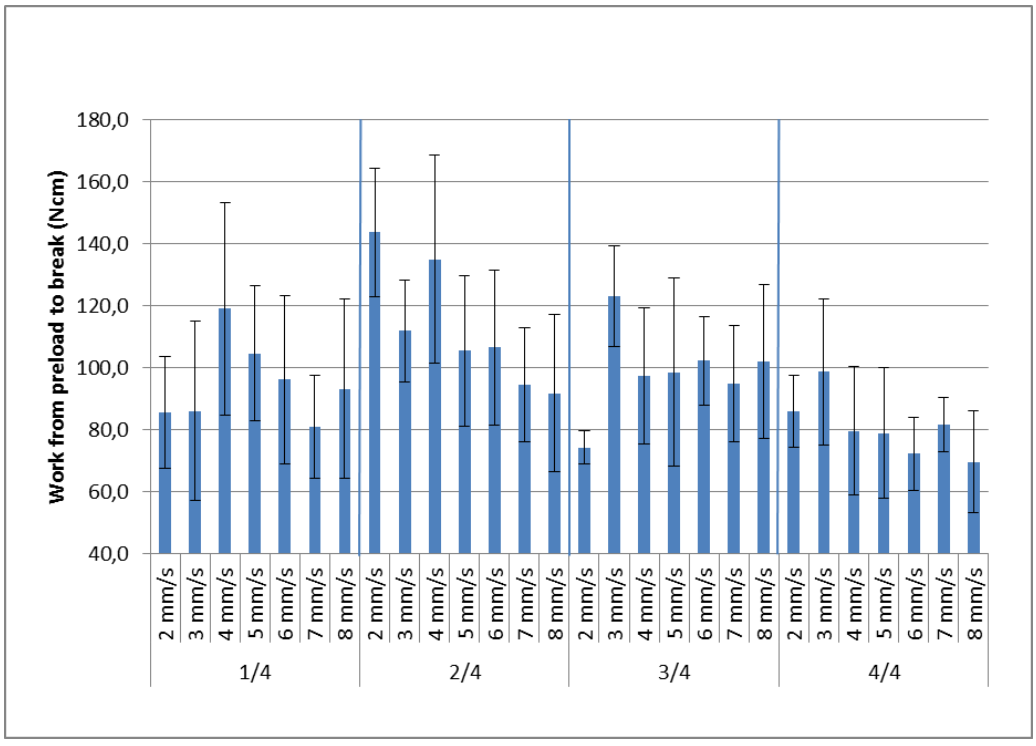

Figure 29. Work by intensity after oven post-curing.

Table 9. Work by speed after oven post-curing.

Group		Work from preload to Break (Ncm)	SD (Ncm)
2 mm/s	1/4	85,7	18,1
	2/4	143,7	20,7
	3/4	74,3	5,4
	4/4	86,0	11,6
3 mm/s	1/4	86,1	29,0
	2/4	112,0	16,4
	3/4	123,0	16,2
	4/4	98,7	23,6
4 mm/s	1/4	119,0	34,4
	2/4	135,1	33,5
	3/4	97,4	22,1
	4/4	79,6	20,8
5 mm/s	1/4	119,0	34,4
	2/4	135,1	33,5
	3/4	97,4	22,1
	4/4	79,6	20,8
6 mm/s	1/4	96,2	27,2
	2/4	106,5	25,0
	3/4	102,2	14,4
	4/4	72,3	11,8
7 mm/s	1/4	80,9	16,7
	2/4	94,5	18,6
	3/4	94,9	18,6
	4/4	81,8	8,8
8 mm/s	1/4	93,3	28,8
	2/4	91,8	25,3
	3/4	102,1	24,8
	4/4	69,6	16,4

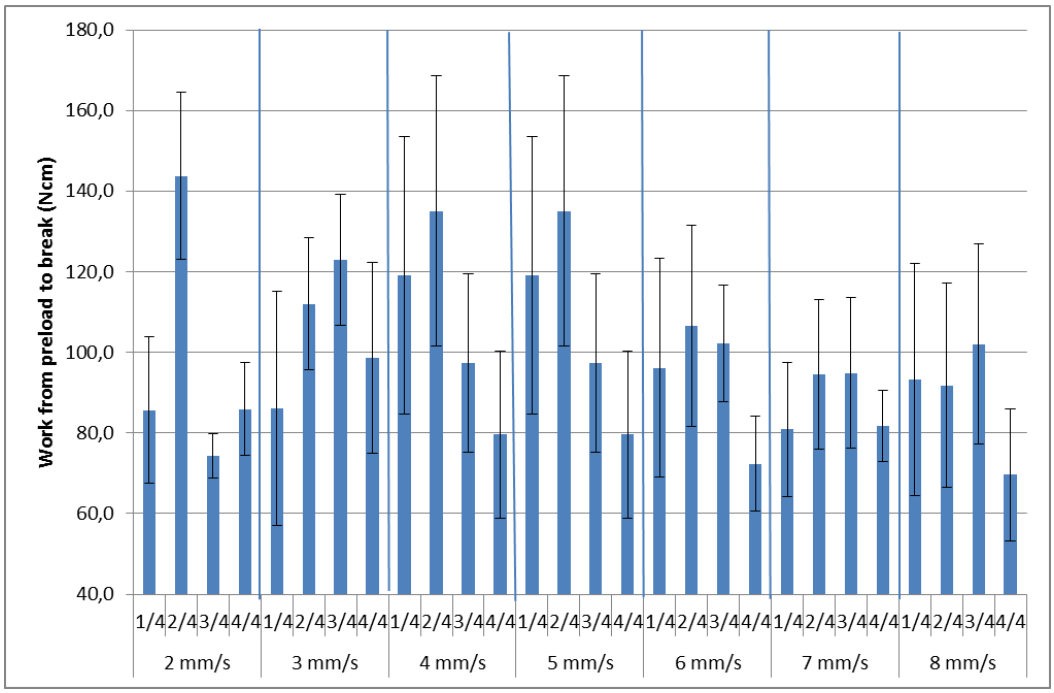

Figure 30. Work by speed after oven post-curing.

The manufactured poles were also studied by SEM imaging (Scanning Electron Microscope, JEOL, Japan) to see the distribution of the fibers and the possible air bubbles (Figure 31). The white lining on the edge may refer to an oxygen inhibition layer (Figure 32).

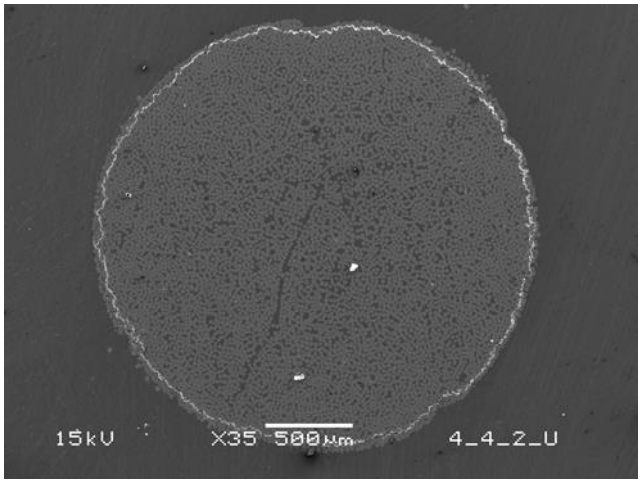

Figure 31. SEM image of the pole cross-section.

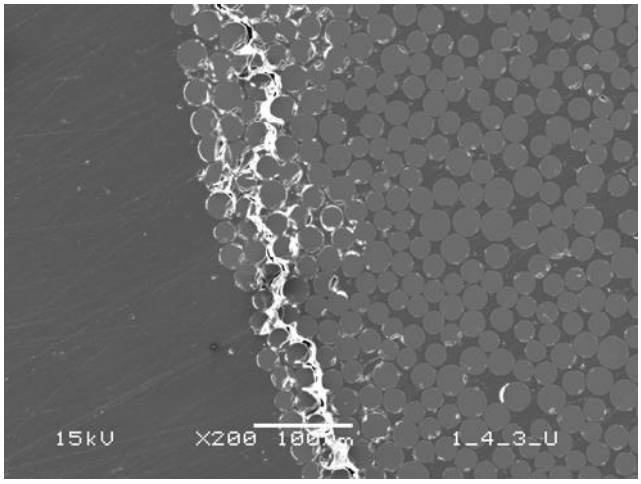

Figure 32. Magnification of the surface area.

10.2 Light intensity and speed without oven post-curing

The test specimens were prepared by using a nozzle with a diameter size of 2.7 mm and 10.3 kg of pre-tensioning weight. The average length of the prepared poles was 158 cm (min 125 cm and max 169 cm) and the diameter varied from 2.57 mm to 2.70 mm, the average being 2.67 mm. The three-point bending test results are listed below (Tables 10-15 and Figures 33-38).

Table 10. Max bending stress and Young's modulus by light intensity without oven post-curing.

Group		Maximum bending stress at maximum load (MPa)	SD (MPa)	Young's modulus of bending (GPa)	SD (GPa)
1/4	2 mm/s	1208,4	74,0	46,4	0,8
	3 mm/s	1026,7	86,7	37,4	1,0
	4 mm/s	1051,6	89,9	36,2	3,6
	5 mm/s	863,0	164,5	27,3	3,3
	6 mm/s	873,8	80,5	30,9	3,1
	7 mm/s	866,3	88,4	28,0	4,9
	8 mm/s				
2/4	2 mm/s	1175,8	65,6	49,9	3,6
	3 mm/s	1095,9	119,6	47,5	5,8
	4 mm/s	990,4	114,9	44,2	5,9
	5 mm/s	1105,3	78,9	38,3	3,6
	6 mm/s	1184,2	96,2	42,3	2,5
	7 mm/s	1001,4	55,7	37,3	5,8
	8 mm/s	996,3	61,8	35,2	4,0
3/4	2 mm/s	1231,2	56,0	52,2	3,4
	3 mm/s	1192,2	72,5	46,4	2,7
	4 mm/s	1083,6	76,7	46,7	2,3
	5 mm/s	1079,6	93,9	39,4	2,6
	6 mm/s	1005,8	42,8	36,7	1,7
	7 mm/s	1006,7	109,2	38,6	4,1
	8 mm/s	863,2	57,1	30,9	3,7
4/4	2 mm/s	1140,3	86,2	50,4	2,3
	3 mm/s	1156,5	76,2	47,9	3,5
	4 mm/s	1146,3	50,7	48,4	3,3
	5 mm/s	1101,9	54,4	40,8	3,6
	6 mm/s	928,6	71,5	34,1	3,4
	7 mm/s	939,0	88,2	35,3	3,5
	8 mm/s	920,0	64,0	32,9	4,2

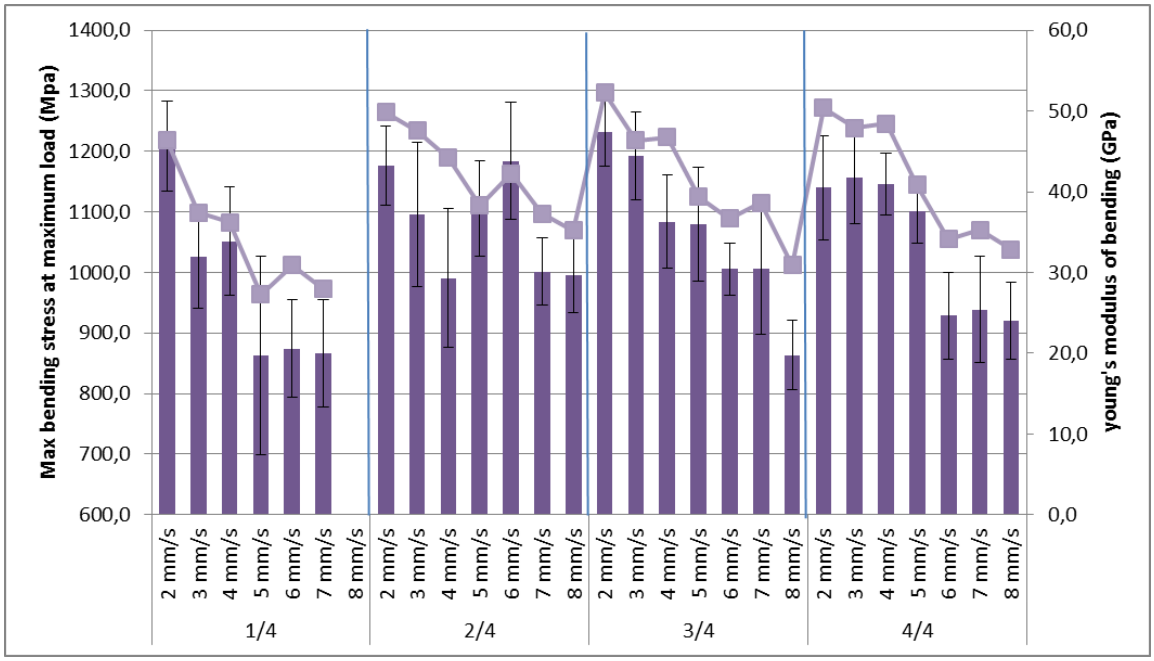

Figure 33. Max bending stress (bar) and Young's modulus (line) by light intensity without oven post-curing.

Table 11. Max bending stress and Young's modulus by speed without oven post-curing.

Group		Maximum bending stress at maximum load (MPa)	SD (MPa)	Young's modulus of bending (GPa)	SD (GPa)
2 mm/s	1/4	1208,4	74,0	46,4	0,8
	2/4	1175,8	65,6	49,9	3,6
	3/4	1231,2	56,0	52,2	3,4
	4/4	1140,3	86,2	50,4	2,3
3 mm/s	1/4	1026,7	86,7	37,4	1,0
	2/4	1095,9	119,6	47,5	5,8
	3/4	1192,2	72,5	46,4	2,7
	4/4	1156,5	76,2	47,9	3,5
4 mm/s	1/4	1051,6	89,9	36,2	3,6
	2/4	990,4	114,9	44,2	5,9
	3/4	1083,6	76,7	46,7	2,3
	4/4	1146,3	50,7	48,4	3,3
5 mm/s	1/4	863,0	164,5	27,3	3,3
	2/4	1105,3	78,9	38,3	3,6
	3/4	1079,6	93,9	39,4	2,6
	4/4	1101,9	54,4	40,8	3,6
6 mm/s	1/4	873,8	80,5	30,9	3,1
	2/4	1184,2	96,2	42,3	2,5
	3/4	1005,8	42,8	36,7	1,7
	4/4	928,6	71,5	34,1	3,4
7 mm/s	1/4	866,3	88,4	28,0	4,9
	2/4	1001,4	55,7	37,3	5,8
	3/4	1006,7	109,2	38,6	4,1
	4/4	939,0	88,2	35,3	3,5
8 mm/s	1/4				
	2/4	996,3	61,8	35,2	4,0
	3/4	863,2	57,1	30,9	3,7
	4/4	920,0	64,0	32,9	4,2

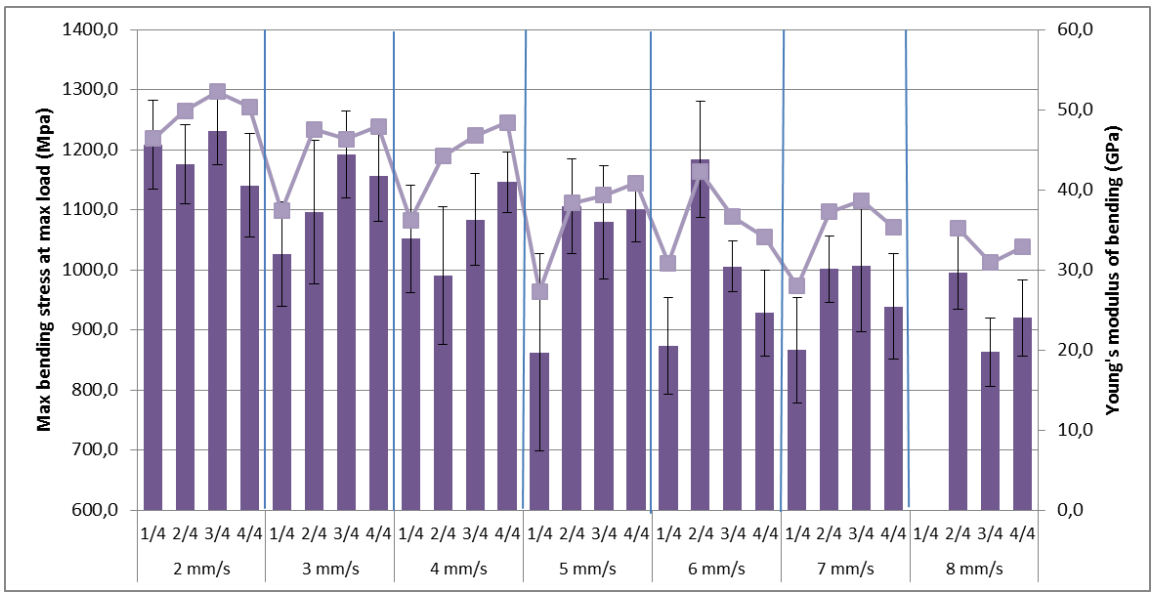

Figure 34. Max bending stress (bar) and Young's modulus (line) by speed without oven post-curing.

Table 12. Max load by light intensity without oven post-curing.

Group		Load at Maximum Load (N)	SD (N)
1/4	2 mm/s	185,0	9,9
	3 mm/s	156,5	13,7
	4 mm/s	153,5	12,3
	5 mm/s	126,4	23,9
	6 mm/s	116,7	10,6
	7 mm/s	125,7	16,1
	8 mm/s		
2/4	2 mm/s	178,8	8,3
	3 mm/s	167,2	17,0
	4 mm/s	138,3	16,4
	5 mm/s	167,8	9,0
	6 mm/s	183,1	12,2
	7 mm/s	148,8	10,2
	8 mm/s	148,9	8,3
3/4	2 mm/s	187,2	8,3
	3 mm/s	178,9	10,0
	4 mm/s	165,0	12,2
	5 mm/s	153,3	11,9
	6 mm/s	152,0	5,3
	7 mm/s	155,2	17,2
	8 mm/s	129,1	9,1
4/4	2 mm/s	173,1	12,6
	3 mm/s	178,5	12,0
	4 mm/s	176,0	7,8
	5 mm/s	162,9	8,1
	6 mm/s	138,2	10,3
	7 mm/s	138,3	13,1
	8 mm/s	127,4	9,0

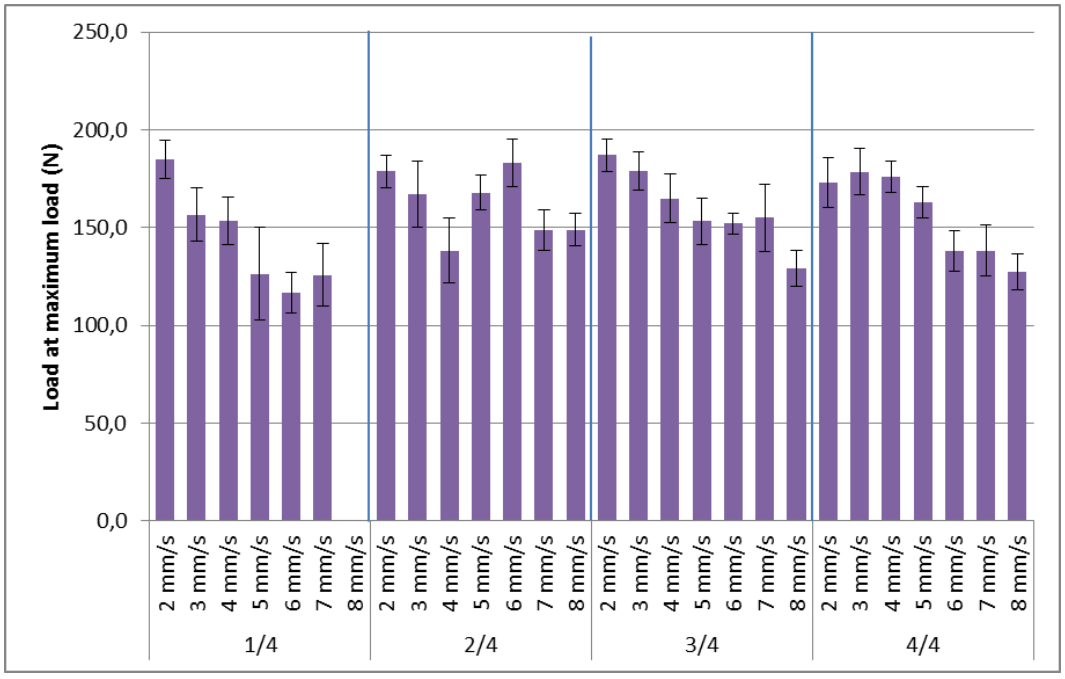

Figure 35. Max load by light intensity without oven post-curing.

Table 13. Max load by speed without oven post-curing.

Group		Load at Maximum Load (N)	SD (N)
2 mm/s	1/4	185,0	9,9
	2/4	178,8	8,3
	3/4	187,2	8,3
	4/4	173,1	12,6
3 mm/s	1/4	156,5	13,7
	2/4	167,2	17,0
	3/4	178,9	10,0
	4/4	178,5	12,0
4 mm/s	1/4	153,5	12,3
	2/4	138,3	16,4
	3/4	165,0	12,2
	4/4	176,0	7,8
5 mm/s	1/4	126,4	23,9
	2/4	167,8	9,0
	3/4	153,3	11,9
	4/4	162,9	8,1
6 mm/s	1/4	116,7	10,6
	2/4	183,1	12,2
	3/4	152,0	5,3
	4/4	138,2	10,3
7 mm/s	1/4	125,7	16,1
	2/4	148,8	10,2
	3/4	155,2	17,2
	4/4	138,3	13,1
8 mm/s	1/4		
	2/4	148,9	8,3
	3/4	129,1	9,1
	4/4	127,4	9,0

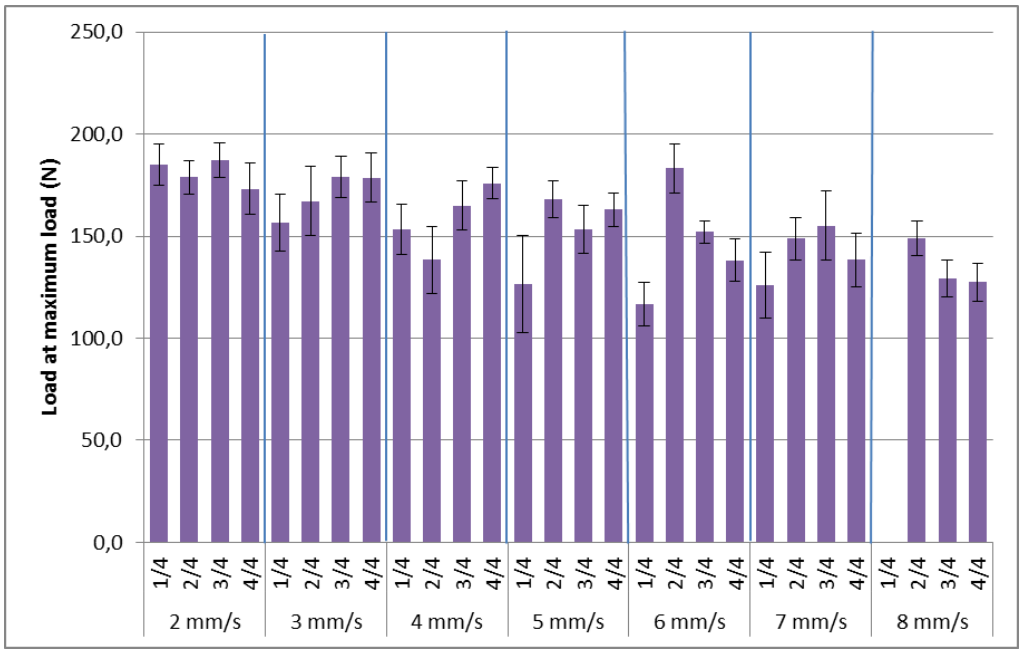

Figure 36. Max load by speed without oven post-curing.

Table 14. Work by light intensity without oven post-curing.

Group		Work from preload to Break (Ncm)	SD (Ncm)
1/4	2 mm/s	110,4	24,0
	3 mm/s	90,0	20,8
	4 mm/s	112,9	19,6
	5 mm/s	84,0	35,3
	6 mm/s	99,4	13,7
	7 mm/s	90,3	17,8
	8 mm/s		
2/4	2 mm/s	82,0	22,9
	3 mm/s	102,0	37,1
	4 mm/s	65,9	10,9
	5 mm/s	108,0	15,3
	6 mm/s	107,8	16,5
	7 mm/s	91,3	13,4
	8 mm/s	83,2	8,3
3/4	2 mm/s	77,8	13,5
	3 mm/s	102,7	19,1
	4 mm/s	79,1	18,6
	5 mm/s	105,0	20,0
	6 mm/s	75,1	12,7
	7 mm/s	72,6	4,7
	8 mm/s	73,5	13,1
4/4	2 mm/s	71,5	10,9
	3 mm/s	93,3	15,1
	4 mm/s	79,4	10,7
	5 mm/s	99,6	7,1
	6 mm/s	72,1	8,0
	7 mm/s	69,1	11,9
	8 mm/s	66,4	11,7

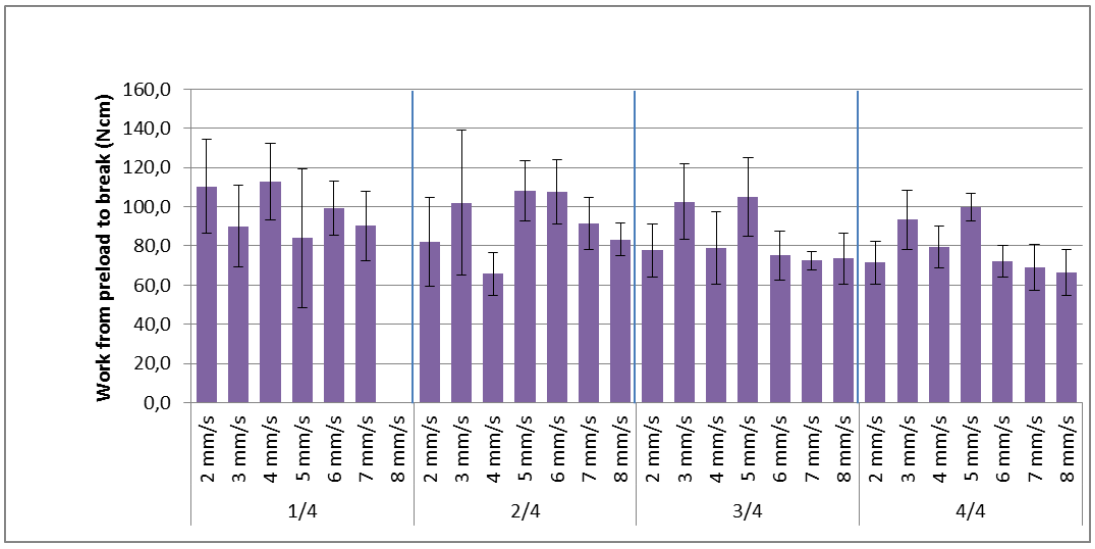

Figure 37. Work by light intensity without oven post-curing.

Table 15. Work by speed without oven post-curing.

Group		Work from preload to Break (Ncm)	SD (Ncm)
2 mm/s	1/4	110,4	24,0
	2/4	82,0	22,9
	3/4	77,8	13,5
	4/4	71,5	10,9
3 mm/s	1/4	90,0	20,8
	2/4	102,0	37,1
	3/4	102,7	19,1
	4/4	93,3	15,1
4 mm/s	1/4	112,9	19,6
	2/4	65,9	10,9
	3/4	79,1	18,6
	4/4	79,4	10,7
5 mm/s	1/4	84,0	35,3
	2/4	108,0	15,3
	3/4	105,0	20,0
	4/4	99,6	7,1
6 mm/s	1/4	99,4	13,7
	2/4	107,8	16,5
	3/4	75,1	12,7
	4/4	72,1	8,0
7 mm/s	1/4	90,3	17,8
	2/4	91,3	13,4
	3/4	72,6	4,7
	4/4	69,1	11,9
8 mm/s	1/4		
	2/4	83,2	8,3
	3/4	73,5	13,1
	4/4	66,4	11,7

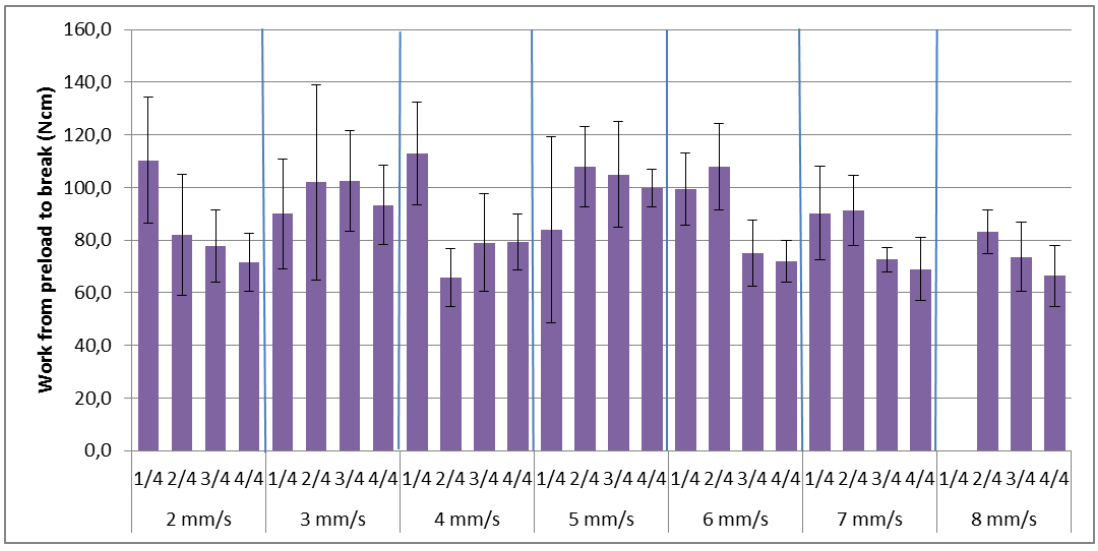

Figure 38. Work by speed without oven post-curing.

10.3 The effect of pre-tensioning

The test specimens were prepared by using a nozzle diameter size of 2.7 mm and different pre-tensioning weights (Table 16). The used light intensity was 1/4 and the speed was 2 mm/s. The prepared poles were post-cured at 120 °C for 60 min. The three-point bending test results are listed below (Tables 17-19 and Figures 39-41).

Table 16. Pre-tensioning weights.

Pretension	Weight (kg)	Tension (N)
1	3,4	33,6
2	7,0	68,6
3	10,3	100,8
4	13,5	132,5
5	17,0	166,7

Table 17. Max bending stress and Young's modulus by pre-tension.

Group	Maximum bending stress at maximum load (MPa)	SD (MPa)	Young's modulus (GPa)	SD (GPa)
pretension_1	1020,3	92,4	49,0	3,2
pretension_2	1111,7	72,5	48,7	1,4
pretension_3	1094,0	65,7	51,0	51,0
pretension_4	1048,6	76,2	51,6	51,6
pretension_5	1024,4	61,9	48,6	48,6

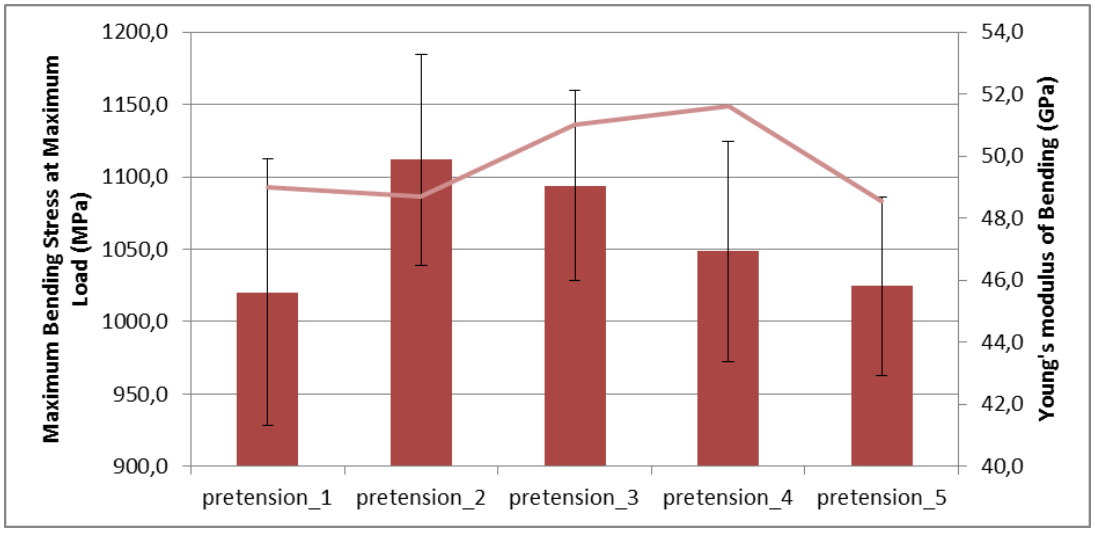

Figure 39. Max bending stress (bar) and Young's modulus (line) by pretension.

Table 18. Max load by pre-tension.

Group	Load at max Load (N)	SD (N)
pretension_1	155,7	13,6
pretension_2	171,8	11,0
pretension_3	169,6	10,2
pretension_4	154,7	9,8
pretension_5	159,9	9,8

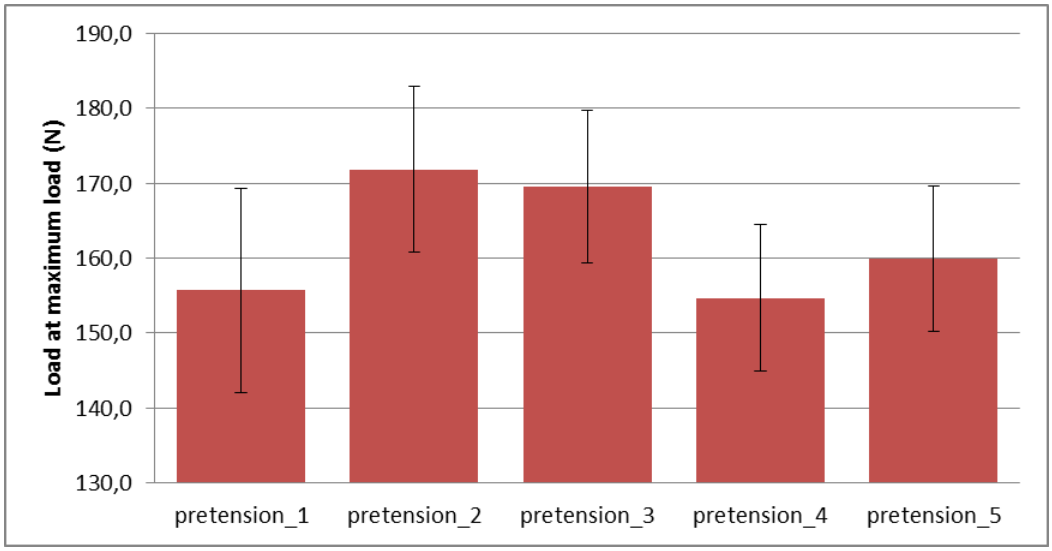

Figure 40. Max load by pre-tension.

Table 19. Work by pre-tension.

Group	Work from preload to break (Ncm)	SD (Ncm)
pretension_1	59,6	10,6
pretension_2	70,3	7,1
pretension_3	57,2	10,6
pretension_4	62,3	17,7
pretension_5	53,3	7,6

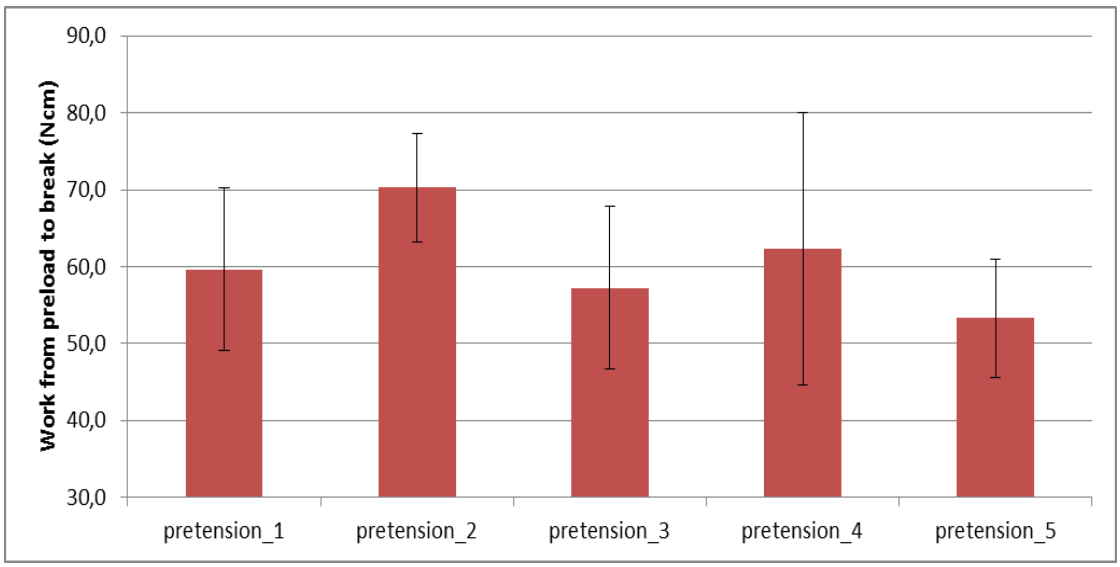

Figure 41. Work by pre-tension.

10.4 The effect of post-curing

The test specimens were prepared by using a nozzle diameter size of 2.7 mm and a pre-tensioning weight of 10.3 kg. The used light intensity was 1/4 and the speed was 2 mm/s. The prepared poles were post-cured at 100 °C, 120 °C and 130 °C for 15 min, 30 min and 60 min. The three-point bending test results are listed below (Tables 20-22 and Figures 42-44).

Table 20. Max bending stress and Young's modulus by post-curing.

Temperature (C)	Time (min)	Maximum Bending Stress at Maximum Load (MPa)	SD (MPa)	Young's Modulus Of Bending (GPa)	SD (GPa)
RT	0 min	840,2	61,3	44992,0	3038,4
100 C	15 min	987,5	81,4	46558,8	1847,4
	30 min	954,9	54,8	42695,1	1268,8
	60 min	1022,7	52,0	44811,6	1986,6
120 C	15 min	1068,2	43,2	47245,3	2766,8
	30 min	1038,0	86,7	47963,0	1710,9
	60 min	1071,8	68,5	48491,6	949,6
130 C	15 min	944,4	72,1	48734,7	1450,5
	30 min	970,4	50,1	48830,5	1832,1
	60 min	1021,3	49,4	47931,8	3101,6

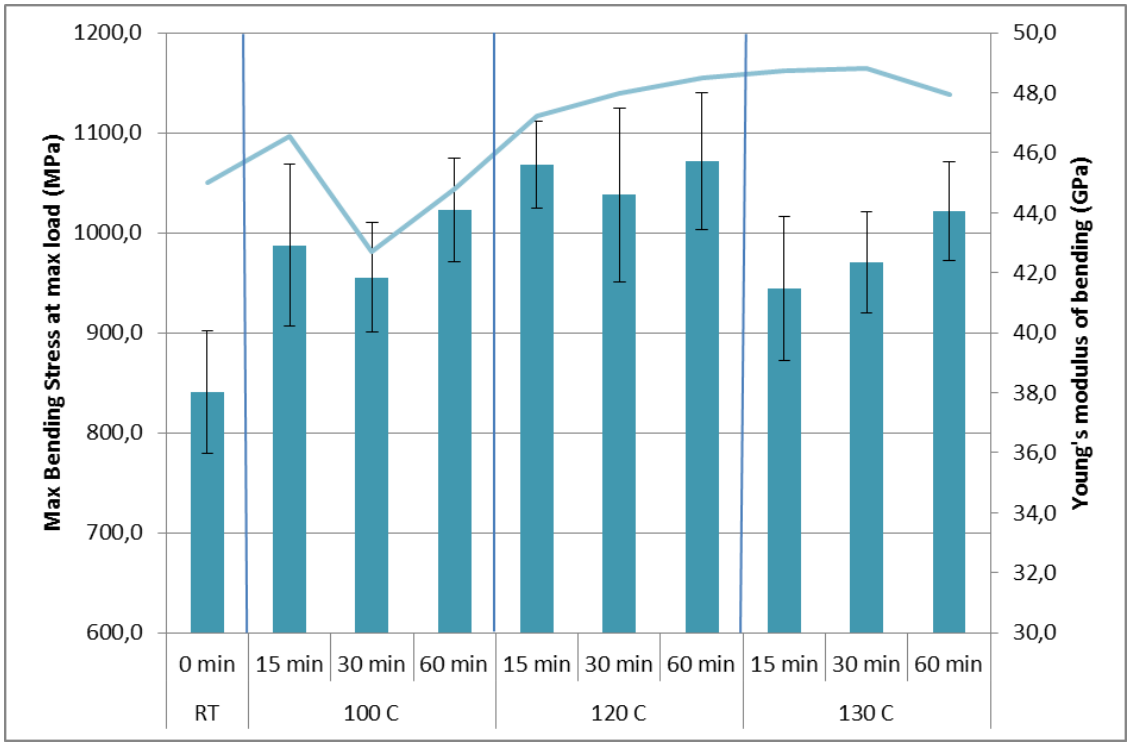

Figure 42. Max bending stress (bar) and Young's modulus (line) by post-curing.

Table 21. Max load by post-curing.

Temperature (C)	Time (min)	Load at Maximum Load (N)	SD (N)
RT	0 min	129,4	9,7
100 C	15 min	155,2	12,2
	30 min	148,6	8,2
	60 min	162,2	11,2
120 C	15 min	163,8	8,5
	30 min	161,6	13,2
	60 min	164,5	10,3
130 C	15 min	149,7	11,1
	30 min	153,2	8,6
	60 min	159,0	8,1

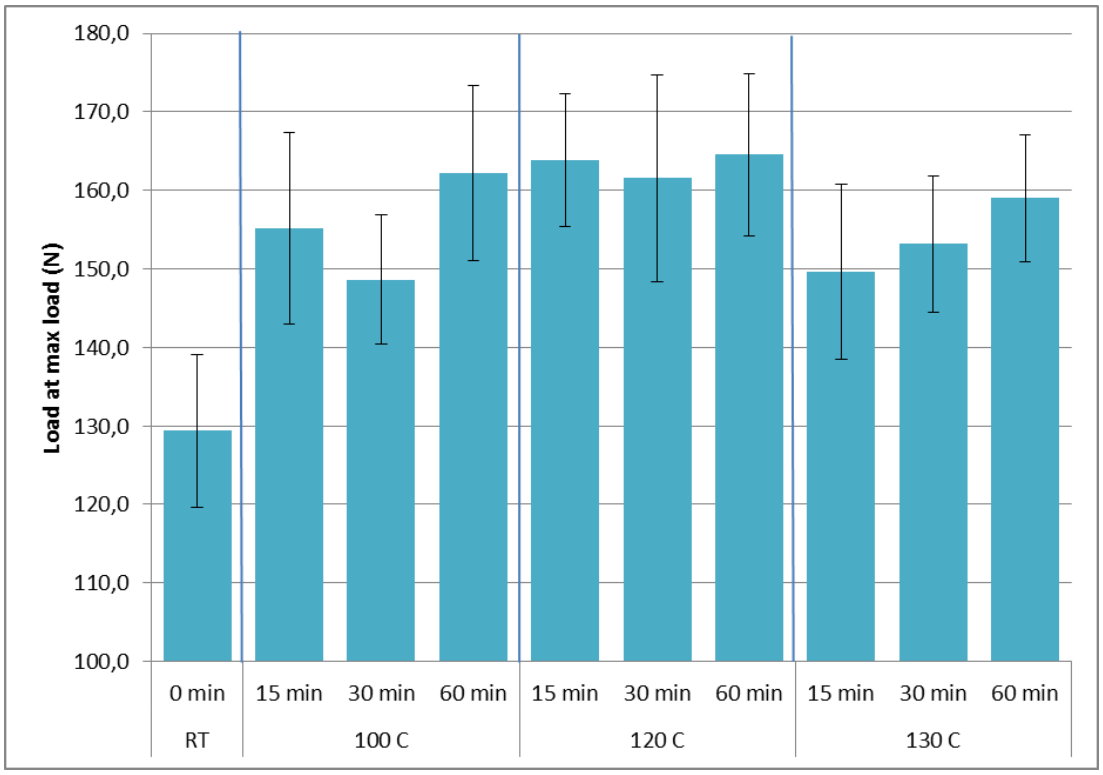

Figure 43. Max load by post-curing.

Table 22. Work by post-curing.

Temperature (C)	Time (min)	Work from preload to Break (Ncm)	SD (Ncm)
RT	0 min	43,4	5,1
100 C	15 min	54,0	15,8
	30 min	57,0	10,1
	60 min	67,9	13,6
120 C	15 min	65,5	18,1
	30 min	63,7	18,3
	60 min	60,6	16,8
130 C	15 min	56,1	15,4
	30 min	60,6	18,8
	60 min	74,5	11,0

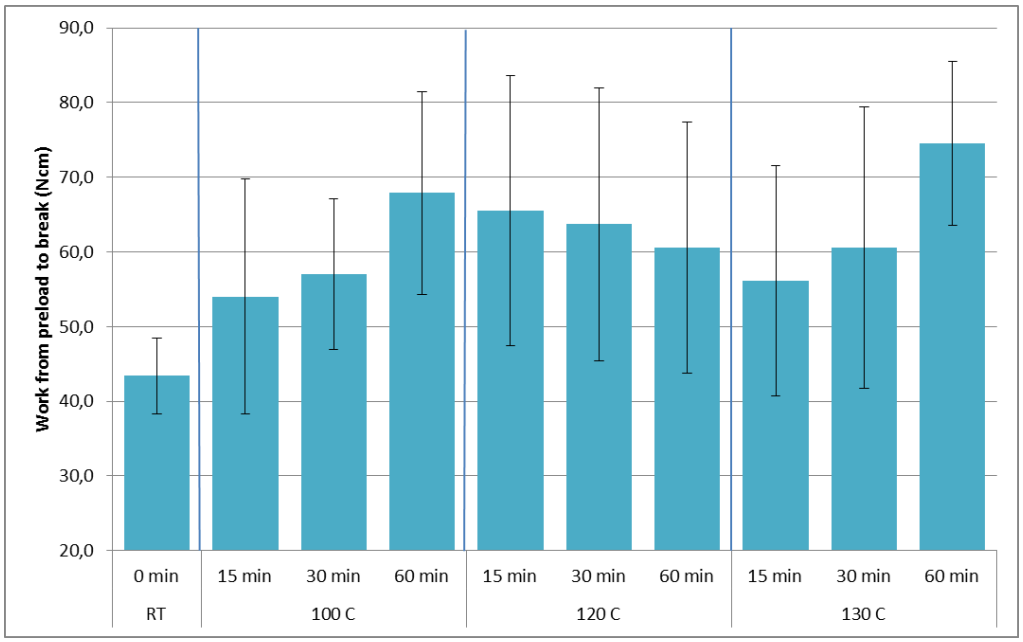

Figure 44. Work by post-curing.

10.5 The effect of the nozzle size

The test specimens were prepared by using a nozzle diameter sizes of 2.6 mm, 2.7 mm and 2.8 mm and a pre-tensioning weight of 10.3 kg. The used light intensity was 1/4 and the speed was 2 mm/s. The prepared poles were post-cured at 120 °C for 60 min. The diameters of the poles prepared with 2.6 mm nozzle had a minimum diameter of 2.68 mm and maximum diameter of 2.70 mm, the average being 2.69 mm. With 2.7 mm nozzle the minimum was 2.70 mm, maximum 2.73 and average 2.72 mm. With 2.8 mm nozzle diameters varied from 2.76 mm to 2.80 mm, the average was 2.78 mm. The three-point bending test results are listed below (Tables 23-25 and Figures 45-47).

Table 23. Max bending stress and Young's modulus by the nozzle size.

Group	Maximum Bending Stress at Maximum Load (MPa)	SD (MPa)	Young's Modulus Of Bending (GPa)	SD (GPa)
2,6 mm	1078,8	48,0	48,6	1,7
2,7 mm	1142,3	94,7	48,8	2,3
2,8 mm	1021,9	51,9	47,1	1,2

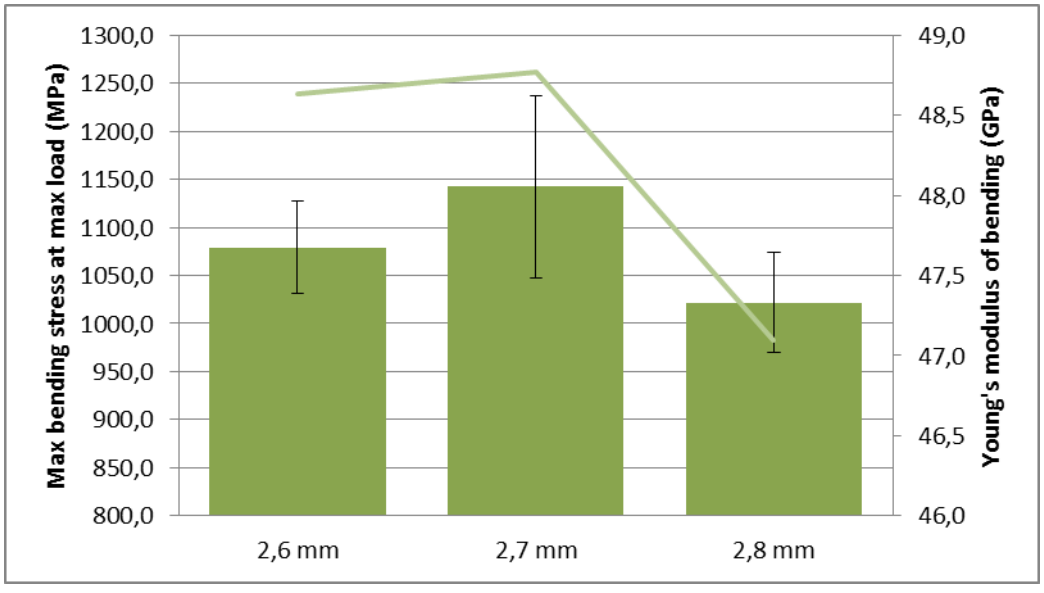

Figure 45. Max bending stress (bar) and Young's modulus (line) by nozzle size.

Table 24. Max load by nozzle size.

Group	Load at Maximum Load (N)	SD (N)
2,6 mm	164,9	6,7
2,7 mm	180,1	15,8
2,8 mm	172,4	7,9

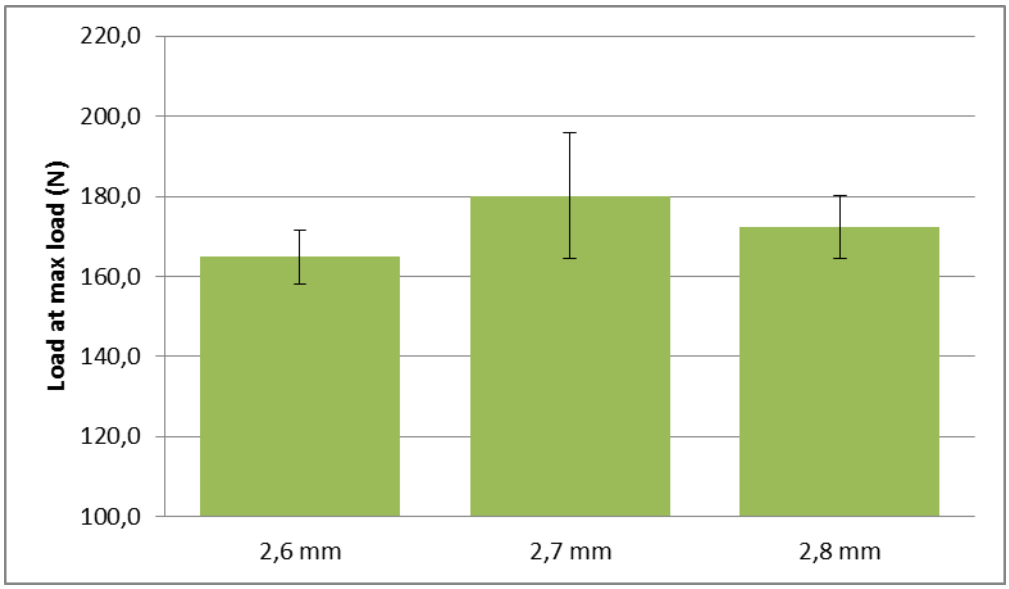

Figure 46. Max load by nozzle size.

Table 25. Work by nozzle size.

Group	Work from preload to Break (Ncm)	SD (Ncm)
2,6 mm	66,97	16,12
2,7 mm	81,35	9,38
2,8 mm	75,55	15,44

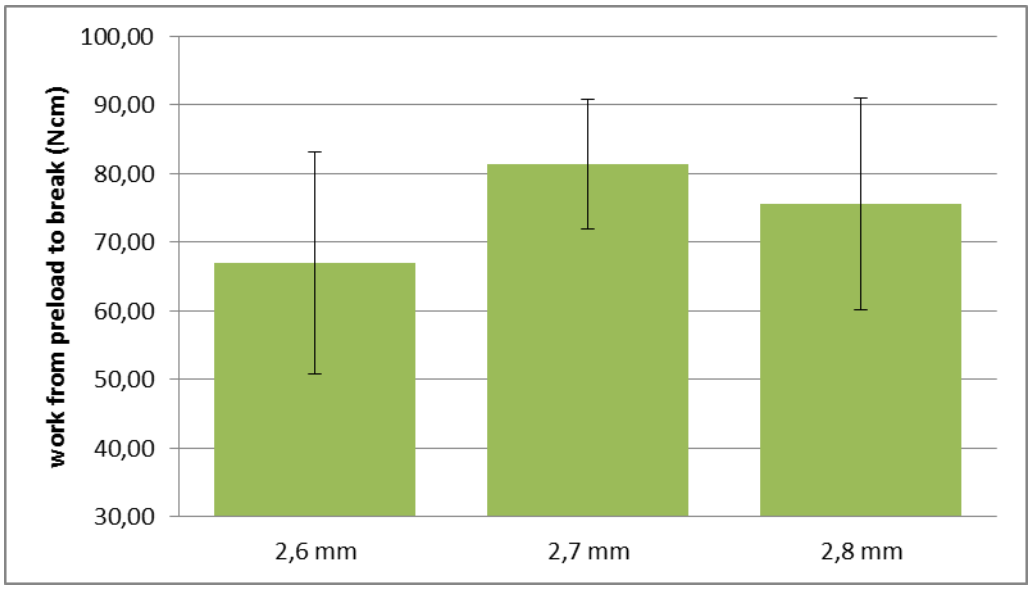

Figure 47. Work by nozzle size.

10.6 Oven and nozzle comparison and light intensity measurements

Because there was only one pole manufactured per test group, one group was chosen as a reference and was remade with every new study. There seemed to be a notable decrease in the test values of this reference group after changing the nozzle and the gutter side (Table 26). The two gutter-ovens were compared and some differences were detected in the heating temperatures (Figure 48). The right-hand side oven reached higher temperatures (max 144 °C) than the left-hand side oven (max 131 °C). There were also slight differences in measured light intensities between the sides (Table 27).

Table 26. Reference values.

Intensity	Speed	Nozzle size	Pretensioning			
1/4	2 mm/s	2,7 mm	10,3 kg			
Study	Max bending stress (MPa)	Young's modulus (MPa)	Max load (N)	Work (Ncm)		
1	1470	51700	226	86	Post-curing, right	Old nozzle
2	1208	46395	185	110	No post-curing	Old nozzle
3	1094	51009	170	57	Post-curing, left	New nozzle
4	840	44992	129	43	No post-curing	New nozzle
4	1072	48492	165	61	Post-curing, left	New nozzle
5	1142	48771	180	81	Post-curing, left	New nozzle
(6)	1224	49875	198	87	Post-curing, right	New nozzle
(6)	1329	50363	185	104	Post-curing, right	Old nozzle
(6)	1176	49733	190	79	Post-curing, left	New nozzle

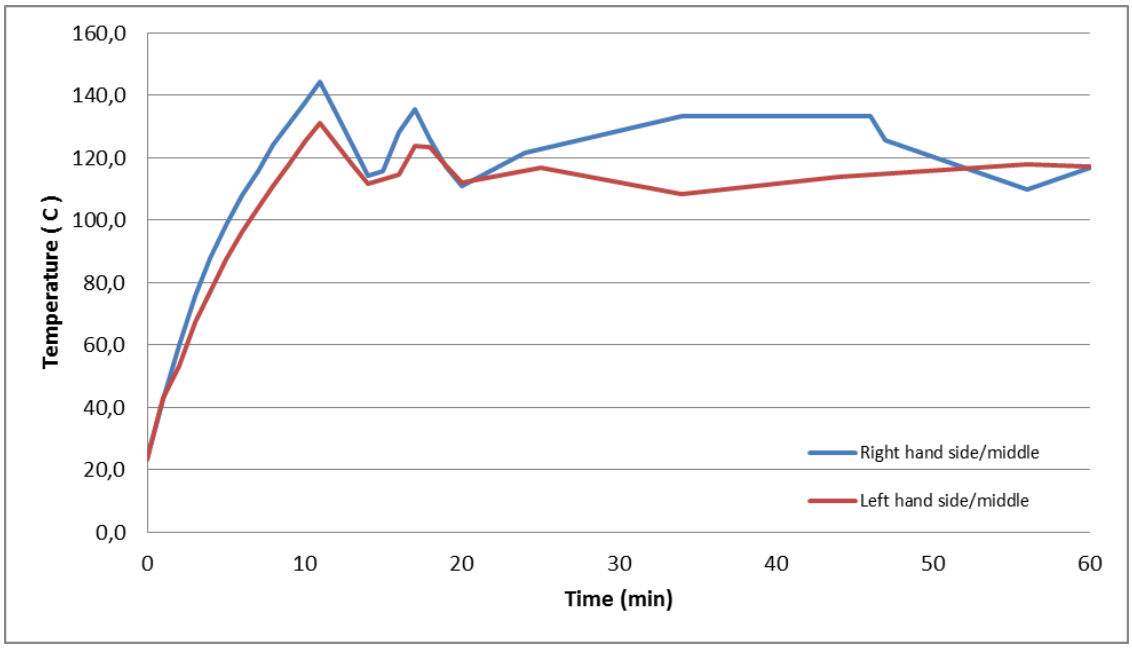

Figure 48. Oven temperature comparison.

Table 27. Light intensities comparison. Left-side oven on the left and right-side oven on the right.

LED/Intensity	1/4	2/4	3/4	4/4	Unit		LED/Intensity	1/4	2/4	3/4	4/4	Unit
1	200	400	500	550	mW/cm2		**1**	200	400	450	500	mW/cm2
2	200	400	500	550	mW/cm2		**2**	200	350	400	400	mW/cm2
3	250	400	500	600	mW/cm2		**3**	200	450	500	550	mW/cm2
Average	200	400	500	600	mW/cm2		Average	200	400	500	500	mW/cm2
SD	29	0	0	29	mW/cm2		SD	0	50	50	76	mW/cm2
RSD	14	0	0	5	%		RSD	0	13	10	15	%
Sum	650	1200	1500	1700	mW/cm2		Sum	600	1200	1350	1450	mW/cm2

Three point-bending tests were also carried out to compare the two ovens and the new and the old nozzle. The three-point bending test results are listed below (Figures 49-51).

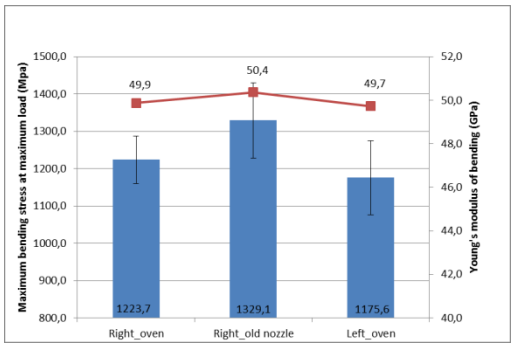

Figure 49. Oven and nozzle comparison by max bending stress (bar) and Young's modulus (line).

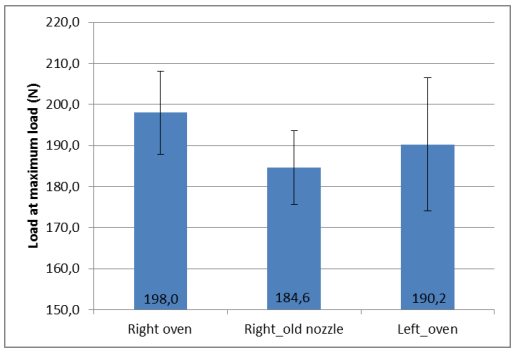

Figure 50. Oven and nozzle comparison by max load.

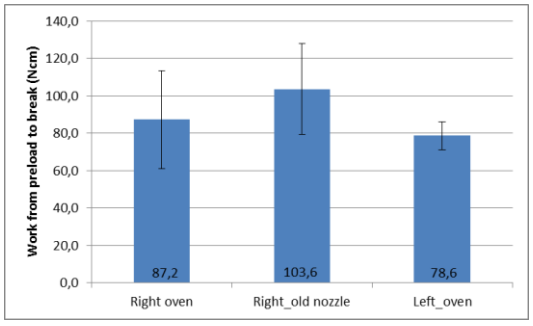

Figure 51. Oven and nozzle comparison by work.

11 DISCUSSION

Heat post-curing was expected to improve materials mechanical properties and therefore the data in the studies 1 (Light intensity and speed with oven post-curing) and 2 (Light intensity and speed without oven post-curing) was also expected to support each other. The results of both studies should follow similar patterns, the post-cured specimens giving higher values. The highest strength value was achieved in the oven post-curing group using light intensity 1/4 and speed 2 mm/s (1470 MPa). The highest value without oven post-curing was 1231 MPa (3/4 intensity and speed 2 mm/s). The lowest value with oven post-curing was 910 MPa and without post-curing 863 MPa. The post-cured specimens gave higher strength, load and work values', indicating that the heat post-curing improves the mechanical properties of the material. This was also the case with the post-curing study, where non-post-cured control showed clearly lower values than all the post-cured groups.

According to the results post-curing does not seem to influence the Young's modulus as strongly as it does other mechanical properties (post-cured 52 GPa - 31 GPa and non-post-cured 52 GPa - 27 GPa). It also seems that post-curing does not have any significant effect when the highest light intensity (4/4) is applied and even after the oven post-curing the strength remains at about the same level as without the post-curing. The highest intensity gave the overall poorest results. This may be due to too fast light-curing that leaves the polymer chains no time for relaxation.

When sorting the data in the studies 1 and 2 according to the light intensity it seems that the flexural strength decreases as the speed rises. This might be due to the shortening curing time with the rising speed. The faster the light passes the impregnated fiber, the shorter the exposure time. It can be roughly estimated that the length of the area that the manufacturing device light system covers is about 10 mm at a time. This gives 5 s of curing time when using the speed 2 mm/s and only about 1 s at 8 mm/s. This is a very short exposure time compared to the 20-40 s curing times often recommended to be used with dental light-curing materials.

The light intensities comparison showed that there are differences in the used intensities. The right-hand side lamps gave slightly lower intensity levels than the left-hand side lamps. The method used to perform the measurements is designed for monitoring the intensity levels of the dentist's hand light-curing devices and the machine LEDs did not fit very well to the radiometer detector. For this reason the measured intensity values should be considered as rough approximates. Also, the lamps have no protective shield and they get dirty by the impregnation resin really easily. This might also cause the differences in the measured values between the sides. Despite the fact that the method is not the best to measure the intensities of the machine LEDs, it indicates that the Dim buttons on both sides of the machine function properly and the light intensity really rises as the buttons are turned clockwise (1/4 ~600 mW/cm^2, 2/4 ~1200 mW/cm^2, 3/4 ~1400 mW/cm^2 and 4/4 ~1600 mW/cm^2). From the used intensity levels 2/4 correlates best with the dental LED light-curing devices (1200 mW/cm^2). Even though the highest strength was achieved using the lowest intensity, the overview of the results suggests that the 2/4 (~1200 mW/cm^2) and the 3/4 (~1400 mW/cm^2) intensity levels are worth further studies.

To be able to calculate flexural strength and Young's modulus one needs to know the diameter of the specimen. The diameters of the poles were not very symmetrical and this causes some uncertainty in the test values. On the other hand in this case it is possible to use the load-values to compare the groups. This is because all the manufactured poles should contain the same amount of fiber and resin. When the load-value patterns are compared to that of strength-value patterns, it can be seen that in studies 1 and 2 the load-values support the strength-values.

When comparing the work values in the studies 1 and 2 the patterns are not that clear and the deviations are quite high. When comparing the work needed to break the specimens the lowest values were obtained using the highest intensity.

SEM images taken from the post-cured specimens (Figure 31) suggested that the fibers have even distribution across the poles and that there are very few air

bubbles in the structures. Even though according to the studies of Gauthier *et al.* post-curing at a temperature above ~110 °C should eliminate the sticky oxygen inhibition layer, the images suggested that the layer still existed on the poles even after post-curing at 120 °C for 1 h. The sticky surface could also be detected when handling the poles. This may be a problem in the milling process.

When studying the effect of different pre-tensioning weights on the mechanical properties of the poles it showed that the smallest weight (3.4 kg) gained the smallest strength. The highest value was obtained using a 7.0 kg weight (1112 MPa) and from that on the values had a slight decrease as the amount of weight increases. This is consistent with the studies made by Schlichting *et al.* and Keulemans *et al.*, the pre-tensioning increases the flexural strength but there is an optimal limit for it. The Young's modulus-values between the groups varied from 52 GPa to 49 GPa. The pattern of the load values is about the same as that of the strength values. Despite the consistency with the previous studies the Spearman correlation coefficient showed no significant correlation between the pretension and the max bending stress ($p=0.41$), the Young's modulus ($p=0.34$), the load ($p=0.52$) and the work ($p=0.11$).

The post-curing study shows very similar patterns when comparing strength, load and work. The highest strength (1072 MPa) and load values were achieved by post-curing at 120 °C for 60 min. The Young's modulus varied between 49 GPa and 43 GPa. Post-curing temperature of 120 °C showed best in all time points (15 min 1068 MPa, 30 min 1038 MPa and 60 min 1072 MPa). The Spearman correlation coefficient showed significant positive correlation between the post-curing and the max bending stress ($p=0.01$), the Young's modulus ($p=0.00$), the load ($p=0.01$) and the work ($p=0.00$).

The highest strength (1142 MPa), load and work were achieved using a nozzle size of 2.7 mm. This is the size calculated for the used fiber amount. The nozzle size between 2.6 mm and 2.8 mm does not seem have a relevant effect on the mechanical properties of the poles. The Spearman correlation coefficient

showed no significant correlation between the nozzle size and the max bending stress (p=0.09), Young's modulus (p=0.11), load (p=0.08) and work (p=0.28).

There were a lot of uncertainty factors within the manufacturing method. When comparing the old and the new nozzle and the two gutter-ovens, some differences were detected. A T-test was performed to make the comparison. It showed that at a 95 % confidence level there is no difference between the poles manufactured with the two gutters, but the stress, load and diameter of the manufactured poles depend on whether the old or the new nozzle was used. The old nozzle had a better fitting to the holder which may have resulted in higher mechanical values in the studies 1 and 2. Too loose fitting does not press the roving into the right shape. The results gained with the old nozzle were also higher in the comparison study, except for the load-value. The contradiction may be caused by the fact that the old nozzle was quite badly damaged when the test-poles were prepared and the diameters were very unsymmetrical. Unsymmetrical diameters make strength and modulus calculations less reliable and also cause problems with the subsequent milling process.

Test-milling could to be carried out by using the ZirkonZahn milling system. This was very time consuming and cannot be the permanent manufacturing method of the root-canal posts. Some basic lathe system is to be developed to produce the final structure. Since the material produced in this study is not the final product, it is very hard to find the suitable values to compare the material with. Elastic modulus of the dentin is 15 GPa and the measured Young's modulus of bending values were between 30 and 50 GPa. The values are not directly comparable because the former is a general modulus value and the latter is the modulus in bending. A similar pre-manufactured glass fiber post, Parapost, from ColteneWhaledent has a flexural strength of 990 MPa and an elastic modulus of 29 GPa. The strength of the final product will be determined when the milling process is fixed. The credit of this study lies in learning about the effects of the different manufacturing parameters on the mechanical properties of the poles, rather than on determining the properties of the final root-canal post. The study

will be continued by developing the milling process. Also different resin compositions will be tested and some filler particles will be added to the structure to create a radio-opaque product.

12 CONCLUSIONS

This study showed that with the designed machine it is possible to produce FRC poles to create root-canal posts. The final milling process is still under development and the properties of the final product could not be measured.

This study showed that the highest flexural strength with the materials used is 1470 MPa and this was achieved by using the light intensity 1/4, a speed of 2 mm/s, a pretension weight of 10.3 kg, a nozzle size of 2.7 mm, a post-curing temperature of 120 °C and duration of 60 min. The Young's modulus of bending values varied between approximately 30 and 50 GPa throughout the tests.

In this study it was also shown that a high light-curing intensity and fast speed give poor mechanical properties to the poles, and that the post-curing strengthens the material and is therefore essential for the manufacturing process. The highest strength was achieved by post-curing at 120 °C for 60 min. The pre-tensioning weights used (3-17 kg) had no significant effect on the mechanical properties, but the highest strength was achieved using a 7.0 kg pre-tensioning weight. In addition the nozzle size which varied between 2.6 mm and 2.8 mm seemed to have no significant effect on the results but the highest values were achieved using a diameter of 2.7 mm.

It was also shown that the nozzle needs to fit tightly in the nozzle holder to get best possible poles. The nozzle might need some adjusting because most of the produced poles are not symmetrical in diameter.

SOURCE MATERIAL

Bagis Y.H., Rueggeberg F.A. (1997), Effect of post-cure temperature and heat duration on monomer conversion of photo-activated dental resin composite, Dental materials, Volume 13, Issue 4, July 1997, pages 228-232.

Bagis Y.H., Rueggeberg F.A. (2000), Effect of post-cure heating on residual, unreacted monomer in a commercial resin composite, Dental materials, Volume 16, Issue 4, July 2000, pages 244-247.

Darvell, B.W., (2009) Materials science for dentistry, chapter 6, 9th ed. Woodhead publishing, Cambridge, UK.

Ferracane J.L., Condon J.R. (1992), Post-cure heat treatments for composites: properties and fractography, Dent Mater 8:290-295.

Fokkinga, W.A., 2007, Post it? Reconstruction of the endotontically treated tooth, Thesis, Radboud University Nijmegen, The Netherlands.

Gauthier, M.A., Stangel, I., Ellis, T.H., Zhu, X.X., Oxygen inhibition in dental resins, J DENT RES 2005 84:725.

Holopainen M., Tenhunen L., Vuorinen P. (2004), Tutkimusaineiston analysointi ja SPSS, Yrityssanoma OY, Kotkan kirjapaino, Hamina.

Keulemans F., Lassila L.V., Vallittu P.K., Kleverlaan C.J., Feilzer A., De Moor R.J. (2012), Prestressed Dental Fibre-Reinforced Composite, IADR Congress 2012 presentation abstract: http://iadr.confex.com/iadr/per12/webprogram/Paper168156.html (referred March 12th 2013).

Le Bell-Rönnlöf, A-M., 2007, Fibre-reinforced composites as root canal posts, Turku University Thesis, Painosalama Oy, Turku, Finland.

3M Espe Dental products (2009), Elipar S10 LED Curing light operating instructions.

3M Espe Dental products (2005), Filtek Z250 restorative material instructions for use.

Outinen, H., Koski, J., Salmi, T., 1998, Lujuusopin perusteet, Pressus Oy, Tampere.

Rich, Jaana, In vitro characterization of bioresorbable polymers and composites for drug delivery and bone replacement. Acta Polytechnica Scandinavica, Chemical Technology Series No. 289, Espoo 2002, 47 pp. Published by the Finnish Academies of Technology, ISBN 951-666-601-9, ISSN 1239-0518.

Rueggeberg, F.A., State-of-the-art: Dental photocuring –A review, Dental materials, 27 (2011), 39-52.

Saarela, O., Airasmaa, I., Kokko, J., Skrifvars, M., Komppa, V., Komposiittirakenteet, Muoviyhdistys ry, Hakapaino Oy, Helsinki 2007.

Schlichting, L.H, de Andrada, M.A.C., Vieira, L.C.C., de Oliviera Barra, G.M., Magne, P., 2010, Composite resin reinforced with pre-tensioned glass fibers. Influence of prestressing on flexural properties, Dental Materials, 26, 2010, 118-125.

Sideridou, I., Tserki, V., Papanastasiou, G., Effect of chemical structure on degree of conversion in light-cured dimethacrylate-based dental resins, Biomaterials, vol. 23, April 2002, pages 1819-1829.

StickTech (2011), EverStick POST instructions for use.

Vallittu, P.K., 2008, Fibre-reinforced composites for dental applications, (ed.) Curtis and Watson, Dental Biomaterials, Woodhead publishing, Cambridge, UK.

Williams, D.F., The Williams dictionary of biomaterials, Liverpool University press, Liverpool 1999.

Raw Data

FRC-poles for root canal posts

Parameters: speeds 2-8 mm/s, light intensities 1-4, post-curing 120C 1h

Hman/TCBC/070312

Specimen info	No	Diameter (mm)	Young's Modulus Of Bending (MPa)	Maximum Bending Stress at Maximum Load (MPa)	Work from preload to Break (Ncm)	Load at Maximum Load (N)
1/4 2mm/s	1	2,70	51483,75368	1527,631306	102,8824625	236,1564022
1/4 2mm/s	2	2,68	51670,02688	1556,051066	94,27057277	235,2437581
1/4 2mm/s	3	2,71	53326,23965	1466,491002	68,24150367	229,2330097
1/4 2mm/s	4	2,70	52107,62859	1483,041951	111,4578501	229,2633373
1/4 2mm/s	5	2,69	50579,89025	1333,808609	79,11132731	203,9108043
1/4 2mm/s	6	2,68	49781,94169	1482,104402	61,76799842	224,0645035
1/4 2mm/s	8	2,69	52949,60435	1441,105299	81,95944653	220,314173
Average		2,69	51699,87	1470,03	85,67	225,46
SD		0,01	1248,57	71,23	18,11	11,04
RSD (%)		0,41	2,42	4,85	21,14	4,90

Specimen info	No	Diameter (mm)	Young's Modulus Of Bending (MPa)	Maximum Bending Stress at Maximum Load (MPa)	Work from preload to Break (Ncm)	Load at Maximum Load (N)
1/4 3mm/s	1	2,69	49151,06932	1188,775089	54,97306764	181,7382816
1/4 3mm/s	2	2,73	47999,75793	1259,56078	58,81405916	201,2782981
1/4 3mm/s	3	2,71	48342,56443	1244,714308	91,00988712	194,5662174
1/4 3mm/s	4	2,69	52705,88118	1302,034044	111,0548385	199,0531529
1/4 3mm/s	5	2,68	51600,78587	1277,619756	137,4676782	193,1505202
1/4 3mm/s	6	2,69	48031,59696	1347,531203	91,61485399	206,0086953
1/4 3mm/s	7	2,70	50287,24155	1225,411916	56,90350883	189,4363307
1/4 3mm/s	8	2,71	48755,7398	1179,370354	87,16118086	184,3520455
Average		2,70	49609,33	1253,13	86,12	193,70
SD		0,02	1758,14	56,52	28,99	8,34
RSD (%)		0,59	3,54	4,51	33,66	4,31

Specimen info	No	Diameter (mm)	Young's Modulus Of Bending (MPa)	Maximum Bending Stress at Maximum Load (MPa)	Work from preload to Break (Ncm)	Load at Maximum Load (N)
1/4 4mm/s	1	2,68	49992,54015	1388,776268	183,8140386	209,9551587
1/4 4mm/s	2	2,67	47232,0559	1378,639154	112,8272927	206,0980862
1/4 4mm/s	3	2,68	51496,90667	1324,357966	140,296721	200,2164015
1/4 4mm/s	4	2,69	46983,11779	1291,680895	116,6352442	197,4703779
1/4 4mm/s	6	2,69	50765,72248	1204,718328	94,18959565	184,1756617
1/4 4mm/s	7	2,71	45278,23688	1290,637224	107,1630865	201,74461
1/4 4mm/s	8	2,72	45434,4372	1255,722672	78,19498237	198,467925
Average		2,69	48169,00	1304,93	119,02	199,73
SD		0,02	2558,05	65,43	34,45	8,14
RSD (%)		0,66	5,31	5,01	28,94	4,08

Specimen info	No	Diameter (mm)	Young's Modulus Of Bending (MPa)	Maximum Bending Stress at Maximum Load (MPa)	Work from preload to Break (Ncm)	Load at Maximum Load (N)
1/4 5mm/s	1	2,71	48485,76419	1036,72424	132,3229525	162,054487
1/4 5mm/s	2	2,68	46262,10702	1317,483105	111,2369506	199,1770602
1/4 5mm/s	3	2,68	47476,61673	1330,127615	114,3999552	201,0886569
1/4 5mm/s	5	2,68	44275,59485	1396,790547	121,4735181	211,1667572
1/4 5mm/s	6	2,70	45322,0901	1368,383967	88,61555548	211,5383686
1/4 5mm/s	7	2,67	46848,6532	1199,938959	96,76608164	179,3836346
1/4 5mm/s	8	2,68	46581,99252	1189,414654	67,66580824	179,8156753
Average		2,69	46464,69	1262,69	104,64	192,03
SD		0,01	1378,93	127,20	21,89	18,65
RSD (%)		0,52	2,97	10,07	20,92	9,71

Specimen info	No	Diameter (mm)	Young's Modulus Of Bending (MPa)	Maximum Bending Stress at Maximum Load (MPa)	Work from preload to Break (Ncm)	Load at Maximum Load (N)
1/4 6mm/s	1	2,66	50213,90345	1053,515101	75,233175	155,7311735
1/4 6mm/s	2	2,67	42076,52668	948,9297392	47,6224895	141,8592708
1/4 6mm/s	3	2,67	45634,92062	1209,214024	111,0622383	180,7702009
1/4 6mm/s	4	2,66	42006,03374	1203,432187	107,3660387	177,8919986
1/4 6mm/s	5	2,67	47470,59018	1201,410912	122,510938	179,6036828
1/4 6mm/s	6	2,66	46165,23159	1110,754072	76,70441717	164,1922693
1/4 6mm/s	7	2,66	47506,7343	1179,065035	126,2533151	174,2900329
1/4 6mm/s	8	2,67	51302,54837	1190,46641	102,6969899	177,9675458
Average		2,67	46547,06	1137,10	96,18	169,04
SD		0,01	3368,31	93,68	27,16	14,01
RSD (%)		0,20	7,24	8,24	28,24	8,29

Specimen info	No	Diameter (mm)	Young's Modulus Of Bending (MPa)	Maximum Bending Stress at Maximum Load (MPa)	Work from preload to Break (Ncm)	Load at Maximum Load (N)
1/4 7mm/s	1	2,68	42366,12595	1169,022748	77,71323667	176,7328275
1/4 7mm/s	2	2,66	46175,40471	1275,071506	80,91667303	188,4817615
1/4 7mm/s	3	2,70	42368,46745	1097,032465	84,4749937	169,5901615
1/4 7mm/s	4	2,67	45257,06787	1169,272939	68,21187689	174,7992497
1/4 7mm/s	5	2,67	45155,78489	1245,980238	102,7816777	186,266528
1/4 7mm/s	6	2,66	46925,17376	1336,441883	106,6508527	197,5535639
1/4 7mm/s	7	2,69	46577,59956	1203,446006	63,13050549	183,9811509
1/4 7mm/s	8	2,68	45756,67919	1199,268342	63,39471198	181,3053556
Average		2,68	45072,79	1211,94	80,91	182,34
SD		0,01	1775,21	73,43	16,68	8,78
RSD (%)		0,53	3,94	6,06	20,61	4,81

Specimen info	No	Diameter (mm)	Young's Modulus Of Bending (MPa)	Maximum Bending Stress at Maximum Load (MPa)	Work from preload to Break (Ncm)	Load at Maximum Load (N)
1/4 8mm/s	1	2,68	44678,2928	1190,774229	104,7769254	180,0212159
1/4 8mm/s	2	2,66	42159,94943	1128,855247	116,8760063	166,8679948
1/4 8mm/s	3	2,66	43714,12055	1102,770232	104,2891976	163,0120938
1/4 8mm/s	4	2,65	45746,74457	1206,169193	52,32434577	176,2932707
1/4 8mm/s	5	2,67	42523,3673	1213,529924	90,55651256	181,415402
1/4 8mm/s	6	2,65	45392,55827	1232,360756	68,53408881	180,1214205
1/4 8mm/s	7	2,67	47643,89227	1233,57135	139,5120575	184,4114742
1/4 8mm/s	8	2,68	42920,77955	1225,700134	69,22901636	185,3013132
Average		2,67	44347,46	1191,72	93,26	177,18
SD		0,01	1873,70	49,44	28,84	8,11
RSD (%)		0,45	4,23	4,15	30,93	4,58

Specimen info	No	Diameter (mm)	Young's Modulus Of Bending (MPa)	Maximum Bending Stress at Maximum Load (MPa)	Work from preload to Break (Ncm)	Load at Maximum Load (N)
2/4 2mm/s	1	2,67	50655,45389	1456,918175	133,2453502	217,800477
2/4 2mm/s	2	2,66	48425,60246	1342,843127	137,0349776	198,4997993
2/4 2mm/s	3	2,67	51559,01601	1383,89888	166,3580209	206,8845329
2/4 2mm/s	4	2,69	53115,55931	1331,564277	154,8712625	203,5676939
2/4 2mm/s	5	2,68	47750,31461	1428,444262	152,393893	215,952165
2/4 2mm/s	6	2,68	49428,17882	1309,21341	122,3307162	197,926848
2/4 2mm/s	7	2,67	50222,46398	1584,137292	170,6657563	236,8189674
2/4 2mm/s	8	2,68	50686,25602	1435,326976	112,9415477	216,9926935
Average		2,68	50230,36	1409,04	143,73	211,81
SD		0,01	1712,54	88,64	20,69	12,91
RSD (%)		0,35	3,41	6,29	14,40	6,10

Specimen info	No	Diameter (mm)	Young's Modulus Of Bending (MPa)	Maximum Bending Stress at Maximum Load (MPa)	Work from preload to Break (Ncm)	Load at Maximum Load (N)
2/4 3mm/s	1	2,68	50557,00061	1469,194398	98,36971089	222,1127694
2/4 3mm/s	2	2,68	49474,90237	1510,330499	124,2034489	228,3317241
2/4 3mm/s	3	2,69	49976,4217	1417,344016	109,2131735	216,6815811
2/4 3mm/s	4	2,68	45728,77497	1540,688959	84,46191105	232,9213152
2/4 3mm/s	5	2,68	48750,1365	1446,656927	123,4882134	218,7055551
2/4 3mm/s	6	2,69	50730,02718	1358,441343	101,179619	207,6766223
2/4 3mm/s	7	2,70	46042,50577	1376,651669	132,4387685	212,8164721
2/4 3mm/s	8	2,68	52435,3479	1320,601069	122,6377605	199,6484339
Average		2,69	49211,89	1429,99	112,00	217,36
SD		0,01	2316,05	76,17	16,39	10,79
RSD (%)		0,28	4,71	5,33	14,64	4,97

Specimen info	No	Diameter (mm)	Young's Modulus Of Bending (MPa)	Maximum Bending Stress at Maximum Load (MPa)	Work from preload to Break (Ncm)	Load at Maximum Load (N)
2/4 4mm/s	1	2,67	45410,51923	1238,019446	183,7161204	185,0764378
2/4 4mm/s	2	2,66	49080,74559	1493,964753	115,3060243	220,83868
2/4 4mm/s	3	2,67	49595,90571	1417,599072	140,8668235	211,9225084
2/4 4mm/s	4	2,66	47135,04657	1354,053609	118,0250039	200,1569388
2/4 4mm/s	5	2,68	48876,50994	1434,887735	189,4662084	216,926289
2/4 4mm/s	6	2,67	46904,8649	1353,295614	112,9642526	202,3095293
2/4 4mm/s	7	2,67	45726,80143	1292,728533	116,6263937	193,2551161
2/4 4mm/s	8	2,66	48395,70646	1468,090269	103,6068425	217,0138997
Average		2,67	47640,76	1381,58	135,07	205,94
SD		0,01	1577,87	88,09	33,51	12,78
RSD (%)		0,27	3,31	6,38	24,81	6,21

Specimen info	No	Diameter (mm)	Young's Modulus Of Bending (MPa)	Maximum Bending Stress at Maximum Load (MPa)	Work from preload to Break (Ncm)	Load at Maximum Load (N)
2/4 5mm/s	1	2,68	48430,95715	1415,106295	107,0333342	213,9357315
2/4 5mm/s	2	2,70	51423,18343	1290,743546	141,7377764	199,5359421
2/4 5mm/s	3	2,69	52541,76322	1309,797267	107,9152642	200,2399837
2/4 5mm/s	4	2,70	50239,26564	1273,809045	80,97116534	196,9180391
2/4 5mm/s	5	2,70	47026,9748	1263,311434	74,41292981	195,2952142
2/4 5mm/s	6	2,69	49023,03535	1323,271276	86,31288137	202,2998715
2/4 5mm/s	7	2,69	49401,64643	1422,908026	134,9467514	217,5321992
2/4 5mm/s	8	2,70	51560,331	1318,079204	110,5668869	203,7617594
Average		2,69	49955,89	1327,13	105,49	203,69
SD		0,01	1835,20	60,42	24,35	7,96
RSD (%)		0,28	3,67	4,55	23,08	3,91

Specimen info	No	Diameter (mm)	Young's Modulus Of Bending (MPa)	Maximum Bending Stress at Maximum Load (MPa)	Work from preload to Break (Ncm)	Load at Maximum Load (N)
2/4 6mm/s	1	2,69	47883,1765	1236,781507	75,24796346	189,0774359
2/4 6mm/s	2	2,70	47632,98357	1296,909947	139,8112262	200,4892056
2/4 6mm/s	3	2,70	46732,41128	1287,384167	83,1400006	199,0166161
2/4 6mm/s	4	2,70	48776,87142	1303,213155	104,8745922	201,4636181
2/4 6mm/s	5	2,69	46048,73614	1336,559927	135,1026279	204,3314219
2/4 6mm/s	6	2,68	46362,07884	1215,037272	125,019581	183,689302
2/4 6mm/s	7	2,69	45039,00779	1183,385067	82,78679955	180,9142624
2/4 6mm/s	8	2,69	45187,67472	1312,53902	106,3879818	200,6591391
Average		2,69	46707,87	1271,48	106,55	194,96
SD		0,01	1318,48	53,42	24,95	9,01
RSD (%)		0,26	2,82	4,20	23,42	4,62

Specimen info	No	Diameter (mm)	Young's Modulus Of Bending (MPa)	Maximum Bending Stress at Maximum Load (MPa)	Work from preload to Break (Ncm)	Load at Maximum Load (N)
2/4 7mm/s	2	2,68	50681,10308	1425,807644	96,69050065	215,5535611
2/4 7mm/s	3	2,69	52336,05969	1147,217058	86,86216069	175,3849475
2/4 7mm/s	4	2,70	49433,88616	1130,601807	56,39542383	174,7796434
2/4 7mm/s	5	2,70	48592,62356	1197,16491	109,805886	185,0696282
2/4 7mm/s	6	2,70	49352,7008	1238,967568	101,1121787	191,5318978
2/4 7mm/s	7	2,70	50404,15792	1193,152303	109,5558344	184,4493196
2/4 7mm/s	8	2,70	48815,56224	1262,674898	101,414641	195,196812
Average		2,70	49945,16	1227,94	94,55	188,85
SD		0,01	1302,97	98,85	18,56	13,99
RSD (%)		0,29	2,61	8,05	19,63	7,41

Specimen info	No	Diameter (mm)	Young's Modulus Of Bending (MPa)	Maximum Bending Stress at Maximum Load (MPa)	Work from preload to Break (Ncm)	Load at Maximum Load (N)
2/4 8mm/s	1	2,69	46769,77297	1197,432533	79,7564359	183,0618195
2/4 8mm/s	2	2,69	44880,02365	1156,584765	62,55085701	176,8170695
2/4 8mm/s	3	2,69	50577,99546	1020,945316	100,1313705	156,0806994
2/4 8mm/s	4	2,68	40887,1196	1081,414819	50,00373837	163,4882631
2/4 8mm/s	5	2,68	42141,246	1097,569529	96,8852027	165,9305318
2/4 8mm/s	6	2,69	44722,13669	1127,450589	116,2113211	172,3644533
2/4 8mm/s	7	2,68	50323,91978	1189,321749	110,7879275	179,8016299
2/4 8mm/s	8	2,68	49491,65488	1244,913066	117,9890854	188,2059237
Average		2,69	46224,23	1139,46	91,79	173,22
SD		0,01	3702,41	72,28	25,31	10,82
RSD (%)		0,20	8,01	6,34	27,58	6,25

Raw Data

Specimen info	No	Diameter (mm)	Young's Modulus Of Bending (MPa)	Maximum Bending Stress at Maximum Load (MPa)	Work from preload to Break (Ncm)	Load at Maximum Load (N)
3/4_2mm/s	2	2,7	49439,66	1175,77	63,86	181,76
3/4_2mm/s	3	2,69	50253,56	1201,26	73,40	183,65
3/4_2mm/s	4	2,69	51337,49	1247,17	76,45	190,67
3/4_2mm/s	5	2,67	56702,10	1260,20	75,93	188,39
3/4_2mm/s	6	2,71	51293,18	1156,23	81,88	180,74
3/4_2mm/s	7	2,68	54885,84	1163,82	74,91	175,95
3/4_2mm/s	8	2,68	48122,57	1131,16	73,96	171,01
Average		2,7	51719,2	1190,8	74,3	181,7
SD		0,0	3040,4	48,0	5,4	6,8
RSD		0,5	5,9	4,0	7,3	3,7

Specimen info	No	Diameter (mm)	Young's Modulus Of Bending (MPa)	Maximum Bending Stress at Maximum Load (MPa)	Work from preload to Break (Ncm)	Load at Maximum Load (N)
3/4_3mm/s	1	2,69	52536,72462	1296,813866	106,5864776	198,2550995
3/4_3mm/s	2	2,69	50433,26342	1297,85503	120,6165928	198,4142712
3/4_3mm/s	3	2,68	53823,55619	1425,020141	141,8366999	215,4345064
3/4_3mm/s	4	2,70	50896,26828	1499,191062	111,9659389	231,759827
3/4_3mm/s	5	2,69	51889,8654	1334,237432	143,9592949	203,9763622
3/4_3mm/s	6	2,69	54426,22514	1211,63223	110,6165952	185,2326494
3/4_3mm/s	7	2,68	53252,56354	1458,635435	108,549161	220,5164657
3/4_3mm/s	8	2,70	51054,58335	1388,162999	139,9650044	214,5960071
Average		2,69	52289,13	1363,94	123,01	208,52
SD		0,01	1462,82	96,01	16,22	14,83
RSD (%)		0,28	2,80	7,04	13,18	7,11

Specimen info	No	Diameter (mm)	Young's Modulus Of Bending (MPa)	Maximum Bending Stress at Maximum Load (MPa)	Work from preload to Break (Ncm)	Load at Maximum Load (N)
3/4_4mm/s	1	2,68	52497,68626	1420,898877	80,50175326	214,8114539
3/4_4mm/s	2	2,68	55187,56289	1151,940739	117,4849874	174,1503698
3/4_4mm/s	3	2,69	51468,11183	1302,220544	105,7072049	199,0816649
3/4_4mm/s	4	2,69	53148,90796	1466,011417	71,77379174	224,1217856
3/4_4mm/s	5	2,70	52223,85257	1313,532246	66,29795635	203,0588455
3/4_4mm/s	6	2,70	52903,82429	1397,838489	115,2291466	216,0917408
3/4_4mm/s	7	2,69	52740,44735	1336,056584	124,0392352	204,2544716
3/4_4mm/s	8	2,68	49408,98568	1171,283016	98,08636388	177,0745347
Average		2,69	52447,42	1319,97	97,39	201,58
SD		0,01	1627,37	112,46	22,07	17,98
RSD (%)		0,31	3,10	8,52	22,66	8,92

Specimen info	No	Diameter (mm)	Young's Modulus Of Bending (MPa)	Maximum Bending Stress at Maximum Load (MPa)	Work from preload to Break (Ncm)	Load at Maximum Load (N)
3/4_5mm/s	1	2,67	48058,73933	1375,358475	111,0465773	205,6077939
3/4_5mm/s	2	2,67	47288,53544	1046,657935	43,09559975	156,3195525
3/4_5mm/s	3	2,69	47407,04047	1084,700529	128,1119269	165,8275075
3/4_5mm/s	4	2,68	50812,048	1267,01031	92,17954236	191,5465844
3/4_5mm/s	5	2,67	49312,3424	1141,816558	136,4455156	170,6946864
3/4_5mm/s	6	2,67	47000,18547	1233,366357	69,33203679	184,380829
3/4_5mm/s	7	2,67	49183,24217	1246,624042	106,4235185	186,3627729
3/4_5mm/s	8	2,67	49435,65703	1323,512757	102,4851278	197,8571719
Average		2,67	48562,22	1214,76	98,63	182,32
SD		0,01	1332,19	114,98	30,53	16,79
RSD (%)		0,28	2,74	9,47	30,95	9,21

Specimen info	No	Diameter (mm)	Young's Modulus Of Bending (MPa)	Maximum Bending Stress at Maximum Load (MPa)	Work from preload to Break (Ncm)	Load at Maximum Load (N)
3/4_6mm/s	1	2,70	51494,7865	997,1260715	108,5740235	154,1456401
3/4_6mm/s	3	2,68	53845,55815	1224,06428	92,22877963	185,0540048
3/4_6mm/s	4	2,69	48805,47557	1208,933663	115,7778862	184,8200963
3/4_6mm/s	5	2,69	49801,65811	1255,975527	99,4353715	192,011791
3/4_6mm/s	6	2,70	48534,88547	1258,723931	75,76997482	194,5860324
3/4_6mm/s	7	2,70	48031,52713	1354,268109	114,8386278	209,3561992
3/4_6mm/s	8	2,70	49740,28293	1177,588657	108,9395997	182,0433368
Average		2,69	50036,31	1210,95	102,22	186,00
SD		0,01	2023,55	109,44	14,35	16,77
RSD (%)		0,29	4,04	9,04	14,04	9,02

Specimen info	No	Diameter (mm)	Young's Modulus Of Bending (MPa)	Maximum Bending Stress at Maximum Load (MPa)	Work from preload to Break (Ncm)	Load at Maximum Load (N)
3/4_7mm/s	1	2,70	49630,98226	1292,880925	88,51119858	199,8663595
3/4_7mm/s	2	2,70	47111,40771	1157,133232	124,4714813	178,8811344
3/4_7mm/s	3	2,68	51046,06375	1174,597471	103,4398679	177,575614
3/4_7mm/s	4	2,68	52792,64105	1272,721024	106,160534	192,4099301
3/4_7mm/s	5	2,67	51019,43199	1181,120205	82,07296394	176,5703445
3/4_7mm/s	6	2,67	47334,08114	1230,394657	94,54166268	183,9365778
3/4_7mm/s	7	2,67	43770,77418	1113,283875	61,18511893	166,4292224
3/4_7mm/s	8	2,67	52508,73199	1312,164179	98,63827429	196,1606279
Average		2,68	49401,76	1216,79	94,88	183,98
SD		0,01	3111,12	71,24	18,63	11,35
RSD (%)		0,49	6,30	5,85	19,64	6,17

Specimen info	No	Diameter (mm)	Young's Modulus Of Bending (MPa)	Maximum Bending Stress at Maximum Load (MPa)	Work from preload to Break (Ncm)	Load at Maximum Load (N)
3/4_8mm/s	1	2,68	44809,82887	1037,567969	106,017956	156,8594976
3/4_8mm/s	2	2,68	45554,25773	1211,362836	83,52304174	183,1338008
3/4_8mm/s	3	2,68	44417,75844	1241,429134	93,81865387	187,679223
3/4_8mm/s	4	2,68	44941,63033	1286,211717	141,6223871	194,4494527
3/4_8mm/s	5	2,68	44397,9754	1207,18044	98,61146892	182,5015063
3/4_8mm/s	6	2,68	46844,6011	1228,04777	123,7070582	185,6562287
3/4_8mm/s	9	2,69	45740,50342	1068,780832	67,07491376	163,3937265
Average		2,68	45243,79	1182,84	102,05	179,10
SD		0,00	873,98	92,81	24,82	13,67
RSD (%)		0,14	1,93	7,85	24,32	7,63

Specimen info	No	Diameter (mm)	Young's Modulus Of Bending (MPa)	Maximum Bending Stress at Maximum Load (MPa)	Work from preload to Break (Ncm)	Load at Maximum Load (N)
4/4_2mm/s	1	2,66	53038,25	1265,88	91,84	187,12
4/4_2mm/s	2	2,69	51688,30	1194,65	75,24	182,64
4/4_2mm/s	3	2,66	52054,03	1105,03	74,18	163,35
4/4_2mm/s	4	2,67	53129,47	1119,50	100,74	167,36
4/4_2mm/s	5	2,65	51780,58	1327,04	79,00	193,96
4/4_2mm/s	6	2,67	52125,47	1196,01	95,15	178,80
4/4_2mm/s	7	2,65	52676,98	1356,99	73,60	198,34
4/4_2mm/s	8	2,65	53442,73	1188,15	97,88	173,66
Average		2,7	52492,0	1219,2	86,0	180,7
SD		0,0	667,7	90,9	11,6	12,3
RSD		0,5	1,3	7,5	13,4	6,8

Specimen info	No	Diameter (mm)	Young's Modulus Of Bending (MPa)	Maximum Bending Stress at Maximum Load (MPa)	Work from preload to Break (Ncm)	Load at Maximum Load (N)
4/4_3mm/s	1	2,69	49642,77327	1159,91885	140,3629369	177,3267799
4/4_3mm/s	2	2,68	48683,93242	1280,231437	114,4676969	193,5453541
4/4_3mm/s	3	2,69	53434,70216	1202,075073	110,2750108	183,7715646
4/4_3mm/s	4	2,68	52481,90593	1148,437605	73,86464627	173,6207661
4/4_3mm/s	5	2,69	49530,24856	1235,133304	78,50975731	188,8254609
4/4_3mm/s	6	2,69	52879,43145	1098,90907	86,06509483	167,9996896
4/4_3mm/s	7	2,70	49518,58179	1186,233773	76,44734404	183,3797847
4/4_3mm/s	8	2,69	50805,95727	1184,989134	109,4810572	181,15949
Average		2,69	50872,19	1186,99	98,68	181,20
SD		0,01	1817,54	55,06	23,65	8,18
RSD (%)		0,24	3,57	4,64	23,96	4,52

Specimen info	No	Diameter (mm)	Young's Modulus Of Bending (MPa)	Maximum Bending Stress at Maximum Load (MPa)	Work from preload to Break (Ncm)	Load at Maximum Load (N)
4/4_4mm/s	1	2,67	38767,3979	1108,175076	84,50175224	165,6654878
4/4_4mm/s	2	2,67	42626,65667	1027,360992	95,55784515	153,5842698
4/4_4mm/s	3	2,70	42127,24819	1054,091387	111,2831668	162,9519037
4/4_4mm/s	4	2,68	45367,59788	1016,566991	87,90183138	153,6845703
4/4_4mm/s	5	2,68	43760,60125	1121,259722	60,92990652	169,5120145
4/4_4mm/s	6	2,68	43757,99325	932,8158251	43,70402182	141,0230713
4/4_4mm/s	7	2,68	48636,45689	1022,041071	73,26474735	154,5121415
4/4_4mm/s	8	2,68	42164,68422	1086,274576	79,79819776	164,2229611
Average		2,68	43401,07	1046,07	79,62	158,14
SD		0,01	2847,43	60,73	20,80	9,20
RSD (%)		0,35	6,56	5,81	26,13	5,82

Specimen info	No	Diameter (mm)	Young's Modulus Of Bending (MPa)	Maximum Bending Stress at Maximum Load (MPa)	Work from preload to Break (Ncm)	Load at Maximum Load (N)
4/4_5mm/s	1	2,68	39189,83056	1060,428441	55,39763034	160,3155431
4/4_5mm/s	2	2,68	37117,6142	901,5805006	61,65294554	136,3009157
4/4_5mm/s	3	2,68	42428,97331	1018,657722	102,6562674	154,0006469
4/4_5mm/s	4	2,68	46316,7734	1089,971251	91,50813031	164,7818244
4/4_5mm/s	5	2,67	38287,79257	1066,188856	92,74305619	159,3888013
4/4_5mm/s	6	2,67	43515,88329	994,9341421	77,59445332	148,7366514
4/4_5mm/s	7	2,67	43611,92527	1118,814929	100,6717433	167,2560817
4/4_5mm/s	9	2,67	39147,02232	830,5529758	49,61309492	124,1626588
Average		2,68	41201,98	1010,14	78,98	151,87
SD		0,01	3213,25	98,70	21,04	14,91
RSD (%)		0,20	7,80	9,77	26,64	9,82

Specimen info	No	Diameter (mm)	Young's Modulus Of Bending (MPa)	Maximum Bending Stress at Maximum Load (MPa)	Work from preload to Break (Ncm)	Load at Maximum Load (N)
4/4_6mm/s_uu	1	2,68	42417,76226	1005,333085	106,9819806	151,9862286
4/4_6mm/s_uu	2	2,68	39085,01833	946,7415312	74,08084036	143,1283591
4/4_6mm/s_uu	3	2,69	41312,45564	1089,595113	90,34594201	166,5757849
4/4_6mm/s_uu	4	2,68	33733,78999	1001,519203	70,49198659	151,4096461
4/4_6mm/s_uu	5	2,68	37285,40717	885,4500735	46,41740289	133,8623182
4/4_6mm/s_uu	6	2,66	43774,26	1019,274277	78,67112104	150,6696764
4/4_6mm/s_uu	7	2,66	41378,54276	816,4687367	41,8813664	120,6908514
4/4_6mm/s_uu	8	2,67	44782,94771	857,1633326	72,8609862	128,1407466
Average		2,68	40471,27	952,69	72,72	143,31
SD		0,01	3630,92	93,02	21,28	14,96
RSD		0,4	9,0	9,8	29,3	10,4

Specimen info	No	Diameter (mm)	Young's Modulus Of Bending (MPa)	Maximum Bending Stress at Maximum Load (MPa)	Work from preload to Break (Ncm)	Load at Maximum Load (N)
4/4_7mm/s	1	2,66	29771,3477	965,6123973	81,03767194	142,7373482
4/4_7mm/s	2	2,67	32900,54169	941,194867	73,3492331	140,7029541
4/4_7mm/s	3	2,67	14874,70116	590,0785683	85,77121733	88,21318579
4/4_7mm/s	4	2,67	33807,1027	989,5418248	82,13934835	147,9305325
4/4_7mm/s	5	2,68	41148,67038	1028,902015	88,73514521	155,5493788
4/4_7mm/s	6	2,65	22357,73546	781,0164292	97,44687785	114,1530903
4/4_7mm/s	7	2,67	35112,47916	952,479156	74,30103901	142,3897377
4/4_7mm/s	9	2,67	37484,49785	1031,483837	71,38190488	154,2006102
Average		2,67	30932,13	910,04	81,77	135,73
SD		0,01	8532,59	151,22	8,83	23,07
RSD (%)		0,33	27,58	16,62	10,80	16,99

Specimen info	No	Diameter (mm)	Young's Modulus Of Bending (MPa)	Maximum Bending Stress at Maximum Load (MPa)	Work from preload to Break (Ncm)	Load at Maximum Load (N)
4/4_8mm/s	1	2,65	31923,99744	885,9317731	60,06840808	129,4874805
4/4_8mm/s	2	2,65	32898,60148	1023,516537	95,439983	149,5968218
4/4_8mm/s	3	2,65	30103,55912	921,4256327	59,30312574	134,6752507
4/4_8mm/s	5	2,65	36586,70848	1014,022698	68,42232356	148,2092057
4/4_8mm/s	6	2,65	36510,8367	797,1643478	51,963903	116,5132644
4/4_8mm/s	7	2,65	34535,60489	897,5872019	89,37031314	131,1910339
4/4_8mm/s	9	2,65	31564,40142	851,1024001	62,6340544	124,3968314
Average		2,65	33446,24	912,96	69,60	133,44
SD		0,00	2509,08	82,37	16,41	12,04
RSD (%)		0,00	7,50	9,02	23,58	9,02

Raw Data

FRC-posts for rootcanal posts
Light intensity and speed
May 2012/Hmar

Specimen info	No	Diameter (mm)	Young's Modulus Of Bending (MPa)	Load at Maximum Load (N)	Maximum Bending Stress at Maximum Load (MPa)	Work from preload to Break (Ncm)
1/4_2mm/s	1	2,70	46079,18	181,86	1176,42	82,10
1/4_2mm/s	2	2,68	46343,74	185,81	1229,04	151,77
1/4_2mm/s	4	2,68	47688,86	191,59	1267,30	91,39
1/4_2mm/s	5	2,68	47082,28	200,00	1322,90	114,01
1/4_2mm/s	6	2,71	45646,00	188,94	1208,74	130,70
1/4_2mm/s	7	2,69	45405,43	176,65	1155,50	101,49
1/4_2mm/s	8	2,70	46518,65	169,88	1098,89	101,31
Average		2,69	46394,88	184,96	1208,40	110,40
SD		0,01	796,28	9,94	73,96	24,02
RSD		0,5	1,7	5,4	6,1	21,8

Specimen info	No	Diameter (mm)	Young's Modulus Of Bending (MPa)	Load at Maximum Load (N)	Maximum Bending Stress at Maximum Load (MPa)	Work from preload to Break (Ncm)
1/4_3mm/s	1	2,70	37839,64	158,14	1022,97	81,31
1/4_3mm/s	2	2,71	38808,45	177,50	1135,53	64,88
1/4_3mm/s	3	2,70	35722,63	147,44	953,76	75,06
1/4_3mm/s	4	2,69	37843,86	136,68	894,03	97,37
1/4_3mm/s	5	2,68	38004,92	166,82	1103,44	69,66
1/4_3mm/s	6	2,67	37769,78	162,08	1084,18	96,52
1/4_3mm/s	7	2,67	36992,72	141,47	946,35	111,23
1/4_3mm/s	8	2,68	36229,83	162,26	1073,30	123,68
Average		2,69	37401,48	156,55	1026,70	89,96
SD		0,01	1015,97	13,71	86,69	20,79
RSD		0,6	2,7	8,8	8,4	23,1

Specimen info	No	Diameter (mm)	Young's Modulus Of Bending (MPa)	Load at Maximum Load (N)	Maximum Bending Stress at Maximum Load (MPa)	Work from preload to Break (Ncm)
1/4_4mm/s	1	2,63	42862,01	141,09	987,48	116,84
1/4_4mm/s	2	2,62	36867,52	154,44	1093,35	110,09
1/4_4mm/s	3	2,65	37977,53	164,76	1127,23	134,46
1/4_4mm/s	4	2,65	33538,02	144,30	987,28	87,37
1/4_4mm/s	5	2,65	35692,45	144,27	987,09	97,89
1/4_4mm/s	6	2,66	30701,28	145,88	986,86	97,42
1/4_4mm/s	7	2,66	38370,16	159,30	1077,66	121,32
1/4_4mm/s	8	2,64	32872,67	178,89	1237,88	148,52
1/4_4mm/s	9	2,68	36896,67	148,14	979,88	102,04
Average		2,65	36197,59	153,45	1051,63	112,88
SD		0,02	3567,80	12,33	89,85	19,57
RSD		0,7	9,9	8,0	8,5	17,3

Specimen info	No	Diameter (mm)	Young's Modulus Of Bending (MPa)	Load at Maximum Load (N)	Maximum Bending Stress at Maximum Load (MPa)	Work from preload to Break (Ncm)
1/4_5mm/s	1	2,65	32027,62	144,12	986,01	100,48
1/4_5mm/s	2	2,63	23814,78	103,01	720,99	39,92
1/4_5mm/s	3	2,66	25106,33	80,68	545,77	20,04
1/4_5mm/s	4	2,66	32101,16	150,16	1015,81	107,15
1/4_5mm/s	5	2,66	26059,09	126,23	853,92	116,12
1/4_5mm/s	6	2,64	27837,01	142,43	985,61	99,02
1/4_5mm/s	7	2,64	27638,29	141,18	976,96	108,88
1/4_5mm/s	8	2,68	23868,97	123,76	818,66	80,22
Average		2,65	27306,66	126,45	862,97	83,98
SD		0,02	3296,64	23,90	164,47	35,32
RSD		0,6	12,1	18,9	19,1	42,1

Specimen info	No	Diameter (mm)	Young's Modulus Of Bending (MPa)	Load at Maximum Load (N)	Maximum Bending Stress at Maximum Load (MPa)	Work from preload to Break (Ncm)
1/4_6mm/s	1	2,61	29216,70	104,72	749,94	83,82
1/4_6mm/s	2	2,59	30530,07	126,62	927,95	111,03
1/4_6mm/s	3	2,58	34798,79	125,97	933,94	106,18
1/4_6mm/s	4	2,55	35748,26	103,70	796,32	110,66
1/4_6mm/s	5	2,56	29217,55	126,89	962,94	110,47
1/4_6mm/s	6	2,56	28518,04	120,16	911,92	78,62
1/4_6mm/s	7	2,55	28116,45	108,58	833,72	95,08
Average		2,57	30877,98	116,66	873,82	99,41
SD		0,02	3107,13	10,63	80,52	13,68
RSD		0,9	10,1	9,1	9,2	13,8

Specimen info	No	Diameter (mm)	Young's Modulus Of Bending (MPa)	Load at Maximum Load (N)	Maximum Bending Stress at Maximum Load (MPa)	Work from preload to Break (Ncm)
1/4_7mm/s	1	2,59	37674,73	94,14	689,90	74,49
1/4_7mm/s	2	2,62	25726,23	118,20	836,79	75,66
1/4_7mm/s	2	2,65	23282,60	130,77	894,67	84,21
1/4_7mm/s	4	2,66	25043,76	143,32	969,57	109,75
1/4_7mm/s	5	2,60	31220,36	125,07	906,02	71,75
1/4_7mm/s	6	2,69	26205,82	131,21	858,25	112,75
1/4_7mm/s	7	2,68	26678,11	137,45	909,19	103,33
Average		2,64	27975,94	125,74	866,34	90,28
SD		0,04	4917,60	16,11	88,45	17,78
RSD		1,5	17,6	12,8	10,2	19,7

Specimen info	No	Diameter (mm)	Young's Modulus Of Bending (MPa)	Load at Maximum Load (N)	Maximum Bending Stress at Maximum Load (MPa)	Work from preload to Break (Ncm)
2/4_2mm/s	1	2,70	45833,39	176,06	1138,90	92,17
2/4_2mm/s	2	2,69	48186,71	174,75	1143,03	62,83
2/4_2mm/s	3	2,71	44837,39	176,73	1130,59	51,61
2/4_2mm/s	4	2,67	52226,85	180,73	1208,98	94,25
2/4_2mm/s	5	2,67	51521,36	191,78	1282,89	99,44
2/4_2mm/s	6	2,68	52358,92	185,68	1228,19	111,87
2/4_2mm/s	7	2,68	53996,63	166,03	1098,22	62,16
Average		2,69	49851,61	178,82	1175,83	82,05
SD		0,02	3558,04	8,28	65,59	22,86
RSD		0,6	7,1	4,6	5,6	27,9

Specimen info	No	Diameter (mm)	Young's Modulus Of Bending (MPa)	Load at Maximum Load (N)	Maximum Bending Stress at Maximum Load (MPa)	Work from preload to Break (Ncm)
2/4_3mm/s	1	2,66	56275,22	174,51	1180,58	132,92
2/4_3mm/s	2	2,67	38178,11	158,72	1061,72	84,77
2/4_3mm/s	3	2,69	42257,61	187,34	1225,42	82,77
2/4_3mm/s	4	2,71	48553,98	140,65	899,78	41,05
2/4_3mm/s	5	2,67	42216,68	153,57	1027,27	170,26
2/4_3mm/s	6	2,68	52023,25	176,56	1167,89	94,00
2/4_3mm/s	7	2,66	47440,83	182,79	1236,58	124,81
2/4_3mm/s	8	2,71	52859,10	148,70	951,28	105,71
2/4_3mm/s	9	2,75	48053,89	181,73	1112,62	81,75
Average		2,69	47539,85	167,18	1095,91	102,00
SD		0,03	5808,24	16,98	119,61	37,09
RSD		1,1	12,2	10,2	10,9	36,4

Specimen info	No	Diameter (mm)	Young's Modulus Of Bending (MPa)	Load at Maximum Load (N)	Maximum Bending Stress at Maximum Load (MPa)	Work from preload to Break (Ncm)
2/4_4mm/s_uusi	1	2,63	53274,391	157,729	1103,964	64,326
2/4_4mm/s_uusi	2	2,63	46591,851	119,803	838,515	76,917
2/4_4mm/s_uusi	3	2,61	39613,120	144,189	1032,571	47,487
2/4_4mm/s_uusi	5	2,61	45691,191	145,510	1042,030	80,773
2/4_4mm/s_uusi	6	2,61	45416,964	153,789	1101,322	60,101
2/4_4mm/s_uusi	7	2,60	33917,694	136,222	986,818	62,039
2/4_4mm/s_uusi	8	2,60	40781,466	109,620	794,109	60,698
2/4_4mm/s_uusi	9	2,59	48286,885	139,688	1023,697	74,570
Average		2,61	44196,70	138,32	990,38	65,86
SD		0,01	5939,27	16,37	114,87	10,92
RSD		0,5	13,4	11,8	11,6	16,6

Specimen info	No	Diameter (mm)	Young's Modulus Of Bending (MPa)	Load at Maximum Load (N)	Maximum Bending Stress at Maximum Load (MPa)	Work from preload to Break (Ncm)
2/4_5mm/s	1	2,67	45794,53	169,66	1134,87	113,13
2/4_5mm/s	2	2,71	39078,48	149,79	958,23	94,85
2/4_5mm/s	3	2,65	36564,85	177,86	1216,88	130,19
2/4_5mm/s	4	2,68	41607,95	176,99	1170,71	123,73
2/4_5mm/s	5	2,67	37592,21	167,89	1123,03	90,22
2/4_5mm/s	6	2,71	35619,64	171,92	1099,82	118,76
2/4_5mm/s	7	2,66	36163,64	161,97	1095,73	95,22
2/4_5mm/s	8	2,73	35121,37	166,69	1043,08	98,17
Average		2,69	38317,83	167,84	1105,29	108,03
SD		0,03	3635,56	8,99	78,86	15,26
RSD		1,1	9,5	5,4	7,1	14,1

Specimen info	No	Diameter (mm)	Young's Modulus Of Bending (MPa)	Load at Maximum Load (N)	Maximum Bending Stress at Maximum Load (MPa)	Work from preload to Break (Ncm)
2/4_6mm/s	1	2,66	43735,51	187,09	1265,66	128,13
2/4_6mm/s	2	2,71	39688,06	172,47	1103,36	100,93
2/4_6mm/s	3	2,72	39894,27	176,06	1113,92	102,62
2/4_6mm/s	4	2,70	46793,28	185,01	1196,75	101,39
2/4_6mm/s	5	2,73	42326,16	169,57	1061,16	80,65
2/4_6mm/s	6	2,73	41971,51	194,81	1219,06	116,10
2/4_6mm/s	7	2,68	39790,35	175,09	1158,13	101,56
2/4_6mm/s	8	2,68	43838,69	204,98	1355,85	130,71
Average		2,70	42254,73	183,13	1184,24	107,76
SD		0,03	2496,23	12,22	96,19	16,47
RSD		1,0	5,9	6,7	8,1	15,3

Specimen info	No	Diameter (mm)	Young's Modulus Of Bending (MPa)	Load at Maximum Load (N)	Maximum Bending Stress at Maximum Load (MPa)	Work from preload to Break (Ncm)
2/4_7mm/s	1	2,66	33725,91	147,55	998,20	99,55
2/4_7mm/s	2	2,65	48010,06	144,23	986,82	87,73
2/4_7mm/s	3	2,64	41386,15	138,60	959,08	82,72
2/4_7mm/s	4	2,68	38127,82	156,06	1032,31	102,42
2/4_7mm/s	5	2,68	36553,28	161,22	1066,42	111,03
2/4_7mm/s	6	2,68	30944,46	148,64	983,21	95,65
2/4_7mm/s	7	2,67	38895,20	160,90	1076,28	69,29
2/4_7mm/s	8	2,65	30392,40	132,84	908,84	82,38
Average		2,66	37254,41	148,76	1001,40	91,35
SD		0,02	5807,08	10,25	55,68	13,36
RSD		0,6	15,6	6,9	5,6	14,6

Specimen info	No	Diameter (mm)	Young's Modulus Of Bending (MPa)	Load at Maximum Load (N)	Maximum Bending Stress at Maximum Load (MPa)	Work from preload to Break (Ncm)
2/4_8mm/s	1	2,67	37368,73	153,95	1029,79	73,43
2/4_8mm/s	2	2,67	35899,65	153,12	1024,25	74,42
2/4_8mm/s	3	2,68	30994,52	133,94	885,98	80,86
2/4_8mm/s	4	2,68	34429,12	156,04	1032,14	100,10
2/4_8mm/s	5	2,68	27846,96	141,30	934,65	80,65
2/4_8mm/s	6	2,67	39813,54	143,48	959,80	84,66
2/4_8mm/s	7	2,65	38285,13	152,75	1045,08	85,29
2/4_8mm/s	8	2,66	36879,92	156,49	1058,67	86,11
Average		2,67	35189,70	148,88	996,30	83,19
SD		0,01	3985,05	8,26	61,83	8,32
RSD		0,4	11,3	5,5	6,2	10,0

Raw Data

Specimen info	No	Diameter (mm)	Young's Modulus Of Bending (MPa)	Load at Maximum Load (N)	Maximum Bending Stress at Maximum Load (MPa)	Work from preload to Break (Ncm)
3/4 2mm/s	1	2,68	49125,66	185,55	1227,35	51,10
3/4 2mm/s	2	2,69	51447,27	187,69	1227,73	73,64
3/4 2mm/s	3	2,69	49512,34	178,84	1169,84	83,27
3/4 2mm/s	4	2,68	50220,03	193,41	1279,34	74,33
3/4 2mm/s	5	2,68	56808,30	171,50	1134,41	76,96
3/4 2mm/s	6	2,70	49582,61	190,94	1235,12	78,59
3/4 2mm/s	7	2,68	57378,94	195,52	1293,31	99,24
3/4 2mm/s	8	2,68	53910,97	193,84	1282,18	84,92
Average		2,69	52248,27	187,16	1231,16	77,76
SD		0,01	3358,98	8,32	56,00	13,54
RSD		0,3	6,4	4,4	4,5	17,4

Specimen info	No	Diameter (mm)	Young's Modulus Of Bending (MPa)	Load at Maximum Load (N)	Maximum Bending Stress at Maximum Load (MPa)	Work from preload to Break (Ncm)
3/4 3mm/s	1	2,66	48124,82	180,67	1222,20	112,08
3/4 3mm/s	2	2,67	47473,49	177,11	1184,74	93,37
3/4 3mm/s	3	2,66	45170,95	192,03	1299,10	115,61
3/4 3mm/s	4	2,68	41020,56	160,45	1061,31	94,15
3/4 3mm/s	5	2,68	47663,75	176,29	1166,06	130,78
3/4 3mm/s	6	2,68	48902,05	173,46	1147,38	103,96
3/4 3mm/s	7	2,68	44337,99	190,45	1259,77	65,91
3/4 3mm/s	8	2,68	48138,72	181,01	1197,33	105,38
Average		2,67	46354,04	178,93	1192,24	102,66
SD		0,01	2664,36	9,95	72,51	19,15
RSD		0,3	5,7	5,6	6,1	18,7

Specimen info	No	Diameter (mm)	Young's Modulus Of Bending (MPa)	Load at Maximum Load (N)	Maximum Bending Stress at Maximum Load (MPa)	Work from preload to Break (Ncm)
3/4 4mm/s_uusit	1	2,68	49498,86	151,92	1004,89	47,84
3/4 4mm/s_uusit	2	2,66	46296,54	166,75	1128,04	97,54
3/4 4mm/s_uusit	3	2,69	49945,21	182,16	1191,55	86,77
3/4 4mm/s_uusi	4	2,68	43449,02	160,88	1064,18	102,56
3/4 4mm/s_uusit	5	2,70	44689,24	178,89	1157,18	57,26
3/4 4mm/s_uusit	6	2,69	48244,97	147,36	963,91	80,48
3/4 4mm/s_uusit	7	2,70	46279,63	170,71	1104,25	78,85
3/4 4mm/s_uusit	8	2,69	45451,49	161,31	1055,12	81,33
Average		2,69	46731,87	165,00	1083,64	79,08
SD		0,01	2306,95	12,16	76,70	18,56
RSD		0,5	4,9	7,4	7,1	23,5

Specimen info	No	Diameter (mm)	Young's Modulus Of Bending (MPa)	Load at Maximum Load (N)	Maximum Bending Stress at Maximum Load (MPa)	Work from preload to Break (Ncm)
3/4 5mm/s	1	2,65	39525,60	158,65	1085,44	126,72
3/4 5mm/s	2	2,64	41709,77	130,63	903,92	87,99
3/4 5mm/s	3	2,64	37437,28	151,59	1048,99	71,97
3/4 5mm/s	4	2,66	39754,63	155,24	1050,20	112,83
3/4 5mm/s	5	2,61	39435,02	160,09	1146,46	92,35
3/4 5mm/s	6	2,61	43406,95	175,42	1256,26	103,46
3/4 5mm/s	7	2,62	40638,06	147,79	1046,26	108,56
3/4 5mm/s	8	2,61	34680,06	149,33	1069,37	138,30
3/4 5mm/s	9	2,59	37563,10	151,36	1109,23	102,54
Average		2,63	39350,05	153,34	1079,57	104,97
SD		0,02	2562,91	11,91	93,86	20,01
RSD		0,9	6,5	7,8	8,7	19,1

Specimen info	No	Diameter (mm)	Young's Modulus Of Bending (MPa)	Load at Maximum Load (N)	Maximum Bending Stress at Maximum Load (MPa)	Work from preload to Break (Ncm)
3/4 6mm/s	1	2,67	37320,95	158,15	1057,89	81,26
3/4 6mm/s	3	2,67	37622,93	154,20	1031,46	71,88
3/4 6mm/s	4	2,70	33494,33	143,32	927,07	49,53
3/4 6mm/s	5	2,67	38314,68	156,20	1044,84	67,45
3/4 6mm/s	6	2,68	35475,18	149,13	986,45	82,06
3/4 6mm/s	7	2,69	38159,11	157,20	1028,27	81,91
3/4 6mm/s	8	2,69	37306,18	150,62	985,24	74,81
3/4 6mm/s	9	2,67	35578,96	147,30	985,31	91,65
Average		2,68	36659,04	152,01	1005,82	75,07
SD		0,01	1663,08	5,28	42,79	12,70
RSD		0,4	4,5	3,5	4,3	16,9

Specimen info	No	Diameter (mm)	Young's Modulus Of Bending (MPa)	Load at Maximum Load (N)	Maximum Bending Stress at Maximum Load (MPa)	Work from preload to Break (Ncm)
3/4 7mm/s	1	2,70	40809,65	129,12	835,26	74,01
3/4 7mm/s	2	2,69	34964,51	141,03	922,47	74,34
3/4 7mm/s	3	2,69	40519,18	165,96	1085,54	79,76
3/4 7mm/s	4	2,70	37594,17	159,00	1028,55	65,30
3/4 7mm/s	5	2,69	45248,68	164,76	1077,74	68,35
3/4 7mm/s	6	2,70	32825,05	146,73	949,14	72,73
3/4 7mm/s	7	2,71	38489,13	179,50	1149,34	74,06
Average		2,70	38635,77	155,16	1006,72	72,65
SD		0,01	4089,67	17,15	109,24	4,65
RSD		0,3	10,6	11,1	10,9	6,4

Specimen info	No	Diameter (mm)	Young's Modulus Of Bending (MPa)	Load at Maximum Load (N)	Maximum Bending Stress at Maximum Load (MPa)	Work from preload to Break (Ncm)
3/4 8mm/s	1	2,67	31120,88	136,78	914,93	52,53
3/4 8mm/s	2	2,68	32505,46	146,23	967,25	67,29
3/4 8mm/s	3	2,69	28303,36	125,82	823,00	73,76
3/4 8mm/s	4	2,65	27643,29	120,56	824,84	68,55
3/4 8mm/s	5	2,67	37495,66	123,32	824,90	95,72
3/4 8mm/s	6	2,67	27153,75	132,51	886,40	74,51
3/4 8mm/s	7	2,67	28773,03	119,33	798,22	68,69
3/4 8mm/s	8	2,66	34349,11	128,06	866,32	87,19
Average		2,67	30918,07	129,08	863,23	73,53
SD		0,01	3663,13	9,08	57,10	13,14
RSD		0,4	11,8	7,0	6,6	17,9

Specimen info	No	Diameter (mm)	Young's Modulus Of Bending (MPa)	Load at Maximum Load (N)	Maximum Bending Stress at Maximum Load (MPa)	Work from preload to Break (Ncm)
4/4 2mm/s	1	2,67	47397,18	178,43	1193,57	55,48
4/4 2mm/s	2	2,68	53340,72	195,83	1295,36	82,12
4/4 2mm/s	3	2,69	50906,52	181,91	1189,89	75,24
4/4 2mm/s	4	2,70	50541,98	176,32	1140,55	80,02
4/4 2mm/s	5	2,70	48757,58	158,21	1023,44	70,15
4/4 2mm/s	6	2,68	52800,18	167,41	1107,35	58,94
4/4 2mm/s	7	2,68	47569,87	159,32	1053,87	84,91
4/4 2mm/s	8	2,67	51747,37	167,16	1118,16	65,43
Average		2,68	50382,67	173,07	1140,27	71,53
SD		0,01	2274,79	12,61	86,23	10,90
RSD		0,4	4,5	7,3	7,6	15,2

Specimen info	No	Diameter (mm)	Young's Modulus Of Bending (MPa)	Load at Maximum Load (N)	Maximum Bending Stress at Maximum Load (MPa)	Work from preload to Break (Ncm)
4/4 3mm/s	1	2,70	42066,35	174,57	1129,22	87,81
4/4 3mm/s	2	2,70	51167,33	189,32	1224,66	86,04
4/4 3mm/s	3	2,71	48252,04	177,05	1132,64	95,87
4/4 3mm/s	4	2,69	50891,00	177,32	1159,86	82,03
4/4 3mm/s	5	2,70	50592,64	172,72	1117,25	98,55
4/4 3mm/s	6	2,70	44384,85	167,88	1085,99	117,34
4/4 3mm/s	7	2,69	45582,66	166,83	1091,25	108,56
4/4 3mm/s	8	2,70	50363,37	202,71	1311,27	70,26
Average		2,70	47912,53	178,55	1156,52	93,31
SD		0,01	3480,98	11,98	76,25	15,05
RSD		0,2	7,3	6,7	6,6	16,1

Specimen info	No	Diameter (mm)	Young's Modulus Of Bending (MPa)	Load at Maximum Load (N)	Maximum Bending Stress at Maximum Load (MPa)	Work from preload to Break (Ncm)
4/4 4mm/s	1	2,70	45667,69	174,79	1130,66	72,59
4/4 4mm/s	2	2,69	50663,49	176,47	1154,29	85,72
4/4 4mm/s	3	2,69	44365,92	168,94	1105,06	82,01
4/4 4mm/s	4	2,70	51295,63	185,82	1202,00	87,89
4/4 4mm/s	5	2,70	49028,55	170,73	1104,41	68,67
4/4 4mm/s	6	2,69	50985,97	175,25	1148,33	72,48
4/4 4mm/s	7	2,69	51690,80	189,02	1236,39	97,87
4/4 4mm/s	8	2,69	43709,80	166,87	1091,54	67,82
Average		2,69	48425,98	175,99	1146,34	79,38
SD		0,01	3319,89	7,83	50,68	10,71
RSD		0,2	6,9	4,4	4,4	13,5

Specimen info	No	Diameter (mm)	Young's Modulus Of Bending (MPa)	Load at Maximum Load (N)	Maximum Bending Stress at Maximum Load (MPa)	Work from preload to Break (Ncm)
4/4 5mm/s	1	2,67	43438,40	179,04	1197,64	113,66
4/4 5mm/s	2	2,65	48176,37	161,58	1105,48	98,84
4/4 5mm/s	3	2,66	37331,84	157,88	1068,07	95,12
4/4 5mm/s	4	2,64	39324,43	166,67	1153,36	92,56
4/4 5mm/s	5	2,67	40803,97	153,82	1028,91	105,46
4/4 5mm/s	6	2,64	38622,56	156,15	1080,53	97,85
4/4 5mm/s	7	2,67	41062,82	167,40	1119,76	100,81
4/4 5mm/s	8	2,68	37978,69	160,46	1061,35	92,83
Average		2,66	40842,38	162,87	1101,89	99,64
SD		0,02	3552,33	8,07	54,40	7,10
RSD		0,6	8,7	5,0	4,9	7,1

Specimen info	No	Diameter (mm)	Young's Modulus Of Bending (MPa)	Load at Maximum Load (N)	Maximum Bending Stress at Maximum Load (MPa)	Work from preload to Break (Ncm)
4/4 6mm/s	1	2,66	37286,18	136,83	925,62	68,98
4/4 6mm/s	2	2,66	37232,77	155,46	1051,66	56,92
4/4 6mm/s	3	2,68	35227,90	151,06	999,21	80,28
4/4 6mm/s	4	2,71	28556,14	131,39	840,54	66,06
4/4 6mm/s	5	2,65	35555,92	140,43	960,83	80,68
4/4 6mm/s	6	2,65	33280,01	125,96	861,78	76,21
4/4 6mm/s	7	2,65	29408,07	131,47	899,52	72,19
4/4 6mm/s	8	2,67	36255,23	132,94	889,29	75,48
Average		2,67	34100,28	138,19	928,56	72,10
SD		0,02	3410,57	10,28	71,90	7,98
RSD		0,8	10,0	7,4	7,7	11,1

Specimen info	No	Diameter (mm)	Young's Modulus Of Bending (MPa)	Load at Maximum Load (N)	Maximum Bending Stress at Maximum Load (MPa)	Work from preload to Break (Ncm)
4/4 7mm/s	1	2,64	40854,35	148,94	1030,66	60,18
4/4_7mm/s	2	2,64	33122,96	119,17	824,65	72,01
4/4 7mm/s	3	2,66	32572,06	137,68	931,42	89,72
4/4 7mm/s	4	2,64	33289,47	129,38	895,32	60,33
4/4 7mm/s	5	2,65	36969,29	145,81	997,63	63,07
4/4 7mm/s	6	2,66	31852,00	126,04	852,65	75,75
4/4 7mm/s	7	2,66	38846,74	161,61	1093,30	83,01
4/4 7mm/s	8	2,68	38679,14	143,50	949,19	53,24
4/4 7mm/s	9	2,68	31526,83	132,46	876,20	64,25
Average		2,66	35301,43	138,29	939,00	69,06
SD		0,02	3535,25	13,09	88,17	11,93
RSD		0,6	10,0	9,5	9,4	17,3

Specimen info	No	Diameter (mm)	Young's Modulus Of Bending (MPa)	Load at Maximum Load (N)	Maximum Bending Stress at Maximum Load (MPa)	Work from preload to Break (Ncm)
4/4 8mm/s	1	2,64	36208,67	124,42	861,00	45,60
4/4 8mm/s	2	2,60	28053,98	109,19	790,97	79,59
4/4 8mm/s	3	2,64	31129,68	139,29	963,88	68,02
4/4 8mm/s	4	2,58	33148,23	127,84	947,80	83,85
4/4 8mm/s	5	2,58	29357,01	124,38	922,19	60,57
4/4 8mm/s	6	2,58	32182,90	128,73	954,42	64,72
4/4 8mm/s	7	2,60	41417,04	136,24	986,97	64,66
4/4 8mm/s	8	2,60	31484,17	128,71	932,37	64,14
Average		2,60	32872,71	127,35	919,95	66,39
SD		0,02	4229,70	9,05	63,98	11,70
RSD		1,0	12,9	7,1	7,0	17,6

Raw Data

Effect of pretension on mechanical properties

August 2012/Hmar

Specimen info	No	Diameter (mm)	Young's Modulus Of Bending (MPa)	Load at Maximum Load (N)	Maximum Bending Stress at Maximum Load (MPa)	Work from preload to Break (Ncm)
pretension_1	1	2,70	47808,27	180,64	1168,49	62,39
pretension_1	2	2,70	45855,91	148,40	959,93	63,09
pretension_1	3	2,71	44670,88	133,62	854,79	75,28
pretension_1	4	2,68	50479,27	151,04	999,08	38,36
pretension_1	5	2,68	49901,67	160,89	1064,23	59,15
pretension_1	6	2,68	53303,40	149,87	991,34	52,99
pretension_1	7	2,68	52781,06	159,80	1057,02	62,39
pretension_1	8	2,68	47071,75	161,39	1067,52	63,53
Av.		2,7	48984,0	155,7	1020,3	59,6
SD		0,0	3152,8	13,6	92,4	10,6
RSD		0,5	6,4	8,7	9,1	17,7

Specimen info	No	Diameter (mm)	Young's Modulus Of Bending (MPa)	Load at Maximum Load (N)	Maximum Bending Stress at Maximum Load (MPa)	Work from preload to Break (Ncm)
pretension_2	1	2,69	50518,35	180,17	1178,51	70,66
pretension_2	2	2,70	49034,17	155,54	1006,15	71,67
pretension_2	3	2,70	47140,53	167,74	1085,07	65,71
pretension_2	4	2,71	48860,42	180,27	1153,26	58,12
pretension_2	6	2,70	47059,29	159,07	1028,98	75,17
pretension_2	7	2,71	48115,12	178,57	1142,41	69,96
pretension_2	8	2,69	50240,82	181,51	1187,28	80,61
Av.		2,7	48709,8	171,8	1111,7	70,3
SD		0,0	1371,3	11,0	72,5	7,1
RSD		0,3	2,8	6,4	6,5	10,1

Specimen info	No	Diameter (mm)	Young's Modulus Of Bending (MPa)	Load at Maximum Load (N)	Maximum Bending Stress at Maximum Load (MPa)	Work from preload to Break (Ncm)
pretension_3	1	2,70	54021,68	181,79	1175,97	56,31
pretension_3	2	2,70	51288,55	179,30	1159,87	61,38
pretension_3	3	2,71	49054,03	175,93	1125,47	61,48
pretension_3	4	2,69	53251,07	157,24	1028,52	35,20
pretension_3	5	2,70	51441,35	165,81	1072,56	66,34
pretension_3	6	2,71	50704,70	169,07	1081,59	50,18
pretension_3	7	2,70	49962,36	173,91	1124,96	58,49
pretension_3	8	2,71	48345,26	153,66	983,02	68,52
Av.		2,7	51008,6	169,6	1094,0	57,2
SD		0,0	1944,7	10,2	65,7	10,6
RSD		0,3	3,8	6,0	6,0	18,5

Specimen info	No	Diameter (mm)	Young's Modulus Of Bending (MPa)	Load at Maximum Load (N)	Maximum Bending Stress at Maximum Load (MPa)	Work from preload to Break (Ncm)
pretension_4	1	2,68	50986,24	136,25	901,22	36,92
pretension_4	2	2,65	51536,18	160,92	1100,98	79,02
pretension_4	3	2,65	52059,23	161,20	1102,88	73,10
pretension_4	4	2,66	50380,33	154,15	1042,83	54,39
pretension_4	5	2,65	51088,12	155,21	1061,92	72,87
pretension_4	6	2,65	52073,44	155,17	1061,65	38,60
pretension_4	7	2,66	52662,09	168,26	1138,29	82,55
pretension_4	8	2,67	52031,49	146,41	979,34	61,16
Av.		2,7	51602,1	154,7	1048,6	62,3
SD		0,0	744,5	9,8	76,2	17,7
RSD		0,4	1,4	6,3	7,3	28,4

Specimen info	No	Diameter (mm)	Young's Modulus Of Bending (MPa)	Load at Maximum Load (N)	Maximum Bending Stress at Maximum Load (MPa)	Work from preload to Break (Ncm)
pretension_5	1	2,71	46274,80	148,79	951,86	49,39
pretension_5	2	2,71	47720,36	169,43	1083,90	50,99
pretension_5	3	2,71	52019,38	161,66	1034,18	43,12
pretension_5	4	2,71	50742,47	178,34	1140,94	62,98
pretension_5	5	2,71	50766,56	154,39	987,70	53,46
pretension_5	6	2,70	47238,67	155,69	1007,13	45,45
pretension_5	7	2,71	50068,32	158,83	1016,10	56,81
pretension_5	8	2,71	43582,37	152,17	973,51	64,14
Av.		2,7	48551,6	159,9	1024,4	53,3
SD		0,0	2836,6	9,8	61,9	7,6
RSD		0,1	5,8	6,1	6,0	14,3

Raw Data

FRC-poles for root canal posts
The effect of postcuring
Aug2012

Specimen info	No	Diameter (mm)	Young's Modulus Of Bending (MPa)	Load at Maximum Load (N)	Maximum Bending Stress at Maximum Load (MPa)	Work from preload to Break (Ncm)
postcure_ref	1	2,67	47939,97	124,65	833,80	36,73
postcure_ref	2	2,68	47385,03	127,85	845,69	43,89
postcure_ref	3	2,70	44615,61	118,35	765,57	43,87
postcure_ref	4	2,70	46437,38	129,24	836,01	46,48
postcure_ref	5	2,70	38699,82	124,82	807,42	53,70
postcure_ref	6	2,71	45591,29	137,90	882,23	40,76
postcure_ref	7	2,71	46604,17	123,21	788,23	40,84
postcure_ref	8	2,70	42662,99	148,87	962,99	41,15
Average		2,70	44992,03	129,36	840,24	43,43
SD		0,01	3038,37	9,69	61,27	5,06
RSD (%)		0,5	6,8	7,5	7,3	11,6

Specimen info	No	Diameter (mm)	Young's Modulus Of Bending (MPa)	Load at Maximum Load (N)	Maximum Bending Stress at Maximum Load (MPa)	Work from preload to Break (Ncm)
postcure_100C15min	1	2,72	46165,29	145,80	922,50	54,87
postcure_100C15min	2	2,72	48250,37	175,07	1107,70	48,73
postcure_100C15min	3	2,70	48620,56	169,80	1098,38	64,47
postcure_100C15min	4	2,71	43914,41	143,71	919,38	53,17
postcure_100C15min	5	2,72	44126,12	144,18	912,25	41,77
postcure_100C15min	6	2,72	45794,30	155,38	983,13	41,16
postcure_100C15min	7	2,72	47954,50	146,81	928,87	87,42
postcure_100C15min	8	2,71	47644,65	160,66	1027,83	40,74
Average		2,72	46558,77	155,18	987,51	54,04
SD		0,01	1847,37	12,25	81,37	15,79
RSD (%)		0,3	4,0	7,9	8,2	29,2

Specimen info	No	Diameter (mm)	Young's Modulus Of Bending (MPa)	Load at Maximum Load (N)	Maximum Bending Stress at Maximum Load (MPa)	Work from preload to Break (Ncm)
postcure_100C30min	1	2,68	45165,65	133,28	881,58	44,92
postcure_100C30min	2	2,70	42089,03	146,60	948,29	49,43
postcure_100C30min	3	2,69	43881,51	139,44	912,11	62,44
postcure_100C30min	4	2,72	43324,25	146,49	926,84	71,14
postcure_100C30min	5	2,71	44827,70	152,05	972,75	39,76
postcure_100C30min	6	2,69	42162,32	163,78	1071,29	49,30
postcure_100C30min	7	2,72	41350,39	154,37	976,73	63,11
postcure_100C30min	8	2,72	41130,39	148,15	937,33	57,84
postcure_100C30min	9	2,70	42794,92	138,22	894,14	62,90
Average		2,71	42695,06	148,64	954,94	56,99
SD		0,01	1268,80	8,24	54,78	10,11
RSD (%)		0,5	3,0	5,5	5,7	17,7

Specimen info	No	Diameter (mm)	Young's Modulus Of Bending (MPa)	Load at Maximum Load (N)	Maximum Bending Stress at Maximum Load (MPa)	Work from preload to Break (Ncm)
postcure_100C60min	1	2,70	46952,20	150,46	973,27	45,09
postcure_100C60min	2	2,71	46941,30	155,85	997,04	73,40
postcure_100C60min	3	2,72	45943,78	152,90	967,44	63,87
postcure_100C60min	4	2,72	41393,65	167,62	1060,56	74,69
postcure_100C60min	5	2,71	44473,10	157,31	1006,34	50,98
postcure_100C60min	6	2,75	43482,93	173,86	1064,41	73,18
postcure_100C60min	7	2,72	45996,86	157,48	996,41	76,77
postcure_100C60min	8	2,75	43308,88	182,25	1115,78	85,07
Average		2,72	44811,59	162,22	1022,66	67,88
SD		0,02	1986,56	11,20	52,03	13,63
RSD (%)		0,7	4,4	6,9	5,1	20,1

Specimen info	No	Diameter (mm)	Young's Modulus Of Bending (MPa)	Load at Maximum Load (N)	Maximum Bending Stress at Maximum Load (MPa)	Work from preload to Break (Ncm)
postcure_120C15min	1	2,68	46026,36	153,00	1012,04	45,26
postcure_120C15min	2	2,69	46808,18	160,47	1049,64	59,35
postcure_120C15min	3	2,70	46588,21	169,08	1093,73	74,63
postcure_120C15min	4	2,71	44392,54	169,61	1085,04	45,45
postcure_120C15min	5	2,68	49778,40	159,77	1056,82	53,97
postcure_120C15min	6	2,69	50315,82	156,46	1023,40	65,76
postcure_120C15min	7	2,71	43325,29	179,49	1148,29	93,16
postcure_120C15min	8	2,68	50727,73	162,79	1076,78	86,75
Average		2,69	47245,32	163,83	1068,22	65,54
SD		0,01	2766,78	8,51	43,19	18,06
RSD (%)		0,5	5,9	5,2	4,0	27,6

Specimen info	No	Diameter (mm)	Young's Modulus Of Bending (MPa)	Load at Maximum Load (N)	Maximum Bending Stress at Maximum Load (MPa)	Work from preload to Break (Ncm)
postcure_120C30min	1	2,71	50145,62	159,15	1018,16	48,34
postcure_120C30min	2	2,70	50682,74	179,01	1157,96	69,04
postcure_120C30min	3	2,71	46904,77	164,15	1050,12	87,30
postcure_120C30min	4	2,71	46300,30	172,86	1105,85	64,10
postcure_120C30min	5	2,69	47736,21	159,06	1040,42	56,12
postcure_120C30min	6	2,71	47616,95	134,25	858,85	34,54
postcure_120C30min	7	2,71	45938,21	158,47	1013,77	88,28
postcure_120C30min	8	2,71	48379,27	165,52	1058,89	62,02
Average		2,71	47963,01	161,56	1038,00	63,72
SD		0,01	1710,87	13,21	86,73	18,27
RSD (%)		0,3	3,6	8,2	8,4	28,7

Specimen info	No	Diameter (mm)	Young's Modulus Of Bending (MPa)	Load at Maximum Load (N)	Maximum Bending Stress at Maximum Load (MPa)	Work from preload to Break (Ncm)
postcure_120C60min	1	2,70	47227,83	176,98	1144,85	76,88
postcure_120C60min	2	2,69	47183,45	159,88	1045,79	62,61
postcure_120C60min	3	2,69	49629,31	180,50	1180,68	49,62
postcure_120C60min	4	2,70	49156,52	162,05	1048,27	86,06
postcure_120C60min	5	2,70	48390,76	156,82	1014,40	47,01
postcure_120C60min	6	2,69	49591,01	169,51	1108,80	72,55
postcure_120C60min	7	2,68	48272,68	159,90	1057,67	52,36
postcure_120C60min	8	2,70	48481,26	150,60	974,18	37,50
Average		2,69	48491,61	164,53	1071,83	60,57
SD		0,01	949,57	10,27	68,47	16,76
RSD (%)		0,3	2,0	6,2	6,4	27,7

Specimen info	No	Diameter (mm)	Young's Modulus Of Bending (MPa)	Load at Maximum Load (N)	Maximum Bending Stress at Maximum Load (MPa)	Work from preload to Break (Ncm)
postcure_130C15min	1	2,72	49665,16	153,36	970,29	54,87
postcure_130C15min	2	2,72	46347,97	130,14	823,39	34,03
postcure_130C15min	3	2,72	48979,58	168,94	1068,92	48,79
postcure_130C15min	4	2,72	49525,98	156,28	988,82	50,33
postcure_130C15min	5	2,73	47812,64	147,40	922,37	53,68
postcure_130C15min	6	2,73	47523,80	148,02	926,27	61,58
postcure_130C15min	7	2,71	50986,69	150,20	960,89	57,03
postcure_130C15min	8	2,73	49035,97	142,96	894,61	88,47
Average		2,72	48734,73	149,66	944,45	56,10
SD		0,01	1450,47	11,11	72,07	15,40
RSD (%)		0,3	3,0	7,4	7,6	27,5

Specimen info	No	Diameter (mm)	Young's Modulus Of Bending (MPa)	Load at Maximum Load (N)	Maximum Bending Stress at Maximum Load (MPa)	Work from preload to Break (Ncm)
postcure_130C30min	1	2,72	51065,29	138,60	876,91	31,15
postcure_130C30min	2	2,73	46668,91	157,66	986,58	52,92
postcure_130C30min	3	2,73	48150,85	167,38	1047,44	43,73
postcure_130C30min	4	2,71	46493,97	151,28	967,81	87,76
postcure_130C30min	5	2,72	50699,61	152,19	962,90	63,80
postcure_130C30min	6	2,72	48512,44	159,91	1011,77	53,23
postcure_130C30min	7	2,71	48233,42	151,31	967,97	75,45
postcure_130C30min	8	2,71	50819,67	147,21	941,76	76,47
Average		2,72	48830,52	153,19	970,39	60,56
SD		0,01	1832,10	8,65	50,05	18,84
RSD (%)		0,3	3,8	5,6	5,2	31,1

Specimen info	No	Diameter (mm)	Young's Modulus Of Bending (MPa)	Load at Maximum Load (N)	Maximum Bending Stress at Maximum Load (MPa)	Work from preload to Break (Ncm)
postcure_130C60min	1	2,70	45641,69	150,43	973,06	62,15
postcure_130C60min	2	2,69	43938,91	156,73	1025,18	65,87
postcure_130C60min	3	2,71	48891,25	167,82	1073,60	80,43
postcure_130C60min	4	2,70	49645,34	153,94	995,82	60,87
postcure_130C60min	5	2,69	43477,39	166,41	1088,49	75,54
postcure_130C60min	6	2,71	49980,03	148,98	953,07	86,99
postcure_130C60min	7	2,73	50656,38	169,74	1062,22	89,80
postcure_130C60min	8	2,72	51223,49	157,88	998,93	74,67
Average		2,71	47931,81	158,99	1021,30	74,54
SD		0,01	3101,62	8,05	49,38	10,95
RSD (%)		0,5	6,5	5,1	4,8	14,7

Raw Data

FRC-poles for root canal posts
The effect of the nozzle size
Aug2012

Light intensity 1/4, speed 2mm/s, post-curing 120C 1h

Specimen info	No	Diameter (mm)	Young's Modulus Of Bending (MPa)	Load at Maximum Load (N)	Maximum Bending Stress at Maximum Load (MPa)	Work from preload to Break (Ncm)
2,6	1	2,70	49204,59	157,06	1015,97	79,98
2,6	2	2,68	46020,10	161,91	1070,96	77,13
2,6	3	2,68	49479,04	170,45	1127,46	90,91
2,6	4	2,69	50301,32	168,66	1103,20	71,68
2,6	5	2,69	48851,88	177,32	1159,87	47,97
2,6	6	2,70	47020,85	163,50	1057,61	44,45
2,6	7	2,70	47181,71	160,41	1037,67	65,60
2,6	8	2,68	51030,42	159,86	1057,44	58,03
Average		2,69	48636,24	164,90	1078,77	66,97
SD		0,01	1738,38	6,73	48,02	16,12
RSD		0,34	3,57	4,08	4,45	24,06

Specimen info	No	Diameter (mm)	Young's Modulus Of Bending (MPa)	Load at Maximum Load (N)	Maximum Bending Stress at Maximum Load (MPa)	Work from preload to Break (Ncm)
2,7	1	2,72	52071,61	171,08	1082,44	90,06
2,7	2	2,70	50295,54	183,76	1188,69	77,82
2,7	3	2,70	48949,44	163,31	1056,40	82,27
2,7	4	2,73	47793,11	207,19	1296,55	92,95
2,7	5	2,73	44314,79	179,87	1125,59	82,24
2,7	6	2,72	48689,18	167,75	1061,35	78,46
2,7	7	2,72	50398,26	168,90	1068,63	84,91
2,7	8	2,72	47656,99	198,94	1258,70	62,12
Average		2,72	48771,12	180,10	1142,29	81,35
SD		0,01	2328,70	15,78	94,65	9,38
RSD		0,43	4,77	8,76	8,29	11,52

Specimen info	No	Diameter (mm)	Young's Modulus Of Bending (MPa)	Load at Maximum Load (N)	Maximum Bending Stress at Maximum Load (MPa)	Work from preload to Break (Ncm)
2,8	1	2,78	46877,07	164,73	976,23	78,68
2,8	2	2,78	49232,95	173,59	1028,76	62,57
2,8	3	2,79	47334,16	174,97	1025,80	92,80
2,8	4	2,76	47164,34	168,26	1018,97	58,53
2,8	5	2,78	47096,54	181,92	1078,10	81,30
2,8	6	2,77	46135,99	185,14	1109,13	62,15
2,8	7	2,78	47905,64	165,72	982,11	67,69
2,8	8	2,80	45013,07	164,86	956,23	100,64
Average		2,78	47094,97	172,40	1021,91	75,55
SD		0,01	1230,08	7,91	51,85	15,44
RSD		0,43	2,61	4,59	5,07	20,44

Oven comparason
FRC-poles for root canal posts
nov2012

Specimen info	No	Diameter (mm)	Young's Modulus Of Bending (MPa)	Load at Maximum Load (N)	Maximum Bending Stress at Maximum Load (MPa)	Work from preload to Break (Ncm)
Oikea_1	1	2,76	49561,76	200,67	1215,27	96,01
Oikea_1	2	2,74	50140,39	206,76	1279,74	121,50
Oikea_1	3	2,74	49633,76	188,45	1166,41	60,73
Oikea_1	4	2,74	48631,44	212,51	1315,31	79,44
Oikea_1	5	2,74	48815,32	185,42	1147,65	118,88
Oikea_1	6	2,72	51348,03	193,57	1224,76	65,04
Oikea_1	7	2,75	50847,78	189,19	1158,30	101,93
Oikea_1	8	2,74	50017,77	207,20	1282,50	54,02
Average		2,74	49874,5	198,0	1223,7	87,2
SD		0,01	928,3	10,2	63,7	26,3
RSD		0,41	1,86	5,14	5,21	30,12

Specimen info	No	Diameter (mm)	Young's Modulus Of Bending (MPa)	Load at Maximum Load (N)	Maximum Bending Stress at Maximum Load (MPa)	Work from preload to Break (Ncm)
Oikea_3_vanhas	1	2,65	47686,40	180,09	1232,12	146,49
Oikea_3_vanhas	2	2,65	47273,48	179,44	1227,70	99,41
Oikea_3_vanhas	3	2,62	48852,69	192,30	1361,37	115,40
Oikea_3_vanhas	4	2,60	49807,77	188,94	1368,75	112,20
Oikea_3_vanhas	5	2,52	55652,13	180,94	1439,57	84,28
Oikea_3_vanhas	6	2,58	50971,86	203,74	1510,55	120,14
Oikea_3_vanhas	7	2,60	50721,47	178,68	1294,43	59,45
Oikea_3_vanhas	8	2,61	50181,68	182,72	1308,47	95,43
Oikea_3_vanhas	9	2,63	52123,98	174,22	1219,39	99,14
Average		2,60	50363,5	184,6	1329,1	103,6
SD		0,04	2522,6	9,0	100,7	24,4
RSD		1,50	5,01	4,89	7,57	23,54

Specimen info	No	Diameter (mm)	Young's Modulus Of Bending (MPa)	Load at Maximum Load (N)	Maximum Bending Stress at Maximum Load (MPa)	Work from preload to Break (Ncm)
Vasen_4	1	2,74	44599,91	194,64	1204,74	79,19
Vasen_4	2	2,74	51900,47	183,27	1134,34	79,62
Vasen_4	3	2,74	51009,22	191,72	1186,69	76,93
Vasen_4	4	2,76	45775,76	199,02	1205,24	91,58
Vasen_4	5	2,73	52587,25	202,17	1265,16	85,65
Vasen_4	5	2,73	50934,53	160,55	1004,70	71,26
Vasen_4	6	2,75	50988,37	177,45	1086,39	76,03
Vasen_4	6	2,74	50064,55	212,89	1317,70	68,43
Average		2,74	49732,5	190,2	1175,6	78,6
SD		0,01	2918,2	16,2	99,2	7,4
RSD		0,36	5,87	8,54	8,44	9,45

Raw Data

Old and new nozzle

F	T		F	T		F	T		F	T	
0,24	0,02	stress	0,74	0,01	Load	0,83	0,20	Work	0,00	0,00	Diameter
0,02	0,60	modulus									

Right side and left side ovens

F	T		F	T		F	T		F	T	
0,26	0,27	stress	0,24	0,27	Load	0,00	0,40	Work	0,74	1,00	Diameter
0,01	0,90	modulus									

F.TEST
The two-tailed propability that the variances are not different

T.TEST
Propability associated with students T-test

P-value higher than 0,05 means that there is no significant difference between groups

Correlations

			Pretension (kg)	Max bending stress at max load (MPa)	Young's modulus (MPa)	Load at max load (N)	Work from preload to break (Ncm)	Diameter (mm)
Spearman's rho	Pretension (kg)	Correlation Coefficient	1,000	-,134	,158	-,105	-,263	,176
		Sig. (2-tailed)	.	,414	,338	,524	,106	,284
		N	39	39	39	39	39	39

Correlations

			Postcuring	Max bending stress at max load (MPa)	Young's modulus of bending (MPa)	Load at maximum load (N)	Work from preload to break (Ncm)
Spearman's rho	Postcuring	Correlation Coefficient	1,000	,280*	,538**	,305**	,354**
		Sig. (2-tailed)	.	,011	,000	,006	,001
		N	81	81	81	81	81

Correlations

			Nozzle size (mm)	Diameter (mm)	Max bending stress at max load (MPa)	Young's modulus of bending (MPa)	Load at maximum load (N)	Work from preload to break (Ncm)
Spearman's rho	Nozzle size (mm)	Correlation Coefficient	1,000	,931**	-,354	-,339	,369	,229
		Sig. (2-tailed)	.	,000	,090	,105	,076	,283
		N	24	24	24	24	24	24